

ALTERNATING FLOW MODEL FOR DISPERSION IN PACKED BEDS

By

KAREN J. KLINGMAN

A DISSERTATION PRESENTED TO THE GRADUATE SCHOOL
OF THE UNIVERSITY OF FLORIDA IN
PARTIAL FULFILLMENT OF THE REQUIREMENTS
FOR THE DEGREE OF DOCTOR OF PHILOSOPHY

UNIVERSITY OF FLORIDA

1985

ACKNOWLEDGEMENTS

The author wishes to thank all who directly and indirectly made this work possible: Professor Hong H. Lee for finally believing in and pushing forward these ideas, Dr. Carlos Smith for long-time enthusiasm and encouragement, and Dr. Lyn Clawson for those much-needed nudges toward the finish line. Thanks are also due to Drs. G. Lyberatos, P.J. McKenna, S. Svoronos and G.B. Westermann-Clark for their time on the advisory committee.

The author also wishes to express her gratitude to Dr. J.C. Hong for his input in the early stages of the work (especially Appendix I) and to Derbra Owete for typing the manuscript.

Sincere appreciation is extended to the author's family, E.S. Griffin and J.A. Klingman, for holding back on the ever-looming question, "When are you going to finish?"; to W.D. Stock for unrelenting moral support; and to her office mates (I. A. T. and E. C. S.) and friends for their infinite tolerance.

TABLE OF CONTENTS

	<u>Page</u>
ACKNOWLEDGEMENTS	ii
NOTATION	v
ABSTRACT	xi
CHAPTERS	
I INTRODUCTION	1
II MASS DISPERSION	6
Concept and Rationale for Proposed Model	6
General Description of Alternating Flow Model	12
Model Development	16
Alternating Flow Model Parameters	23
Model Limitations	40
Comparison with Experimental Data	41
III HEAT DISPERSION	55
Model Development	61
Model Parameters	71
Determination of Film Coefficients	79
Comparison with Experimental Data	83
Summary of AFM for Heat Dispersion	102
IV REACTION	104
Model Development	104
Condensation of Equations and Solution Technique	114
Model Parameters	116
Example Problems	117
Summary of AFM for Reaction	135
V CONCLUSIONS	136

	<u>Page</u>
APPENDICES	
A HYDRAULIC RESISTANCES.	138
B REFERENCE LIST FOR DISPERSION COEFFICIENT STUDIES.	142
C AXIAL VOIDAGE VARIATION DETERMINATION.	143
D REFERENCE LIST FOR VOID FRACTION STUDIES	148
E TRANSIENT SIMULATION TECHNIQUE	149
F COMPARISON OF AFM FLOW PROFILES BASED ON EMPTY ANNULUS AND ERGUN-TYPE HYDRAULIC RESISTANCES.	157
G FICKIAN HEAT DISPERSION PARAMETER REFERENCES	159
H TWO-SIDED EFFECTIVENESS FACTOR FOR GENERAL INTRINSIC KINETICS.	160
I PACKING ARRANGEMENT FROM POTENTIAL ENERGY MINIMIZATION . .	164
J SUGGESTIONS FOR FUTURE WORK.	173
K FORTRAN PROGRAM LISTINGS	192
BIBLIOGRAPHY	236
BIOGRAPHICAL SKETCH.	249

NOTATION

a_i	constants for Cohen-Metzner porosity correlations
$a(j,k)$	interfacial area between j-th and k-th radial plugs per unit bed length (equations (20), (22)) (L)
$a(s,w)$	interfacial area between N-th solid plug and stagnant wall film per unit bed length (L)
A_i	void cross-sectional area of i-th radial plug (L^2)
\underline{A}_n	concentration vector for A-half-cell of n-th A/B cell
A^*	heat transfer area ratio (equation (27)) (L/L)
A_t	total tube cross-sectional area (L^2)
A_{tube}	A_t
B	collection of heat transfer terms (equation (28) or (35))
\underline{B}_n	concentration vector for B-half-cell of n-th A/B cell
C	concentration (mol/L^3)
C^*	two plug verage concentration (equation 54) (mol/L^3)
\underline{CA}	A-half-cell concentration vector equations (74), (75))
\underline{CB}	B-half-cell concentration vector (equations (74), (75))
C_p	fluid specific heat ($q/M-\theta$)
d	diameter of cylindrical pellet (equation (28)) (L)
d_i	delay time in i-th radial plug
dp	pellet diameter (L)

Da	axial mass dispersion coefficient (equation (1)) (L^2/t)
De	effective diffusivity of key component in catalyst material (L^2/t)
Dr	radial mass dispersion coefficient (equation (1)) (L^2/t)
Dt	tube diameter (L)
f	friction factor
g	rate constant exponent (equation 52) (θ)
g_c	units conversion factor (e.g. 32.2 ft.-lb _m /lb _f -5 ²)
G	mass velocity ($M/L^2 - t$)
hp	pellet film heat transfer coefficient ($q/t-L^2-\theta$)
hw	wall film heat transfer coefficient ($q/t-L^2-\theta$)
h*	stagmant film heat transfer coefficient (equation (33)) ($q/t-L^2-\theta$)
(-ΔH)	heat of reaction (q/mol)
H _i	hydraulic resistance of i-th radial plug
k	reaction rate constant
k _o	rate constant premultiplier (equation (51))
K'	constant for equation (41)
K''	constant for equation (42)
Kw	constant for equation (45)
ℓ	length of cylindrical pellet (equation (46))(L)
L	total vessel length; or, if used in conjunction with catalyst pellet, $L = V_p/S_p$ (L)

m	flow rate exponent (equation (45))
N	total number of radial plugs in any half-cell (or, total number of void plugs in one A/B cell)
N_{axial}	number of repeating A/B cells in a packed bed
N_{rad}	N
P	general physical property (equations (79), (80)); pressure elsewhere
Q_t	total volumetric flow rate (L^3/t)
Q_{tot}	Q_t
Q_j	volumetric flow rate through j -th radial plug (L^3/t)
r	radial position (dimensional for equations (1), (19); dimensionless elsewhere)
r_c	intrinsic reaction rate (equation (51)) ($\text{mol}/t \cdot L^3_{\text{catalyst}}$)
$r_{i,j}$	(i,j) -th element of \underline{R}
\underline{R}	A-to-B mixing matrix
R_t	tube radius (L)
R_{tube}	R_t
Re	Reynolds number
R_G	global rate of reaction (mol/t); $R_G^i = R_G/z$ ($\text{mol}/t \cdot L$)
R_h	hydraulic radius (L)
s	Laplace variable ($1/t$)
$s_{i,j}$	(i,j) -th element of \underline{S}
\underline{S}	B-to-A mixing matrix
S_p	catalyst pellet surface area (L^2)

Sp'	Sp per unit vessel length (equation (60)), (L)
t	solid temperature (θ)
t_{in}	temperature of solid plug at inner radius (equations (25), (34)), (θ)
t_{out}	temperature of solid plug at outer radius (equation (26)) (θ)
T	fluid temperature (θ)
T^*	two-plug average temperature (equation (54)), (θ)
<u>TA</u>	A-half-cell temperature (equations (74), (75))
<u>TB</u>	B-half-cell temperature vector (equations (74), (75))
T_{wall}	wall temperature (θ)
u	fluid velocity (L/t)
u'	bed average velocity (L/t)
V_p	catalyst pellet volume (L^3)
w_i	weighting factors for <u>R</u> and <u>S</u> (equation (8))
x	radial distance inward from tube wall (units of dp)
Y	parameter group for equation (70)
z	axial coordinate (L)
Z	Z_{tot}
Z_c	length of one A/B cell (L)
Z_{tot}	total bed length (L)

Greek

β	proportionality constant
γ	shape factor for hp (equation (50)) ($\gamma = 1.0$ for spheres, 1.33 for cylinders)
δ	tube material roughness (L)
ϵ	bed void fraction (L^3/L^3)
$\underline{\theta}_A$	A-half-cell delay time matrix
$\underline{\theta}_B$	B-half-cell delay time matrix
λ	effective thermal conductivity (equation (19)) ($q/L-t-\theta$)
λ_s	thermal conductivity of solid packing material ($q/L-t-\theta$)
μ	fluid viscosity (M/L^2-t)
ρ	fluid density (M/L^3)
τ	bed-averaged hold-up time (t)
ϕ	Thiele modulus (equation (52)); or functional form (Table 6)

Subscripts

a	radially averaged value
b	bulk or bed-averaged
base	base case value
c	at bed centerline
h	hydraulic
hi	upper value
in	inlet
int	interstitial
lo	lower value
n	axial cell number
out	outlet
p	particle (except for C_p)
s	solid (packing) material
sup	superficial
t	two or total

Units

L	length
M	mass
q	heat (e.g. cal)
t	time
θ	temperature

Abstract of Dissertation Presented to the Graduate School
of the University of Florida in Partial Fulfillment of the
Requirements for the Degree of Doctor of Philosophy

ALTERNATING FLOW MODEL FOR DISPERSION IN PACKED BEDS

By

KAREN J. KLINGMAN

December, 1985

Chairman: Dr. H. H. Lee
Major Department: Chemical Engineering

The Alternating Flow Model (AFM) views dispersion in packed beds as a sequence of streamline plugs which must repeatedly split and merge as the bulk fluid traverses the vessel. Thus, the flow in the AFM is ordered, as opposed to the random flow implied by the Fickian analogy.

For mass dispersion only, model parameters arise from a priori consideration of packing geometry. Steady-state and transient data ($5.6 < Dt/dp < 54.4$, $100 < Re_p < 1000$, gases and liquids) show the AFM to surpass the Fickian analogy in most cases. Further, the AFM can describe well the radial velocity profiles in packed beds.

Alternating Flow Model heat transfer parameters wall and pellet film resistances are not a priori functions of packing geometry. Fitting the AFM to steady-state temperature data (air, $5 < Dt/dp < 14$, $2 < Re_p < 1300$, cylindrical and spherical pellets) validates a single correlation of h_p versus dp and flow rate and justifies a simple form for correlating h_w versus flow rate. Comparison with experiments shows the AFM to equal or surpass the back-fit Fickian analogy.

For reaction, the AFM combines the concepts of simple mass and heat dispersion with the only additional parameters associated directly with the reaction itself (e.g. intrinsic rate expression, heat of reaction, etc.) AFM-predicted conversion and temperature profiles in both wall-cooled and adiabatic reactors differ significantly from those predicted by the Fickian analogy for the given example system. The difference in the models' predictions of reactor stability characteristics can be attributed to their respective radial flow profiles. This implies that the AFM, with its ability to describe this flow behavior, should be further explored as a packed bed reactor design tool.

CHAPTER I INTRODUCTION

Consider the problem of describing the concentration profile which develops as dye is injected into a clear fluid flowing through a tubular packed bed. After some period of time, the dye concentration will be maximum at the injection point and will decrease as the distance from the injection point increases both radially and axially in the direction of flow. This dye dilution is the simplest case of dispersion in packed beds. If the dye reacts in the bulk fluid or on the pellets, or if the dye adsorbs on the solid surfaces and if heat dispersion accompanies the dispersion of mass, the problem becomes more complex, but a basic understanding of the mass dispersion phenomenon alone is needed before moving up the hierarchy. It is therefore the intent in this paper to present a packed bed dispersion model which is based on the physical behavior of the bulk fluid as it travels around the packing.

Dispersion in packed beds has traditionally been modeled by analogy to Fickian diffusion, e.g., for a constant density fluid

$$\frac{\partial C}{\partial t} + u \frac{\partial C}{\partial z} - Da \frac{\partial^2 C}{\partial z^2} - Dr \frac{1}{r} \frac{\partial}{\partial r} \left(r \frac{\partial C}{\partial r} \right) = 0 \quad (1)$$

where the axial and radial dispersion coefficients D_a and D_r are effective parameters which account for the presence of packing material. It should be noted here that equation (1) can be developed by assuming random motion of particles moving through the vessel (Baron, 1952; Jacques and Vermeulen, 1957; Klinkenberg and Sjenitzer, 1956). The usual procedure for modeling packed beds is to obtain the dispersion coefficients and then to solve (1) either analytically or numerically for the appropriate boundary conditions.

An acceptable dispersion model should at the very least adequately describe the simplest problem of injecting non-reacting dye into a clear stream flowing through a bed packed with non-porous beads. The solution of (1) for the simple dye injection problem predicts backmixing in the steady state (Hiby, 1963) where none is observed experimentally.

Mixing cell models (Deans and Lapidus, 1960; Lapidus and Amundson, 1977; Olbrich et al., 1966) overcome the backmixing problem but predict that concentration wavefronts travel at infinite speed, i.e. any change in inlet concentration is immediately seen at the bed outlet. Experimental observations (Sundaresan et al., 1980) indicate that concentration propagates at a finite speed. Also, no standard technique for sizing the individual mixing cells is available.

A more recent crossflow model (Hinduja, 1977; Hinduja et al., 1980) is based on the concept that the flow around pellets creates two regimes--a stagnant wake behind each pellet and moving streams

travelling between pellets. The wakes are assumed to shed/receive a certain amount of fluid to/from the moving streams and the packing is characterized by a parameter which accounts for the radial distance over which the packing pattern repeats itself. Hinduja (1977) recommends determining the cross-flow characteristic parameters from the correlations of effective Fickian dispersion coefficients. It should also be noted that for the simple dye injection problem, the cross-flow model equations reduce to the Fickian dispersion model.

Other researchers have also proposed stochastic (Schmalzer and Hoelscher, 1971), capillary (Lippert and Schneider, 1979), and probabilistic time-delay models (Buffham, 1971) for packed beds. In addition, the literature provides several reviews of and cautions regarding packed bed models (Aris and Amundson, 1957; Beek, 1962; Bischoff and Levenspiel, 1962; Froment, 1967, 1972; Gunn, 1968; Hiby, 1963; Levenspiel, 1963; Vortmeyer and Winter, 1984).

What, then, are the characteristics of an acceptable packed bed dispersion model? The model should provide the correct steady-state form (axial and radial spreading, no back-mixing, agreement with experimental data) and should predict the correct transient behavior (finite speed of propagation, conservation system) Sundaresan et al., (1980). The model should also properly represent the flow around packing, its solution, analytical or numerical, should be straightforward, and its corresponding parameters should be well-defined. Table 1 indicates that none of the currently available models meet all acceptability criteria.

The objectives here are to present a model which describes the flow in packed beds as a series of alternating annular plugs, the so-called Alternating Flow Model (AFM), and then to develop the corresponding mathematical model. Conceptually, this AFM meets all the criteria set forth in Table 1. Its applicability thus depends on adequate representation of the packing interstices as a regular pattern of concentric annular voids. The second chapter justifies the AFM by physical and other reasoning and the remaining chapters develop the pertinent equations for cases of varying degrees of complexity. As each case is considered, corresponding model parameters will be evaluated. While at first glance the number of parameters may seem quite large, the AFM utilizes an a priori distribution of voids based on the relative size of tube to pellets and on packing geometry, rather than on back-fitting those parameters to experimental data.

First, cases of mass dispersion only, both steady-state and transient, will be considered so that the physical dimensions of the individual plugs can be determined. Next, the case of heat dispersion only will be used to extend the applicability of the AFM and to identify the additional parameters which may be needed to describe energy dispersion. And, finally, because the AFM is particularly applicable to vessels with small tube- to pellet-diameter ratios, equations for combined heat and mass dispersion (i.e., reaction within the catalytic packing) will be presented, since highly exothermic reactions are normally carried out in tubes with a small number of pellets across the tube diameter to facilitate cooling.

Table 1

Dispersion Model Acceptability Criteria

	Fickian	Mixing Cell		Crossflow	AFM
		1-D	2-D		
Finite wavefront speed	depends on BC's	No	No	depends on BC's	Yes
Conservation system	depends on BC's	Yes	Yes	depends on BC's	Yes
Radial and axial spreading	if all terms used	No	Yes	Yes	Yes
No back-mixing	depends on BC's & terms	Yes	Yes	depends on BC's & terms	Yes
Agreement with data	if fit disp. coeffs.	for avg. conc.	if fit params	?? ??	Yes Yes
Easy to solve	depends on BC's etc.	Yes	sec. ODE's	simult. PDE's	Yes
Account for packing	adjust coeffs	-empirical- cell size		uses Fickian coeffs	a-priori based on Dt/dp

CHAPTER II MASS DISPERSION

Concept and Rationale for Proposed Model

Traditionally, two experiments have been used to characterize mass dispersion in empty tubes: steady-state injection of dye at some point along the centerline axis (as mentioned earlier) and time-dependent variation (e.g., step change or sine wave) in the cross-sectional inlet concentration. The steady-state case results in a parabolic shape profile emanating from the point of injection in the direction of bulk flow whereas the transient case yields the residence time distribution (or the so-called "F-curve," if the input is a step-change) which uses the bulk average outlet concentration as an indication of deviation from plug-flow. General practice, as established by Aris (1956, 1958, 1959) and Taylor (1953, 1954a, 1954b), is then to describe this dispersion behavior by a Fick's Law analog (equation (1)). These axial and radial dispersion coefficients, D_a and D_r , (in the form of a dimensionless Peclet Number) are correlated for each of the three flow regimes (laminar, turbulent, transition) (Hoffmann, 1961) in terms of Reynolds and Schmidt Numbers. It is generally accepted that use of the dispersion parameters obtained from these correlations together with the numerical or analytical solution of equation (1)

and its corresponding boundary conditions accurately predicts observed concentration profiles and residence time distributions in empty tubes.

If these same two experiments are carried out in a packed bed, similar (but not exactly equivalent) dispersion characteristics are observed (Danckwerts, 1953; Hiby, 1963). Thus, usual practice is to again employ Fick's Law, together with numerical or readily available analytical solutions of equation (1) (Carberry, 1976; Froment and Bischoff, 1979; Wen and Fan, 1975), but to use effective parameters to account for the fact that the tube is partially occupied by packing. Again, the effective Peclet Numbers (both radial and axial) are correlated in terms of Reynolds and Schmidt Numbers (Wen and Fan, 1975; see also list of pertinent references in Appendix A). Unlike empty tubes, however, these parameters are not well-correlated; there is much spread in the data. The spread exists within the data of single researchers as well as between average values reported by different researchers. One might attribute this spread in Peclet numbers to several factors:

1. misrepresentation of the Reynolds Number,
2. variations in void fraction,
3. erroneous application of the Fickian analogy.

First, consider calculation of the Reynolds number for a packed bed. While in empty tubes it is the diameter that affects transition from laminar to turbulent flow, there is some doubt as to what length actually characterizes this behavior in packed beds, which have,

essentially, two competing lengths: tube diameter and pellet diameter. Usual practice is to employ the pellet diameter since flow around single spheres is well-documented (Bird et al., 1960). However, it has been suggested that it is not the pellet diameter, per se, which induces turbulence but rather the size of the voids, i.e., interstitial hydraulic radius, through which the fluid moves that dominates flow patterns, and that this hydraulic radius should determine a more correct Reynolds number (Cairns and Prausnitz, 1960; Bird et al., 1960; Schertz and Bischoff, 1969; Ergun, 1952; Ergun and Orning, 1949; Lapin, 1962; Leva, 1947a, 1947b; Leva and Grummer, 1947a; Martin et al., 1951). The hydraulic radius for beds with spherical pellets can be calculated from the bed voidage in two ways:

$$1. \quad Rh' = \frac{Dt \, \epsilon}{1.5 \frac{Dt}{dp} (1-\epsilon) + 2} \quad (\text{Cairns and Prausnitz, 1960});$$

$$2. \quad Rh = \frac{dp \, \epsilon}{6(1-\epsilon)} \quad (\text{Bird et al., 1960})$$

In either case, however, re-plotting the Peclet number in terms of this corrected Reynolds number, i.e., with Rh as the characteristic length, does not significantly reduce the spread. Figure 8 of Cairns and Prausnitz (1960) illustrates this point for the case of Rh' . For the case of Rh consider the relationship between the pellet-

and hydraulic-Reynolds numbers: $Re_h = Re_p \epsilon / 6(1-\epsilon)$. Since the usual practice is to plot Peclet number versus Reynolds number on logarithmic axes, all data would translate horizontally by the same amount since $\log(Re_h) = \log(Re_p) + \log(\epsilon / 6(1-\epsilon))$. Given that ϵ falls within a narrow range, the second term is essentially constant.

Second, although packed beds are inherently non-homogeneous merely by the presence of packing, the void fraction within a bed is not constant throughout but depends on radial position (see Appendix C for list of appropriate references). Thus, although the dispersion parameters, i.e., Peclet numbers, are effectively adjusted to account for that portion of the bed unavailable for flow (and mixing), use of the average bed void fraction to do so can induce errors, since the void fraction, in general, determines the average velocity of equation (1). If velocity varies as a function of radial position, then it follows that the dispersion characteristics should also vary radially. Cohen and Metzner (1981) summarize the radial fluctuations in void fraction in terms of a tri-regional (wall, transition, bulk) equation. Their correlation documents maximum voidage near the tube wall with sinusoidal variations about the average bed voidage whose amplitude decays exponentially as one moves from the wall to the centerline. While voidage variations are thus well-established, the corresponding velocity variations are not. In fact, while one would expect minimum velocity to correspond to maximum cross-sectional area, the converse has been consistently observed

(Carbonell, 1980; Gunn, 1969; Karabelas, et al., 1973; Mickley et al., 1965; Schertz and Bischoff, 1969; Schwartz and Smith, 1953; Standish, 1984; Vortmeyer, 1983; Vortmeyer and Schuster, 1984). This maximum velocity/maximum voidage effect can be attributed to channelling--that more fluid will take the path of least hydraulic resistance, i.e. maximum cross-sectional area. In addition, other researchers (Fahien and Smith, 1955; Edisath et al., 1983; Dorweiler and Fahien, 1959; Oliveros and Smith, 1982) have shown that allowing the individual dispersion coefficients to be functions of radial position improves the accuracy of the Fickian description (equation (1)) of packed beds; Fahien and Smith (1955) showed that the dispersion coefficient also varies axially.

Third, consider the possibility that it may be the model itself, rather than the corresponding parameters, that is in error. Why does the Fickian analogy work so well for empty tubes but present difficulties when applied to packed beds? Some researchers have attributed this to the dubious applicability of the usual boundary conditions to packed beds (Burghardt and Zaleski, 1968; Chen et al., 1983; Choi and Perlmutter, 1976; Deckwer and Mahlmann, 1976; Rasmuson and Neretnieks, 1980; Rasmuson, 1981; Ray et al., 1972; Standart, 1968; Wehner and Wilhelm, 1956), but the key here is to examine the underlying assumption of randomness implied by the application of Fick's Law. It has been shown (Baron, 1952; Jacques and Vermeulen, 1957) that if a particle exhibits random motion, with no preference for direction of travel, as it traverses the length of the vessel, then

statistical analysis will lead to equation (1). The question then arises as to whether the presence of packing within the tube would impose some order to the flow.

Gunn and Pryce (1969) carried out several experiments in packed beds of two types: one with the packing intentionally arranged in a regular pattern and another with random (dumped) packing. Their goal was to compare the applicability of the Fickian analogy to the tanks-in-series model. The initial hypothesis was that the tanks-in-series model should more closely fit the ordered packing arrangement since regular pockets would be available for the formation of perfect mixers, whereas the Fickian analogy should better describe the random packing arrangement. They reasoned that if the parameters associated with each of these models could be fit within reasonable statistical significance, the model itself would be applicable to that particular situation. Their data analysis showed that, within the desired accuracy, the tanks-in-series model parameters could not be fit to either the random or regular packing cases, that the Fickian dispersion parameters could not be fit to the regular array case, and that the Fickian parameters did fit the random packing case. This lends support to the idea that equation (1) may not adequately describe conditions of non-random motion.

In addition, other researchers (Hiby, 1963; Bischoff and McCracken, 1966; Kubo et al., 1979) experimented with time-lapse photography to observe the flow patterns around pellets in packed beds.

Patterns, such as those shown schematically in Figure 1, were consistently observed. The experiment illustrated in Figure 1 is for flow around cylinders between two flat plates. This streamline-split/merge pattern did not break down even as the velocity was increased by two orders of magnitude (Hiby, 1963). This lends support to the idea that the packing arrangement dominates the actual fluid velocity in determining mixing characteristics within packed beds.

How, then, is it possible to use this information to aid the description of dispersion in packed beds? If one draws a vertical axis through the middle of the flat plates illustrated by Figure 1 and then rotates these plates about that axis, the void and occupied channels become void and occupied annuli as shown in Figure 2. As the fluid flows through this sequence of void-full annular cells it alternately splits and merges; hence, the name Alternating Flow Model (AFM). The basic premise of this work, then, is that this AFM approximation, developed solely from observations of packed bed flow behavior, accurately describes not only the flow, but also the dispersion behavior in packed beds. Further, the resulting equations can be solved in a straightforward manner and the corresponding physical parameters can be determined a priori, as opposed to being back-fit to laboratory data.

General Description of Alternating Flow Model

The Alternating Flow Model presumes that flow through a packed bed can be described by an axially repeating series of cells as shown in Figure 2, and that the fluid moving through each void space

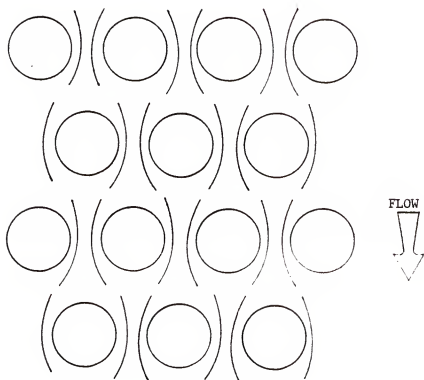


Figure 1: Schematic Representation of Flow Patterns
in Packed Beds

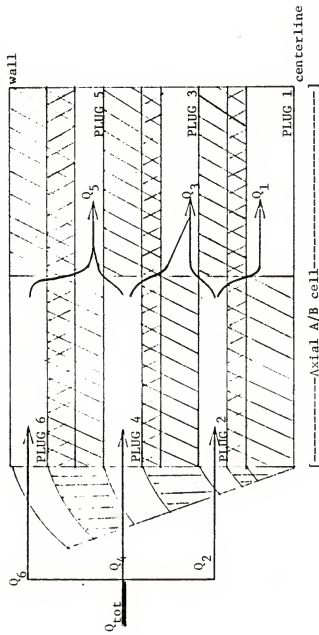


Figure 2: One AFM Repeating A/B cell, $N_{rad}=6$

exhibits plug flow behavior. Thus, dispersion is achieved by repeated splitting and merging of these fluid plugs as the bulk fluid traverses the length of the bed.

Note that the underlying assumption here is that the packing exerts a great influence on the flow pattern, i.e., the packing imposes order on the flow. Hence, the randomness assumption inherent in the Fickian analogy no longer holds. One might argue that if the tube to pellet diameter ratio, D_t/d_p , is large enough, the choice of pathways available to a particle as it traverses the bed will be sufficiently large to validate the randomness assumption. One might intuitively justify this argument by pointing out the large number of possible arrangements the pellets can assume as they are packed in the tube. Consider, however, what happens as D_t/d_p decreases; the number of possible arrangements also decreases. For example, if $D_t/d_p=3$, the only possible arrangement for spheres within a cylinder (or for discs within a larger circle) is one sphere at the center with six spheres tangent to the tube wall. Thus, one can also intuitively argue that randomness decreases as order is imposed on the packing. Recall the experiments of Gunn and Pryce (1969); with the Fickian model, which implies randomness, they were unable to reproduce observed dispersion behavior in intentionally ordered packed beds. (In practice, such ordered cases arise in applications involving highly exothermic catalytic reactions. Usual practice is to pack only a few pellets across the tube diameter so that effective cooling can be achieved and hot spots, particularly at the tube axis, can be avoided.)

Model Development

If a cylindrical tube is packed with inert uniformly sized spheres, the simplest mass dispersion cases are the steady-state injection of dye, or tracer, on the tube axis and a transient step-change in concentration across the entire inlet cross-section. For these cases, two AFM parameters define the dispersion behavior: the number (size) and distribution of radial plugs within each A or B half-cell and the length of each repeating A/B cell (see Figure 2). The distribution of the flow among the individual radial plugs, or the split-merge behavior, follows from these dimensions via a hydraulic resistance argument.

Consider as an example a tube divided into six concentric annuli as shown in Figure 2. Since the flow into a channel or arbitrary cross-section is described by

$$\Delta P = f \left(\frac{L}{R_h} \right) U^2 / 2g_c \quad (2)$$

and

$$f = \begin{matrix} \text{constant/Re} & \text{laminar} \\ \\ \text{constant} & \text{turbulent} \end{matrix} \quad (3)$$

the total flow, Q_t , entering a pipe of pattern A (Figure 2) will be distributed to each plug as

$$Q_i / Q_t = (1/H_i) \sum (1/H_i) \quad i=2,4,6 \quad (4)$$

In the above relationship, the individual hydraulic resistances H_i , depend on annulus dimensions and on flow regime (Appendix B) as

$$\begin{aligned} & A_i R_{h_i}^2 && \text{laminar} \\ 1/H_i = & && (5) \\ & A_i (R_{h_i})^{0.5} && \text{turbulent} \end{aligned}$$

Here, whether the flow be regarded as laminar or turbulent is based on the particle Reynolds number, Re_p (pellet diameter as characteristic length) for flow around individual spheres; $Re_p > 150$ implies turbulence, and $Re_p < 150$ implies laminar flow. As the fluid flows from the A-half-cell to the B-half-cell, the plug 2 flow splits in proportion to the hydraulic resistances presented by plugs 1 and 3, the plug 4 flow splits in proportion to the plug 3 and 5 resistances, and the plug 6 flow must all enter plug 5 (Figure 2), i.e.,

$$\begin{aligned} Q_1/Q_t &= (1-W_3)Q_2/Q_t \\ Q_3/Q_t &= W_3Q_2/Q_t + (1-W_5)Q_4/Q_t \\ Q_5/Q_t &= W_5Q_4/Q_t + Q_6/Q_t \end{aligned} \quad (6)$$

The individual weighing factors are determined by the resistances of those B plugs into which each A plug must split. Consider, for example, A-plug 4 as it splits via two competing resistances into B-plugs 3 and 5 (just as there were three competing resistances for the total flow entering pattern A). Thus

$$Q_5/Q_4 = \frac{1/H_5}{1/H_5 + 1/H_3} = W_5$$

and

(7)

$$Q_3/Q_4 = \frac{1/H_3}{1/H_3 + 1/H_5} = 1-W_5$$

Hence, the weighing factors of equation (6) are given by

$$W_i = \frac{1/H_i}{1/H_i + 1/H_{i-2}} \quad (8)$$

where the subscripts are as illustrated in Figure 2 and the hydraulic resistances are as defined in equation (5), above. As the fluid moves from the B-half-cell into the next A-half-cell, the plugs recombine in such a way as to regain the original A distribution. This implies that the concentration entering each plug is a weighed average of the outlets of preceding plugs:

A to B transition

$$C_1 = C_2$$

$$C_3 = (1-W_5)Q_4 C_4 + W_3 Q_2 C_2 / Q_3$$

$$C_5 = W_5 Q_4 C_4 + C_6 Q_6 / Q_5$$

B to A transition

(9)

$$C_2 = W_3 C_3 + (1-W_3) C_1$$

$$C_4 = (1-W_5) C_4 + W_5 C_3$$

$$C_6 = C_5$$

(Note: the question may arise as to why the AFM employs the A-first pattern as opposed to the B-first pattern. Since the profiles predicted by the AFM are insensitive to the A/B order (Figure 3, Table 2) the A-first pattern was selected.)

Table 2
Centerline Concentrations for two AFM Patterns

<u>Dt/dp</u>	<u>z/dp</u>	<u>C/Ca at r=0</u>	
		<u>A-B</u>	<u>B-A</u>
25.6	52	8.6	8.2
13.3	27	4.2	4.1
11.1	23	4.0	3.7
6.9	14	2.2	2.4
19.2	52	4.8	5.0
8.3	23	2.0	2.3
12.8	52	2.1	2.1
5.3	23	1.3	1.3

These geometries correspond to data taken by Fahien and Smith (1955). Model is compared to data in a later section.

For the simple mass dispersion only cases, the plug flow equation for each radial plug becomes

$$u \, dC/dz + dC/dt = 0 \quad (10)$$

where determination of the individual linear velocities, u , are discussed below. The solution of equation (10) indicates that the concentration at the outlet of each radial plug is simply its input signal delayed by a dead time equal to the half-cell length divided by u . Since the fluid must traverse a series of delays before exiting the bed, a finite time will pass before any inlet changes will propagate to the outlet.

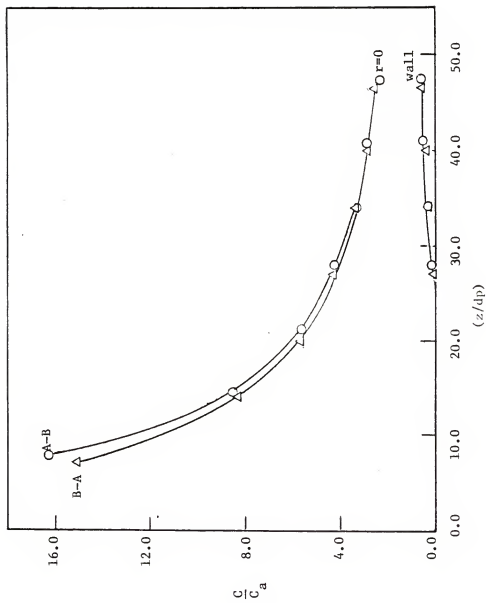


Figure 3: A-first and B-first AFM Concentration Profiles

In the steady-state, enough time has passed so the outlet and inlet concentrations are equal and the concentration profile at the n-th axial segment can be determined from the inlet profile:

$$\begin{aligned} \underline{A}_n &= (\underline{SR})^{n-1} \underline{C}_{in} \\ \underline{B}_n &= \underline{RA}_n \end{aligned} \quad (11-a)$$

where

$$\begin{aligned} \underline{A}_n^T &= [C_{2,n} \ C_{4,n} \ \dots \ C_{Nrad,n}] \\ \underline{B}_n^T &= [C_{1,n} \ C_{3,n} \ \dots \ C_{Nrad-1,n}] \\ \underline{C}_{in}^T &= [C_{2,in} \ C_{4,in} \ \dots \ C_{Nrad,in}] \end{aligned} \quad (11-b)$$

and \underline{R} and \underline{S} are each $(Nrad/2)$ by $(Nrad/2)$ di-diagonal matrices with all elements zero except that

$$\begin{aligned} s_{i,i} &= \begin{cases} 1-W_{2i} & i=1,2,3, \dots, (Nrad/2) \\ 0 & i=Nrad/2 \end{cases} \\ s_{i,i+1} &= \begin{cases} W_{2i} & i=1,2,3, \dots, (Nrad/2) \\ 1 & i=Nrad/2 \end{cases} \end{aligned} \quad (11-c)$$

$$r_{i,i} = \begin{cases} 1 & i=1 \\ \frac{W_{2i-2} Q_{2i-2}}{Q_{2i-1}} & i=2,3,4, \dots, (Nrad/2) \end{cases}$$

$$r_{i,i+1} = \begin{cases} 0 & i=1 \\ \frac{(1-W_{2i}) Q_{2i}}{Q_{2i-1}} & i=2,3,4, \dots, (Nrad/2) \end{cases}$$

Here, N_{rad} signifies the total number of void radial plugs in an A/B cell. Note that a point source of dye is simulated by setting $C_{2,in} = C_{in}$ and $C_{4,in} = C_{6,in} = \dots = C_{N_{rad},in} = 0$. Since the concentration in any given radial plug is solely a function of upstream conditions, no backmixing is predicted.

In the transient case, the dead times are most easily viewed in the Laplace domain. A uniform step-change in inlet concentration is simulated by setting all elements of an $(N_{rad}/2)$ -long column vector equal to (C_{in}/s) . The concentration profile at the n th axial segment and at any given time can be represented in a form analogous to equation (11), above, with additional inclusion of diagonal delay matrices:

$$\begin{aligned}\underline{A}_{out,n} &= \underline{\theta}_A \underline{A}_{in,n} \\ \underline{B}_{out,n} &= \underline{\theta}_B \underline{B}_{in,n}\end{aligned}\tag{12-a}$$

where $\underline{\theta}_A$ and $\underline{\theta}_B$ are diagonal matrices with elements

$$\begin{aligned}(\theta_A)_{i,i} &= \exp(-sd_j) & i=1,2,3, \dots, N_{rad}/2 \\ & & j=2i \\ (\theta_B)_{i,i} &= \exp(-sd_j) & i=1,2,3, \dots, N_{rad}/2 \\ & & j=2i-1\end{aligned}\tag{12-b}$$

so that

$$\begin{aligned}(\underline{A}_{in})_n &= (\underline{S} \underline{\theta}_B \underline{R} \underline{\theta}_A)^{n-1} \underline{C}_{in}/s \\ (\underline{B}_{out})_n &= \underline{\theta}_B \underline{R} \underline{\theta}_A (\underline{S} \underline{\theta}_B \underline{R} \underline{\theta}_A)^{n-1} \underline{C}_{in}/s\end{aligned}$$

Note that equation (12) implies a radial distribution of the total time delay required for an inlet change to be seen at the outlet, i.e., a residence time distribution. The matrix formulation of equation (12) is for convenience. The actual mechanics of real-time simulation are described in Appendix E.

Now that the appropriate describing equations have been established, the corresponding radial plug size distribution axial cell length and individual linear velocities must be determined.

Alternating Flow Model Parameters

As mentioned earlier, radial variations in bed voidage, as porosity, are well-documented experimentally (see Appendix C) and have been correlated via a tri-regional model (Cohen and Metzner, 1981) which is shown below for convenience:

1. wall region ($x < 0.25$)--

$$1 - \varepsilon = 4.5(1 - \varepsilon_b)(x - 7x^2/9)$$

2. transition region ($0.25 < x < 8$)--

$$\frac{\varepsilon - \varepsilon_b}{1 - \varepsilon_b} = a_1 e^{-a_2 x} \cos(a_3 x - a_4) \pi \quad (13)$$

3. bulk region ($x > 8$)--

$$\varepsilon = \varepsilon_b$$

where x is the distance, in pellet diameters, from the tube wall; the constants are $a_1 = 0.3463$, $a_2 = 0.4273$, $a_3 = 2.4509$, $a_4 = 2.2011$. It should be noted that these radial porosities are averaged over the entire bed length.

Although the literature only hints at axial voidage variations (Bennett, 1972; Schwartz and Smith, 1953), they do exist. Consider again the case of dropping spheres into a vertical cylinder whose diameter is three times that of an individual sphere. The densest packing is to have repeating layers of seven spheres (one in the center and six tangent to the wall), with the outside ring of spheres rotated thirty degrees from the layer below and the center spheres stacked one on top of the other. The area void fraction will be maximum, i.e., completely empty, at the tube bottom and will decrease to a minimum at one-half pellet diameter up. The void fraction will again increase (to a different maximum) as one moves halfway to the center plane of the next layer and then decrease (to a different minimum) at the center plane, and so on. One can also extend this idea of repeating axial layers to more complex packing arrangements, i.e., larger D_t/d_p . Figure 5 shows numerically determined axial void variations for $D_t/d_p=3$ whereas Figure 4 shows experimentally measured voidages $D_t/d_p=6.6$. The numerical and experimental techniques are described in Appendix D.

The peak-to-peak distance in the void fraction curves indicates the number of void-full regions expected both radially and axially.

Radially, this distance can be found by determining the points at which $\epsilon=\epsilon_b$ (equation (13)) and are

$$\cos(a_3x-a_4)\pi=0$$

or

$$a_3x-a_4 = \dots -3/2, -1/2, 1/2, 3/2, \dots, \quad (14)$$

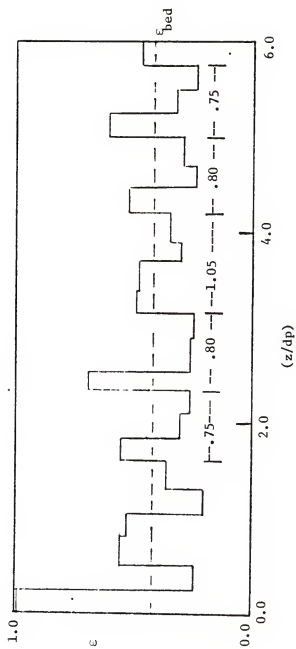


Figure 4: Axial Voidage Variations, $Dt/dp=5.04$, Measured Experimentally

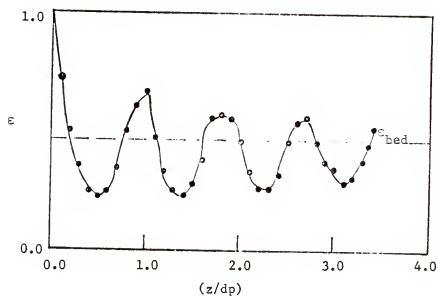


Figure 5: Axial Voidage Variation, $Dt/dp=3.0$,
Determined Numerically

The radial thickness of each void-full region would then be the distance between the i -th and $(i+2)$ th zeros, since each zero indicates a transition from maximum to minimum voidage. Note from Table 3 the distance between successive zeros is 0.408 dp, yielding a radial void-full thickness of 0.816dp. (It may be of interest to also note that the center-to-center distance between spheres arranged in a hexagonal close packed (HCP) pattern is 0.816dp). Thus, $N_{rad} = (Dt/dp)/0.816$, to the next highest even integer, and the radius is divided into $(N_{rad}/2)$ equal increments which are then subdivided to satisfy the radial distribution of void fraction. That is, the voidage of any given A- or B-plug must equal the radially averaged voidage given by equation (13) for that same interval:

$$2 \int_{r_i}^{r_{i+2}} r \epsilon(r) dr = r_{hi}^2 - r_{lo}^2 \quad (15)$$

where the small r 's denote the scaled radial position, R/R_{tube} . The radii r_{hi} and r_{lo} are determined by the half-cell as shown in Figure 6. (Note that for the A-half-cell r_{lo} is unknown, whereas for the B-half-cell r_{hi} is unknown). The corresponding overall bed voidage ϵ_{bed} can be found by integrating the left hand side of equation (15) from $r=0$ to $r=1$ and is not necessarily equal to ϵ_b of equation (13). Thus, ϵ_b must be selected to give ϵ_{bed} within a few percent of the observed value. If the overall bed voidage is unknown, the comprehensive data of Leva and Grummer (1947b) for bed voidage as a function of Dt/dp can be used.

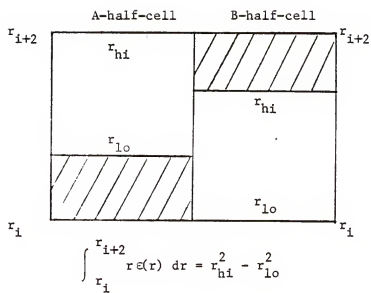


Figure 6: Intermediate Radius Integration Limits

Table 3

Half-cycle Crossings of Radial Void Function

R.H.S. of equation (14)	x-value
-----	-----
-1.5	0.286
-0.5	0.694
0.5	1.102
1.5	1.510
2.5	1.918
3.5	2.326
4.5	2.734

Axially, the peak-to-peak distance can be found in an analogous manner. Figures 5 and 4 show the cycle width, which represents the length of one half-cell, to be approximately $0.82dp$, independent of Dt/dp . Recall that the center-to-center distance for HCP spheres is $0.816dp$; it is therefore assumed that this is the axial voidage cycle width. Thus, the total (A/B) cell length is twice that amount giving $Nz = Z_{tot}/1.632dp$ as the number of repeating (A/B) cells.

The individual linear velocities, u (equation (10)), are calculated as volumetric flow rate (equations (4) and (6)) divided by cross-sectional area of flow, $u_i = Q_i/A_i$, as was implied by employing equation (2) to distribute the flows. The individual cross-sectional areas, A_i , are determined from the radii defined by equation (15). These velocities are scaled by dividing the average interstitial bed velocity, $u = Qt/\epsilon_{bed}Atube$, or

$$u_i/u' = \frac{\epsilon_{bed}(Q_i/Q_t)}{A_i/Atube}$$

The delay times in each annulus are given by the plug (or half-cell) length divided by the corresponding velocity and are scaled by dividing by the average bed hold-up time, $\tau = Z_{tot}/u$, to give

$$d_i/\tau = \frac{A_i/Atube}{2Nz \epsilon_{bed} Q_i/Q_t} \quad (17)$$

since there are $(2 Nz)$ half-cells (plug lengths) across the overall bed length, Z_{tot} .

Figures 7 - 12 compare observed radial profiles of u_1/u' to those predicted by equation (16). In all cases, the AFM predictions follow the data well. In these figures, the AFM profiles are represented by horizontal bars corresponding to the A- or B-plugs (B with hash-marks, A without); the non-vertical dashed segments connect across those regions the AFM considers occupied by solid regardless of half-cell (refer to Figure 2). The experimental data are represented in Figures 8 - 12 by horizontal bars covering the regions in which the respective researchers assumed the velocities to be constant. In these cases, velocities were measured at five radial positions each with 10% of the total tube cross-sectional area on either side so that the radially integrated (average) velocity, u' , would equal the arithmetic average. In Figure 7, the data are represented by single points since so many measurements were made. In this case, the radially averaged velocity, u' , was determined by numerical integration from which the scaled values were calculated.

Because insertion of velocity probes into the packing would disrupt both the flow profile and packing arrangement, velocity data were taken in the empty tube some distance beyond the packed section. As this distance increases, the velocity profile tends to flatten out (Figure 13) and eventually approaches the roughly parabolic shape expected in an empty tube. In addition, velocities will decrease when the fluid expands from the small cross-section

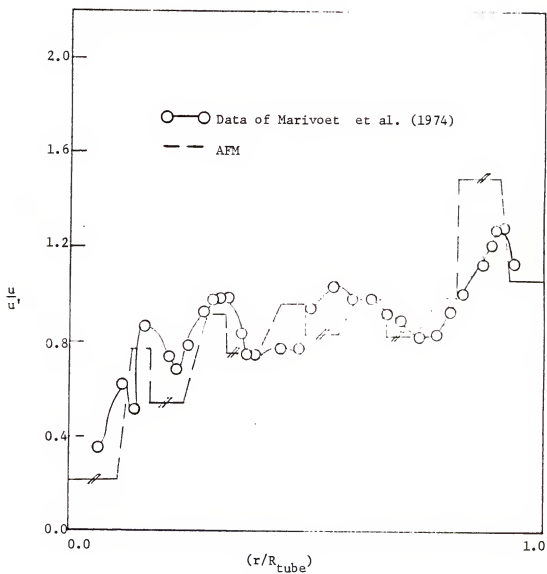


Figure 7: Radial Velocity Profiles, $D_t/d_p=9.4$, 3" Pipe,
Data (Marivoet et al., 1974) Taken 0.5cm
beyond Packed Section

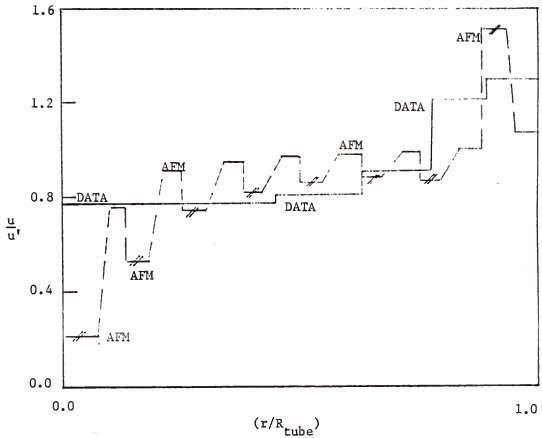


Figure 8: Radial Velocity Profiles, $D_t/d_p=3.2$, 4" Pipe, Data (Schertz and Bischoff, 1969) Taken 1 inch beyond Packed Section

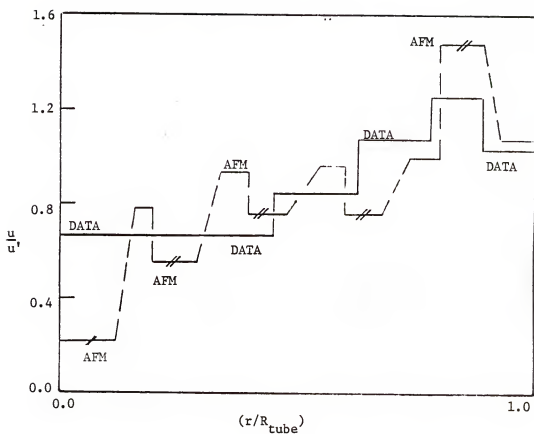


Figure 9: Radial Velocity Profiles, $D_t/d_p=8$, 4" Pipe,
Data (Schwartz and Smith, 1953) Taken 2 inches
beyond Packed Section

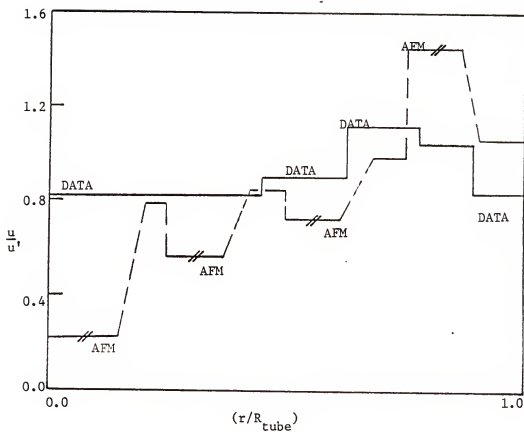


Figure 10: Radial Velocity Profiles, $D_t/d_p=6$, 3" Pipe,
Data (Schwartz and Smith, 1953) Taken 2 inches
beyond Packed Section

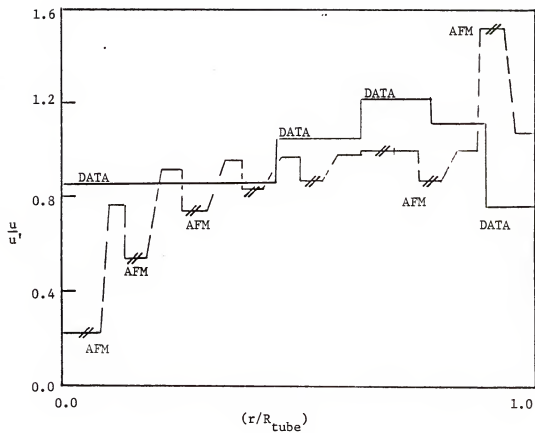


Figure 11: Radial Velocity Profiles, $D_t/d_p=12.8$, 2" Pipe, Data (Schwartz and Smith, 1953) Taken 2 inches beyond Packed Section

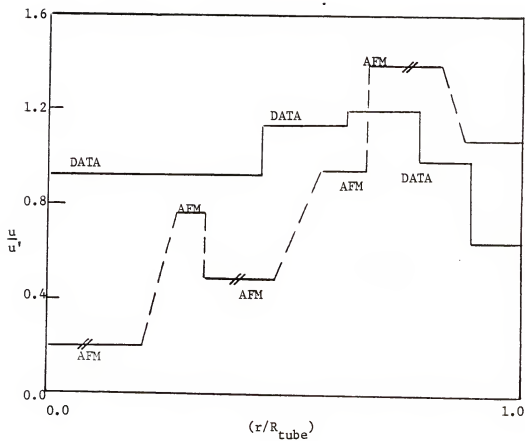


Figure 12: Radial Velocity Profiles, $D_t/d_p=5.3$, 2" Pipe,
Data (Schwartz and Smith, 1953) Taken 2 inches
beyond Packed Section

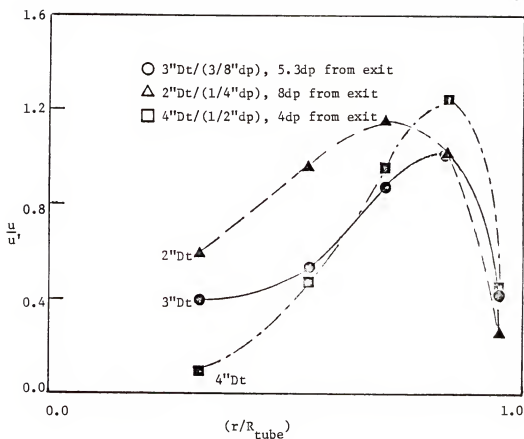


Figure 13: Flattening of Radial Velocity Profile as Distance beyond Packed Section Increases, $Dt/dp=8$, Data (Schwartz and Smith, 1953) Taken 2 inches beyond Packed Section, Regardless of Dt

of the packing interstices into the larger cross-section of the empty tube. The degree of expansion probably varies radially due to the radial porosity profile with the smallest effect at maximum voidage near the wall. But, the empty tube wall drag and tendency for maximum velocity at the centerline would likely combine to dampen out any peaks near the wall more dramatically than at other radial positions. Vortmeyer and Winter (1982) solved the Navier-Stokes equations for an empty tube with a maximum-near-wall velocity profiles at its inlet and showed that the flow pattern quickly redistributes. However, the empty tube measurements should at least indicate the velocity trends within the packing.

In all cases, the AFM predictions follow the observed velocity trends. Moreover, the AFM predictions more closely match data taken either very close to the bed exit (Figure 7) or in larger tubes (Figure 8 and 9) where the empty tube has had less of a chance to influence the flow patterns. This good agreement of predicted and measured velocities gives credibility to using equations (16) and (17) to determine transient characteristics of packed beds.

Examination of these techniques for determining AFM parameters reveals one key point: only geometric factors (Dt/dp , z/dp , ϵ_{bed}) are required to predict mass dispersion in packed beds. Thus the Alternating Flow model is predictive; its parameters are determined a priori with no need for back-fitting them to dispersion data. In a later section, steady-state data will be used to check the sizing of axial cell length, the distribution of radial plugs, and the

distribution of flows. Transient data will be used to check the velocity (delay time) distribution. But first, some limitations of the AFM must be discussed.

Model Limitations

Questions regarding how the Alternating Flow model handles the cases of

1. zero bulk velocity or flow rate,
2. extremely wide beds (i.e., Dt/dp large),
3. extremely long beds (i.e., z/dp large)

may arise. Each is discussed below.

Zero velocity dispersion behavior should reduce to a pure diffusion-like mechanism. Consider the simplest steady-state experiment of injecting dye (tracer) at some point within the packed bed. If there is no bulk velocity, then the dye should disperse equally in both directions; that is, there must be back-mixing. A model, such as the AFM, which alleviates the back-mixing problem described earlier, cannot describe such zero velocity behavior. But, any model, such as the Fickian analogy, which can describe stagnant flow fails to alleviate the back-mixing problem.

For the AFM, extremely wide or long beds result in large numbers of radial plugs or axial cells, respectively. As these numbers become increasingly large, the AFM description of the transient (F-curve) behavior approaches plug flow behavior for the overall bed, i.e., the output signal becomes the input signal delayed by one bed hold-up time. This is a result of flat radial delay-time profiles (equation (17)). As Dt/dp increases, the "wall region" becomes a

smaller proportion of the total bed cross-section thus creating a more uniform porosity profile, which in turn implies more uniform velocity and delay time profiles. As z/d_p increases, N_z follows and the denominator of equation (17) eventually becomes large enough to prevent any noticeable differences between individual delay-times.

Comparison with Experimental Data

Figures 14 - 17 give steady-state radial concentration profiles at a set of positions for $5.6 < Dt/d_p < 54$, $100 < Re_p < 500$, and $10 \leq z/d_p \leq 100$. Figure 18 shows axial profiles at two set radial positions for $Dt/d_p = 12.8$, and Figures 19 and 20 give F-curves for $Dt/d_p = 15.9$ and 8.0 . Both gases and liquids are represented (Table 4). Experiment is compared to prediction via

1. Fickian predictive: dispersion coefficients obtained via correlations available in the literature (Wen and Fan, 1975; Levenspiel, 1962;
 - a) steady-state via equation (15) of Gunn and Pryce (1969),
 - b) transient via equation (19) of Danckwerts (1953),
2. Alternating Flow Model predictions.

These figures do not show profiles obtained by back-fitting dispersion coefficients to the data since, at any given axial position, it is possible to obtain a nearly perfect fit. However, as indicated by the experiments of Fahien and Smith (1955) these coefficients may change with axial position.

Table 4
Data Used for Mass Dispersion Comparison

Source	Type ^a	Dt	dp	Tracer/ bulk	Rep	z/dp
Fahien and Smith (1955)	SS	2"-4"	5/32" -0.36"	CO ₂ /air	150 -900	10-70
Gunn and Pryce (1969)	SS	3.5"	6mm	Ar/air	121	23
Latinen (1951)	SS	2"	.037"	dye/water	102	180
Cairns and Prausnitz (1960)	trans	2"	3.2mm	NaCH/water water	128	191
Jacques and Vermeulen (1957)	trans	6"	.75"	NaCH/ water	130 ^b	32

^aSS=steady-state; trans=transient.

^b Data read directly from their Figure 32, which was assumed to represent Run 217-2 (2gpm) and not Run 217-1 as stated. If this assumption is not made, the data imply that the F-curve reaches 50% only after two vessel hold-up times, a situation that seems highly unlikely.

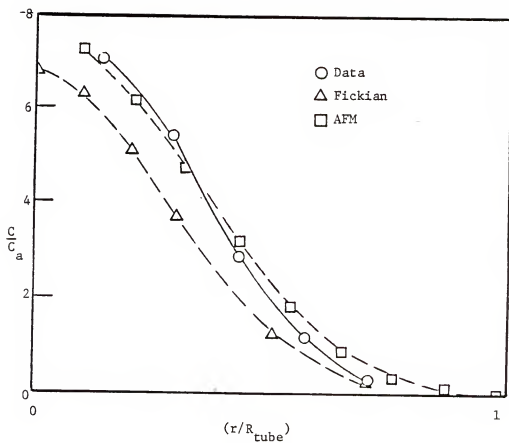


Figure 14: Steady-state Radial Concentration Profiles, $Dt/dp=15$, $Z_{\text{tot}}/dp=23$, Data of Gunn and Pryce (1969)

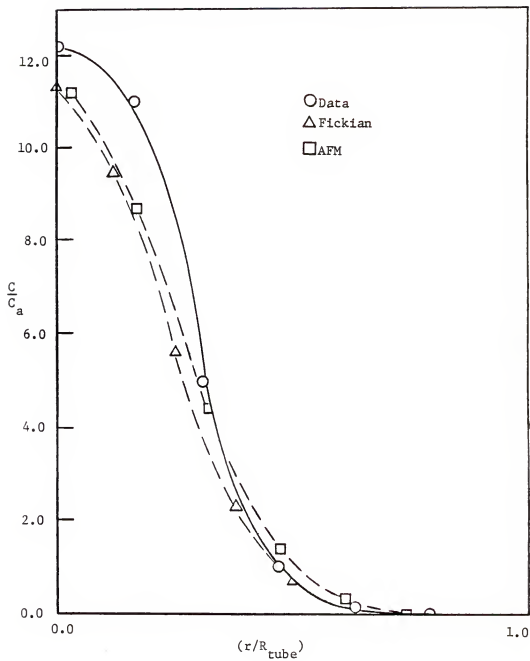


Figure 15: Steady-state Radial Concentration Profiles, $D\tau/d\rho=54.3$, $Z_{\text{tot}}/d\rho=180$, Data of Latinen (1954)

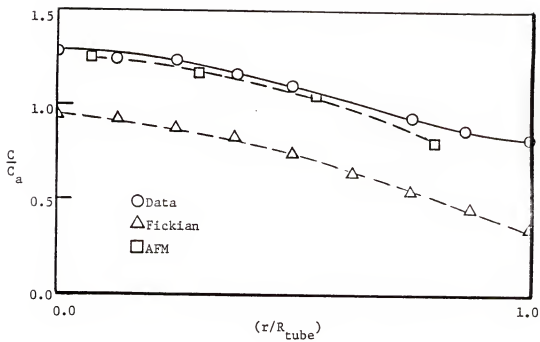


Figure 16: Steady-state Radial Concentration Profiles, $Dt/dp=5.6$, $Z_{tot}/dp=23$, Data of Fahien and Smith (1955)

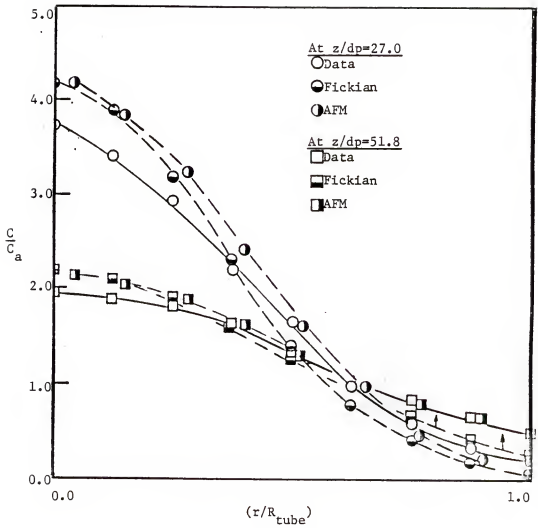


Figure 17: Axial Variation of Steady-state Radial Concentration Profiles, $Dt/dp=12.8$, $z/dp=27$ and 52 , Data of Fahien and Smith (1955)

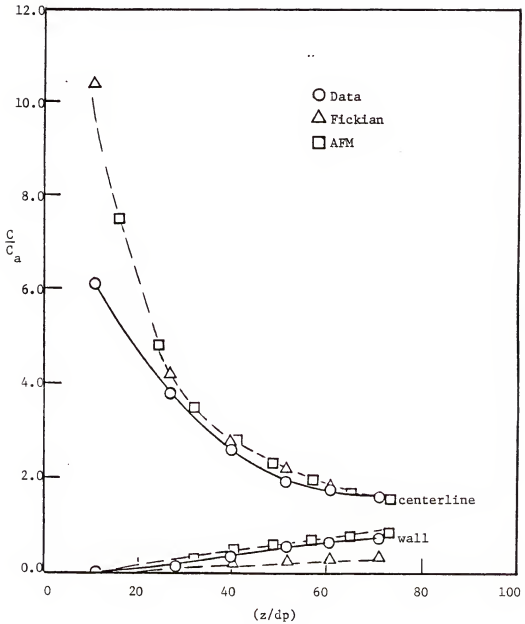


Figure 18: Steady-state Axial Concentration Profiles, $Dt/dp=12.8$, Data of Fahien and Smith (1955)

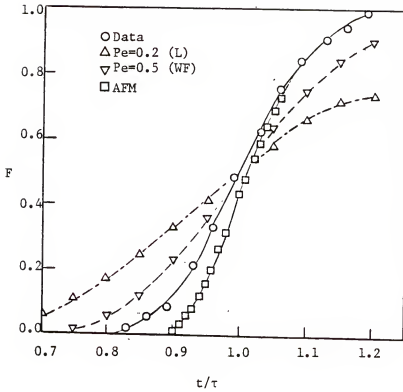


Figure 19: F-curves for $Dt/dp=15.9$, $Z_{tot}/dp=191$,
 Data of Cairns and Prausnitz (1960),
 L=Levenspiel (1962), WF=Wen and Fan (1975)

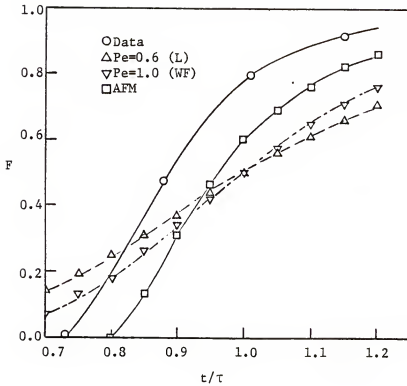


Figure 20: F-curves for $Dt/dp=8.0$, $Z_{tot}/dp=32$,
Data of Jacques and Vermeulen (1957),
L=Levenspiel (1962), WF=Wen and Fan (1975)

In the steady-state Figures (14 - 18), the vertical axis represents point-value concentrations scaled by the average measured effluent concentration, C_a , which can be calculated at any given axial position as $C_a = (\text{total amount of tracer material})/(\text{total amount of fluid})$. Solutions of the Fickian analogy (equation (1)) for C/C_a as function of radial and axial position are given elsewhere (e.g., Roemer et al., 1962; Gunn and Pryce, 1969; Danckwerts, 1953; Cairns and Prausnitz, 1960; Wen and Fan, 1975). For the AFM the scaled concentrations become

$$C_i/C_a = C_i Q_i / \sum (Q_j C_j) \quad (18)$$

with $j=2,4,\dots,N$ for the A-half-cell, and $j=1,3,\dots,N-1$ for the B-half-cell. The subscript "i" implies that the concentration in that given annular plug is constant. To alleviate discrete (step-wise) concentration profiles, Figures 14 - 18 show the values calculated from equation (18) at each plug's midpoint radius.

Figures 14 - 16 indicate good agreement of the AFM with experiment over a wide range of Dt/dp . However, Figures 17 and 18 which show axial variations for $Dt/dp=12.8$ indicate that, at low z/dp , neither the AFM nor the Fickian analogy closely follows the observed dispersion behavior. However, the agreement is quite good at $z/dp > 25.6$ or two tube diameters. This behavior is also borne out in Table 5 which compares AFM and Fickian predictions to observed values of centerline concentrations for $5.6 < Dt/dp < 25.6$ as given by Fahien and Smith (1955). Note the improvement in both models as z/Dt increases. This can probably be attributed to entrance effects

since the tracer injection tube creates a disturbance in the flow pattern and in the packing pattern which may each take some distance to settle out. For example, in empty tubes the flow disturbance created by a barrier requires several pipe diameters to settle out (Daugherty and Franzini, 1977) as compared to an apparent "settling length" here of about two pipe diameters. This shorter distance should be expected since the packing tends to impose order on the flow pattern. Consider also that insertion of a tracer injection tube into the packing will disrupt the "normal" packing arrangement and hence the distribution of voids. Thus, the assumed plug and cell distributions may not be applicable in the vicinity of the injection tube. In fact, Marivoet et al. (1974) showed that insertion of a narrow tube along the axis of a packed bed significantly altered the flow pattern.

Given such arguments, one would expect this entrance effect to disappear if there is no physical barrier inserted into the packing. Since the simplest heat-dispersion-only experiments meet the no-barrier criterion, the corresponding AFM results should provide more insight into this entrance effect.

In all steady-state cases, the AFM results equal or surpass the Fickian predictions. These results lend support to the previously described techniques for sizing plugs (equation (15)), for determining cell length (HCP spacing) and for distributing the flows (equations (6) and (7)).

Table 5

Centerline Concentrations--Data, Fickian, and AFM

Dt/dp	z/dp	z/Dt	Centerline Concentration ^a		
			Data	AFM	Fickian
25.6	52.0	2.0	4.8	8.6	8.7
13.3	27.1	"	2.8	4.2	4.5
11.1	22.6	"	2.3	4.0	3.7
6.9	14.0	"	1.3	2.2	2.3
19.2	52.0	3.0	3.8	4.8	4.9
8.3	22.6	"	1.8	2.0	2.1
12.8	52.0	4.0	2.2	2.1	2.2
5.6	22.6	"	1.3	1.3	.95

^a-----
 All data from Fahien and Smith (1955).

Transient (F-curve) AFM and Fickian predictions using dispersion coefficients from two different sources (Levenspiel, 1962, p. 282; Wen and Fan, 1975, p. 166) are compared to data in Figures 19 and 20 (see Table 4 for system description). These figures indicate that the Alternating Flow model again surpasses the Fickian analogy, even in the case of the longer bed (Figure 19, $z/d_p=191$). In this case, the AFM might be expected to fail because of its tendency to predict plug flow behavior for the overall bed for large z/d_p and Dt/d_p as noted in the "model limitations" discussion, above.

The log of the AFM behind the data may be due to using an incorrect ϵ_{bed} in determining velocity profiles. The ϵ_{bed} value used in the AFM simulations for Figures 19 and 20 were based on the ϵ_{bed} versus Dt/d_p data given by Leva and Grummer (1947b) since neither researcher gave explicit bed porosity values. If ϵ_{bed} is actually larger than the selected values, then the scaled velocities would be proportionately faster and the entire AFM F-curve would shift left in time. The shift should become less pronounced as the number of mixes increases since increasing the exponent (axial cell number, n) or dimension (Dt/d_p or $Nrad$) of equation 11 tends to dampen any discontinuities in the velocity profile. Comparisons of Figures 19 and 20 supports this reasoning since the lag appears constant for the shorter, narrower bed (Figure 20) but approaches zero for the longer, wider bed (Figure 19). The steady-state results are more tolerant of ϵ_b errors: ϵ_b was estimated (from the data of Leva and Grummer, 1947) for some of the cases and AFM predictions still closely

followed the concentration data. This can be attributed to the fact that the number and thickness (or hydraulic radius) of radial plugs determine steady-state mixing characteristics. Recall the assumption that the radial porosity profile will oscillate with the same frequency regardless of its mean value. Thus, the effect of ϵ_b on N_{rad} is nil and on the radial plug thicknesses is minimal.

CHAPTER III HEAT DISPERSION

Consider now the heating of a gas, initially at uniform temperature, T_{in} , as it flows through a packed bed with constant wall temperature, T_{wall} (Figure 21). Heat transfers in from the wall so that radial temperature gradients will be the sharpest just inside the bed and will flatten with increasing axial position. If the bed is long enough, the fluid will eventually reach a uniform temperature of T_{wall} .

The corresponding Fickian analogy assumes that heat flows in at the wall by a film resistance and then disperses radially by conduction through a pseudo-homogeneous medium, or (in the steady-state)

$$u \frac{\partial T}{\partial z} - \lambda \frac{\partial^2 T}{\partial z^2} - \lambda \frac{1}{r} \frac{\partial}{\partial r} \left(r \frac{\partial T}{\partial r} \right) = 0 \quad (19)$$

where λ = effective thermal conductivity of the packed section ("effective" to account for void fraction), $G = \rho G / A_{tube}$ is the mass flux, ρ is the fluid density, and A_{tube} and G are defined earlier. The well-known solution of equation (19) with appropriate boundary conditions and the usual assumption of no axial dispersion is a Bessel function series (e.g., Li and Finlayson, 1977). The boundary conditions give rise to a wall film heat transfer coefficient, h_w . The parameters, h_w and λ , are either fit to experimental data or

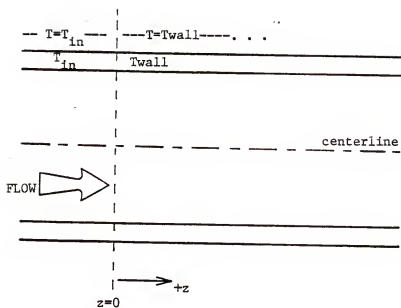


Figure 21: Simplest Heat Dispersion Experiment

obtained from available correlations giving these coefficients in dimensionless form in terms of Re_p (see Appendix G for list of references). However, experimental values of hw depend on axial position and corresponding λ depend on both axial and radial position (Bunnel et al., 1949; Calderbank and Pogorski, 1957; Coberly and Marshall, 1951; deWasch and Froment, 1972; Hall and Smith, 1949; Kunii et al., 1968; Kwong and Smith, 1957; Lerou and Froment, 1977; Li and Finlayson, 1977; Patterson and Carberry, 1983; Plautz and Johnstone, 1955) so that average or asymptotic values must be used. The literature provides many forms of correlations for both hw and λ (e.g., Carberry, 1976; Froment and Bischoff, 1979; Li and Finlayson, 1977; Schlunder, 1978). The "data effect" may cause the "correlation effect" but both may be due to several factors:

1. assumption of radially uniform velocity in equation (19)
2. assumption of radially uniform λ in equation (19)
3. misrepresentation of the Reynolds number (correlation effect only)
4. erroneous application of the Fickian analogy.

Schlunder (1978) points out that using a non-uniform velocity profile decreases the dependency of hw on tube length.

The first two points were also considered by Lerou and Froment (1977) who included a prescribed radial profile in G (i.e., velocity) and a given functional form for λ versus Re (local) in fitting point values of $\lambda(r)$ and overall values of hw to their experimental data. They reasoned that because there are both static and turbulent con-

tributions to λ it must vary radially for two reasons: the porosity profile (static contribution) and the velocity profile (turbulent contribution). To support this reasoning they fit the parameters to the model with uniform λ to the model with point values of $\lambda(r)$. In both models they obtained better fits by allowing G to vary inversely with porosity, in contrast to the observed velocity profiles which were discussed earlier. Although no direct comparison was made between data and temperature profiles predicted by the uniform and point-value models, it was implied that the latter gave better results. However, in over two thirds of the experiments listed, application of the point-value λ model increased the uncertainty in the absolute value of hw ; the relative uncertainty increased in about half of the cases.

Hence, allowing λ to vary radially can improve temperature profile predictions but may decrease the confidence with which hw can be regarded. Note also that it was necessary to employ erroneous velocity profiles to attain these results. Thus the added accuracy may be due to increasing the number of parameters (allowing λ to vary radially) and not due to better representation of the Fickian parameter.

Next, consider the correlation of λ and hw in terms of Re_p . As discussed earlier, the particle Reynolds number may not be the best descriptor of turbulence in packed beds. Some attempt has been made to use other "hydraulic" Reynolds number (Li and Finlayson, 1977), but these have remained relatively unpopular.

And next consider application of the Fickian model to dispersion in packed beds. If the model is truly applicable, then the observed spatial variations in its parameters should be justified. Because the usual practice is to neglect axial heat conduction in the Fickian analogy (equation (19)) the literature provides little information for non-stagnant effective axial thermal conductivities especially in cases where simultaneous axial and radial conduction is considered (Clement and Jorgensen, 1981; Patterson and Carberry, 1983; Wakao, 1976; Wakao et al., 1979; Yagi et al., 1960). But, under the assumption of pseudo-homogeneity implied by equation (19) a total absence of axial heat "conduction" seems unlikely. Thus, spatial variations in radial thermal conductivity may be needed to compensate for otherwise ignored driving forces in the axial direction. The radial variation of conductivity can also be justified on porosity variations since the relative ratio of solid to fluid will change accordingly. But what about the axial variation in h_w ? In empty tubes, h_w will vary from some high value in the entrance region (because of increased turbulence there) and will eventually settle out to some constant value (e.g. McCabe and Smith, 1976). Thus, length-averaged h_w 's for empty tubes depend on total tube length. Packed beds, however, have no single entrance region after which the turbulence settles out. They are, in fact, a large number of entrance regions in series since the fluid moves through repeating layers of pellets. Because each entrance region, or layer, is short

(less than one pellet diameter) one would expect h_w to be constant throughout the length of the bed.

Furthermore, as the mass dispersion chapter points out, the Fickian analogy implies random fluid motion whereas flow through packed beds is orderly. Although heat transfers by many mechanisms (conduction, turbulent and film convection, radiation) which may or may not be orderly, recall the simplicity of the heat dispersion being described. Heat transfers in from the wall at a temperature low enough to rule out radiation, through a film to a gas of low thermal conductivity. The gas moves around packing made from a material (e.g., glass or catalyst support) again of low thermal conductivity. Any heat transferred to the packing must pass through a film, and the amount of heat transferred is small. Thus, the overriding mechanism is convection--through films and by bulk fluid motion.

The acceptability criteria for a packed bed heat dispersion follow those presented earlier for mass dispersion. Heat must be conserved and travel at a finite speed, heat should disperse both radially and axially, and no backmixing should be predicted. The model should also properly represent the flow around packing, its solution should be straightforward and its corresponding parameters should be well-defined. The finite wavefront speed and no back-mixing criteria are based on physical arguments: the inherent non-homogeneity of the packed bed induces a high resistance to heat transfer by pure conduction (consider the small contact area between

pellets); heat must therefore travel near the speed of fluid flow and should not move backwards against the direction of bulk flow. As indicated in Table 1 (mass dispersion chapter), none of the currently available models meets all criteria.

The Alternating Flow Model, therefore, combines the wall and pellets film and bulk flow mechanisms with the previously established flow patterns and mixing characteristics to describe heat dispersion in packed beds. Although the mass dispersion chapter considered spherical pellets, most reaction applications involve packing of other shapes. This chapter, therefore, addresses both spherical and cylindrical pellets. The AFM heat dispersion equations are developed and additional parameters arise, some related to packing characteristics and some related to film heat transfer. Those parameters related to packing characteristics are determined a priori, whereas the film coefficients must be based on heat transfer fundamentals. Model results are compared to experiment for both spherical and cylindrical pellets.

Model Development

The Alternating Flow Model (AFM) assumes that heat disperses axially and radially by the repeated splitting and merging of streams, in a manner analogous to the simplest cases of mass dispersion. However, in the case of heat dispersion, the packing and wall can no longer be considered inert since heat transfers in from the wall and disperses radially from the bulk fluid to the packing. In the context of the AFM, then, equations describing the solid plugs must

also be considered. Note from Figure 2 that since the radial void-full pattern depends on half-cell several types of plugs must be considered:

1. main fluid plug--an annulus surrounded by different packing annuli (e.g., plugs A2, A4, B3, and B5 of Figure 2)
2. main solid plug--an annulus surrounded by different fluid annuli (e.g., plugs A3, A5, B2 and B4 of Figure 2)
3. center solid plug--completely surrounded by same fluid plug (i.e., plug A1 of Figure 2)
4. center fluid plug--completely surrounded by same solid plug (i.e., plug B1 of Figure 2)
5. wall fluid plug--tube wall on one side and solid plug on the other (e.g., plug A6 of Figure 2)
6. wall solid plug--tube wall on one side and fluid plug on the other (e.g., plug B6 of Figure 2).

The AFM assumes that no heat transfers via radiation, that no heat conducts between solid plugs, that heat convects from wall to fluid across a wall film resistance (h_w) and from wall to solid across a stagnant film, and that heat convects from fluid to packing (solid plugs) across a pellet film resistance (h_p). These assumptions, together with the underlying assumptions of plug flow through each of the void radial plugs and the mixing at plug outlets via the matrix mixing equations for mass dispersion, will be used to develop appropriate heat dispersion relationships for each type of plug. The resulting equations will then be expressed within the context of the

AFM. The integral nature of these equations, however, precludes condensation to matrix form. Throughout the development, lower case t refers to solid temperatures and upper case T to fluid temperatures.

Main Fluid Plug

Consider a heat balance on a fluid element as shown in Figure 22-a. The element gains heat due to bulk inflow and from the warmer solid above and loses heat with the bulk outflow and to the cooler solid below. Because of the low gas thermal conductivity, this model neglects radial and axial heat conduction within the fluid itself. The heat balance thus becomes

$$\rho C_p Q_j \frac{dT_j}{dz} = h_p a(j,j+1) [t_{j+1} - T_j] \quad (20)$$

$$- h_p a(j,j-1) [T_j - t_{j-1}]$$

where the coordinate z refers to distance from the plug entrance, and Q_j is the volumetric flow rate through the j th plug as defined for mass dispersion. Note that the mass flux G (equation (19)) is related to AFM parameters via:

$$G = \rho \Sigma Q_j / A_{tube} \quad (21)$$

where $j=2,4,\dots,N$ for the A-half-cell and $j=1,3,\dots,(N-1)$ for the B-half-cell. The areas $a(j,j+1)$ and $a(j,j-1)$ are the areas per unit length available for heat transfer from upper solid to fluid and from fluid to lower solid, respectively. Although Figure 2 represents these areas as a single interface, their values are not simply $2\pi r$.

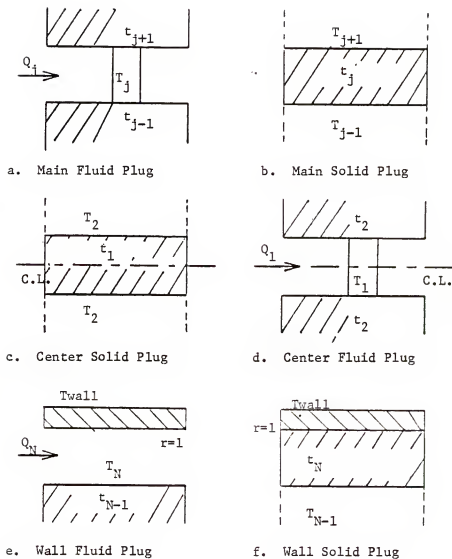


Figure 22: Plug Types for AFM Heat Dispersion Analysis

The pellet to fluid heat transfer areas are based on the total surface area available within a solid plug, i.e., the number of pellets that can fit into the solid plug volume times the surface area per pellet. It is then assumed that half of this area faces up and half down so that

$$\begin{aligned} a(j,j+1) &= 0.5\pi R_{tube}^2 (r_{j+1}^2 - r_j^2) S_p/V_p \\ a(j,j-1) &= 0.5\pi R_{tube}^2 (r_{j-1}^2 - r_{j-2}^2) S_p/V_p \end{aligned} \quad (22)$$

At first glance this may seem inconsistent within the AFM context-- that the bed can be represented by solid and void spaces whose outlines determine the flow pattern. But although the solids are considered to have definite boundaries they are porous media so that the available surface area is actually greater than the overall shape would imply. This is similar to utilization of BET surface area for porous catalysts.

Note that the effect of pellet shape on these area parameters is implied by the term S_p/V_p . For spheres, $S_p/V_p=6dp$ and for cylinders $S_p/V_p=4dp$.

Main Solid Plug

The solid element shown in Figure 22-b receives heat from the fluid above, conducts heat radially inward and then loses heat to the fluid below. This model assumes that axial temperature gradients within the solid are negligible in comparison to radial gradients. Thus, at any given z the steady-state heat balance becomes

$$t_{out} - t_{in} = R_{tube} r_{j-1} q \ln \left[\frac{r_j}{\lambda_s r_{j-1}} \right] \quad (23)$$

where q is the amount of heat transferred through the solid, and λ_s is the solid thermal conductivity. Note that q , R_{tube} , and λ_s must be in a consistent set of units (e.g., CGS, MKS, etc.). But in the steady-state, heat in equals heat out, or

$$\begin{aligned} q &= h_p a(j, j+1) [T_{j+1} - t_{out}] \\ &= h_p a(j, j-1) [t_{in} - T_{j-1}] \end{aligned} \quad (24)$$

Combining these two equations leads to

$$t_{in} = \frac{T_j + (A^* + B) T_{j-1}}{1 + A^* + B} \quad (25)$$

$$t_{out} = \frac{A^* T_{j-1} + (1 + B) T_{j+1}}{1 + A^* + B} \quad (26)$$

where

$$A^* = a(j, j-1) / a(j, j+1) \quad (27)$$

$$B = R_{tube} r_{j-1} h_p a(j, j-1) \ln \left[\frac{r_j}{\lambda_s r_{j-1}} \right] \quad (28)$$

Because the total heat transferred is small, $B \ll 1$ (see note, below) so that the solid has a flat radial profile at any given z , i.e.

$t_{out} = t_{in} = t_j$. And, since half of the solid area faces up and half

down (equation (22)) $A^*=1$ and t_j is the average of the two surrounding fluid temperatures:

$$t_j = \frac{1}{2}(T_{j+1} + T_{j-1}) \quad (29)$$

(Note: $B \ll 1$ can be justified by substituting typical values into equation (28). Suppose $r_j=0.6$, $r_{j-1}=0.5$, $r_{j-2}=0.4$ $R_{tube}=3.6\text{cm}$, $h_p=.001\text{cal/s-cm}^2\text{-K}$, and the spherical pellets, $d_p=.26\text{cm}$, are glass so that $\lambda = .0029\text{cal/s-cm-K}$.) This yields $a(j,j-1)=1.83\text{cm}$ and $B=.02$.

Center Solid Plug

The arguments here follow those for the main solid plug. But, since the solid is completely surrounded by a single fluid plug (Figure 22-c)

$$t_1 = T_2 \quad (30)$$

Note that this is analogous to the Fickian boundary condition of zero temperature gradient at the tube centerline.

Center Fluid Plug

In this case, the fluid element (Figure 22-d) gains heat from the surrounding solid and from bulk inflow and loses heat to bulk flow only (no inner solid), so that

$$\rho C_p Q_1 \frac{dT_1}{dz} = h_p a(1,2) [t_2 - T_1] \quad (31)$$

Wall Fluid Plug

Here, the fluid element (Figure 22-e) gains heat from the wall and from inflow and loses heat to outflow, so that

$$\rho C_p Q_N \frac{dT_N}{dz} = 2\pi R_{tube} h_w [T_{wall} - T_N] \quad (32)$$

$$-h_p a(N, N-1) [T_N - t_{N-1}]$$

where T_{wall} is the wall temperature (constant).

Wall Solid Plug

A solid plug in contact with the wall as shown in Figure 22-f gains heat from the wall across a stagnant film, transfers radially inward via conduction and then loses heat across a pellet film resistance to the fluid at T_{N-1} . Within the solid itself, equation (23) for the main solid plugs holds but equation (24) must be replaced by

$$q = h^* a(s, w) [T_{wall} - t_{out}] \quad (33)$$

$$= h_p a(N, N-1) [t_{in} - T_{N-1}]$$

where h^* is the stagnant wall film coefficient and $a(s, w)$ is the area available for heat transfer across the stagnant film per unit length. Combining (23) and (33) yields

$$t_{in} = \frac{T_{wall} + (A^{**} + B) T_{N-1}}{1 + A^{**} B} \quad (34)$$

where

$$B = R_{tube} r_{N-1} h_p a(N, N-1) \ln\left(\frac{1}{r_{N-1} \lambda_s}\right) \quad (35)$$

Again, because the total amount of heat transfer is small (h_p very low) $B \rightarrow 0$ so that

$$t_{in} = \frac{T_{wall} + A^{**} T_{N-1}}{1 + A^{**}} \quad (36)$$

implying that the solid temperature is some weighted average of the wall and fluid temperatures. For the cases considered in the "Comparison with Experiment" section, it was assumed that

$$t_N = 0.1 T_{wall} + 0.9 T_{N-1} \quad (37)$$

where the 0.1 and 0.9 weighting factors were found empirically to best fit the base case data. In retrospect, these weights can be justified somewhat by physical reasoning.

The moving stream below the solid plug should induce better heat transfer than the stagnant between the solid plug and the tube wall, so that $h_p > h^*$. And, the stagnant film heat transfer area $a(s,w)$ (not well-defined from system geometry) may range from $a(N,N-1)$ down to some fraction of $\pi D t$, so that $a(s,w) < a(N,N-1)$ and hence $A^{**} > 1$. Note that if $a(s,w) = a(N,N-1)$ and $h^* = (.1)h_p$ then equation (36) yields weighting factors of 0.09 and 0.91 (as opposed to the 0.1 and 0.9 of equation (37)). Thus, although h^* and $a(s,w)$ cannot be ascertained from system geometry, the empirically derived weighting given by equation (37) seems reasonable.

Condensation of Equations and Solution Techniques

Description of the complete radial profile at any given z within an A-half-cell requires equations (30), (29) with $j=3,5,\dots,N-1$, (20) with $j=2,4,\dots,N-2$ and (32). (In this section $N=N_{\text{rad}}$, or the total number of plugs in any half-cell.) Equations (29) with $j=2,4,\dots,N-2$, (37), and (20) with $j=3,5,\dots,N-1$ and (32) are required for a B-half-cell. Since the temperatures vary with z , these equation sets must be integrated from plug inlet to outlet before mixing calculations can be made. After the cells and plugs are sized according to Dt/dp and ϵ_{bed} and the flows subdivided and mixing matrices determined as outlined in the mass dispersion chapter, the temperature profile at any given axial position can be obtained in the following manner:

1. set all inlet temperatures (solid and fluid) to T_{in} .
2. within the A-half-cell, integrate equations (32) and (20) for $j=2,4,\dots,N-2$ from $z=0$ to $z=0.816dp$ (the length of one half-cell). Note that this must be done numerically as the interdependence of the equations precludes analytical results. At each integration step, obtain new solid temperatures via equations (30) and (29) for $j=3,5,\dots$. The outlet fluid temperatures (T_2, T_4, \dots, T_N) becomes the elements of the $(N/2)$ -long vector $\underline{T_A}(\text{out},n)$, where n is the current cell number.
3. calculate the next B-half-cell inlet temperatures via the previously-defined mixing matrix, R used in the mass dispersion calculations:

$$\underline{TB}(\text{in},n) = \underline{R} \underline{TA}(\text{out},n)$$

where

(38)

$$\underline{TB}(\text{in},n)^T = [T_1 T_3 \dots T_{N-1}]$$

4. integrate equations (31) and (20) for $j=3,5,\dots,N-1$ from B-half-cell inlet to outlet, calculating new solid temperatures at each integration step (equations (37) and (29) for $j=2,4,\dots,N-2$). The outlet fluid temperatures (T_1, T_3, \dots, T_{N-1}) becomes the elements of the $(N/2)$ -long vector $\underline{TB}(\text{out},n)$.
5. calculate next A-half-cell inlet temperatures via the previously defined mixing matrix, \underline{S} used in the mass dispersion calculations:

$$\underline{TA}(\text{in},n+1) = \underline{S} \underline{TB}(\text{out},n) \quad (39)$$
6. repeat steps 2-5 until the desired number of axial cells has been traversed.

Model Parameters

Of the parameters necessary for heat but not mass dispersion, $a(j,j+1)$ is defined by the AFM in terms of packing geometry (equation (22)) and $a(s,w)$ and h^* (equation (36)) are incorporated into the weighted average of equation (37). The nature of the coefficients h_p and h_w , on the other hand, prevents them from being determined solely by geometry. In fact, previous studies of flow around submerged objects (e.g. Bird et al., 1960) and in empty tubes (e.g.. McCabe and Smith, 1976) show that film coefficients must

be correlated to system variables such as pellet or tube size, total flow rate, friction factor, and fluid properties (e.g., thermal conductivity and specific heat). The AFM thus draws on this experience to obtain general correlation forms for h_p and h_w . Experimental data are needed to determine some of the coefficients.

Pellet Film Coefficient (h_p)

Forced-convection heat transfer from a single sphere in an infinite fluid moving at velocity v^* has been related by Ranz and Marshall (1952)(Bird et al., 1960, p. 409) to system parameters via

$$\frac{h_p d_p}{\lambda_{\text{fluid}}} = 2.0 + \left(\frac{C_p \mu}{\lambda_{\text{fluid}}} \right)^{1/3} \left(\frac{d_p G}{\mu} \right)^{0.5} \quad (40)$$

where λ_{fluid} = fluid thermal conductivity, $G = \rho v^*$, ρ = fluid density, C_p = fluid specific heat and μ = fluid viscosity. At high flow rate, the second term on the RHS of equation (40) will dominate, yielding, for a fluid with constant physical properties,

$$h_p = K' \left(\frac{G}{d_p} \right)^{0.5} \quad (41)$$

where K' is a constant.

For long cylinders of diameter d_p with v^* perpendicular to the axis, Bird et al. (1960, p. 408) also give a graphical correlation from Sherwood and Pigford (1952) of h_p which can be represented by

$$\frac{h_p}{G c_p} \frac{c_p \mu}{\lambda_{\text{fluid}}}^{2/3} = 0.42 \frac{G}{\mu}^{-0.46} \frac{dp}{dp}$$

which yields, for a fluid with constant physical properties

$$h_p = K'' \frac{G^{0.54}}{dp^{0.46}} \approx K'' \frac{G}{dp}^{0.5}$$

where K'' is a constant, not necessarily equal to K' . Note that the interstitial value of G should be used for packed beds to account for the effect of overall bed voidage on velocity.

According to these relationships, then, h_p should vary as $(G/dp)^{0.5}$ whether the pellets are spherical or cylindrical. Schlunder (1978) also notes that the single-pellet dependence of Nu ($Nu = h_p dp / \lambda_{\text{fluid}}$) on the square root of Re_p should hold for packed beds if it is enhanced to account for the extra turbulence. The use of a single h_p correlation form simplifies use of the AFM. However, pellet shape will influence the relative magnitude K'/K'' as follows. Consider the random packing of cylinders versus spheres into a tube. Because spheres have no "corners" the fluid moves around hydraulically smooth surfaces. But, depending on their orientation, cylinders may offer surfaces of smoothness similar to spheres (v^* perpendicular to pellet axis) or surfaces inducing maximum turbulence (v^* parallel to pellet axis). And, at any angle in between the fluid must pass over some sort of corner. Thus, one can reason

that the increased turbulence through cylindrical (versus spherical) packing would lead to higher h_p for the same G and d_p .

Wall Coefficient (h_w)

Forced-convection heat transfer in empty tubes has been related in many forms to system parameters (e.g., Bennett and Myers, 1982; Greenkorn and Kessler, 1972; McCabe and Smith, 1976). McCabe and Smith (1976), for example, give the correlations for smooth and rough pipes shown in Table 6. Note the dependence of h_w on tube length in the first four relationships; this is probably due to the entrance effect discussed earlier. Thus, the AFM uses the fifth equation of Table 6 as a guide for a general form of correlation between h_w and other system parameters.

The relationship f versus Re and relative roughness, (δ/Dt) in pipes is well-established (e.g., Greenkorn and Kessler, 1972, p. 226). Each (δ/Dt) establishes a separate curve (with f decreasing as Re increases) which can be represented by several segments over which

$$f = K_f / Re^n \quad (43)$$

where K_f is a constant. For smooth pipes, n is essentially constant, whereas for rough pipes n is maximum at low Re and equal to zero at "complete turbulence." The Re above which $n=0$ decreases as (δ/Dt) increases. The value of n also decreases as (δ/Dt) increases. Since trends in h_w are desired, equation (43) can be combined with the fifth relationship of Table 6 to give (for $\phi(f)=1$)

Table 6
Correlations for Forced Convection in Empty Tubes

1. Laminar flow ($G D_t / \mu = \text{Re} < 2100$)

$$\frac{h w D_t}{\lambda} = K_L \left(\frac{G C_p}{D_t \lambda L} \right)^{1/3}$$

where K_L is a constant and L is tube length

2. Transition flow ($2100 < \text{Re} < 10000$)

$$\frac{h w}{C_p G} = K_{tr} \left(\frac{D_t}{L} \right)^{1/3} \left(\frac{D_t G}{\mu} \right)^{-2/3} \left(\frac{C_p \mu}{\lambda} \right)^{-2/3}$$

where K_{tr} is a constant, L is tube length

3. Turbulent flow ($\text{Re} > 10000$)

$$\frac{h w}{C_p G} = \frac{K_{tu} \left(\frac{C_p \mu}{\lambda} \right)^{-2/3} \left(1 + \frac{D_t}{L} \right)^{0.7}}{\left(\frac{D_t G}{\mu} \right)^{0.2}}$$

where K_{tu} is a constant and L is tube length

4. Smooth Pipes ($\text{Re} > 50000$)

$$\frac{h w}{C_p G} = K_s \left(\frac{C_p \mu}{\lambda} \right)^{-2/3} f$$

5. Any Re

$$\frac{h w}{C_p G} = \frac{f}{\phi(f)}$$

where f is the friction factor and $\phi(f)$ is some function of f .

$$hw = K_{fc} G Re^{-n} \quad (44)$$

Hence, for a fluid with constant physical properties

$$hw = \frac{K_w G^{1-n}}{Dt^n} = \frac{K_w G^m}{Dt^n} \quad (45)$$

Note that interstitial values of G should be used here to account for the effect of overall bed voidage on velocity. The following trends should be expected in fitting hw to data via equation (45):

1. constant m for smooth pipes over a wide range of flow rates-- m should be higher for rough tubes than for smooth ones, all else being equal;
2. increasing m as G increases--if the range of flow rates is large enough, several different m -values may be needed;
3. increasing m as Dt decreases--that n decreases as (δ/Dt) increases implies n is directly proportional to Dt for a given material with constant δ ; hence, $m=1-n$ is inversely proportional to Dt .

Other Parameters Influenced by Pellet Shape

To solve the AFM equations, the cells and plugs must be sized according to Dt , dp and ϵ_{bed} so that the flow rates and mixing matrices can be determined. The mass dispersion cases established these parameters for spherical packing, where radial and axial porosity profiles showed oscillations about ϵ_{bed} with cycle widths of 0.816 dp . But, one may question whether similar patterns would occur with cylindrical pellets.

The bed porosity, ϵ_{bed} , for cylindrical packing is lower than that for spherical packing of the same D_t/d_p , if d_p for each pellet is taken to be that of a sphere which would occupy the same volume (Leva and Grummer, 1947b; Roblee et al., 1958; Schwartz and Smith, 1953). This implies that because of their irregular shape, more cylinders can pack within a given boundary. And, cylinders are asymmetric, so they can assume any number of orientations upon being poured into a tube. Roblee et al. (1958) report radial porosity profiles for beds packed with cylinders. The profiles indeed show oscillation about the lower ϵ_{bed} . However, no definite conclusions regarding the actual cycle width can be drawn from their work since they present profiles for only one D_t/d_p . The reported data represent segments, or disks, one pellet diameter long. Because of the expected axial oscillations in porosity, one pellet diameter is too short to represent average bed values and too long to yield axial cycle widths. Indeed, the data show two distinct profiles, each with a different period of oscillation.

Schwartz and Smith (1953) also give radial porosity profiles, but the radial increments over which measurements were taken are too wide to reveal oscillatory behavior. These authors also present radial velocity profiles for cylindrical packing which should at least hint at the radial oscillations in porosity. However, as discussed earlier, the measurements were made at only five radial positions in the empty tube some distance beyond the packed section and may not be truly representative of the packed bed itself. And,

Lerou and Froment (1977) showed that velocity measurements could be distorted simply by rearranging the last layer of pellets.

Consider again the orientation of cylindrical pellets into a tube. If it is assumed that the perpendicular (pellet axis at right angle to flow direction) and parallel (pellet axis parallel to flow direction) orientations are equally probable, then the fluid can encounter a barrier of width d or l with equal probability. Thus, the AFM uses the geometric mean

$$dp = \left(\frac{d^2 + l^2}{2} \right)^{0.5} \quad (46)$$

as the effective pellet diameter. Calculating dp in this way assures that if $d=l$, $dp=d$ whereas the equivalent volume argument leads to

$$dp = (1.5)^{0.33} d$$

regardless of the aspect ratio d/l . The relationships presented for spherical pellets then use of the dp of equation (46) (and the corresponding Dt/dp) together with the lower ϵ_{bed} to determine axial cell length and radial plug width as presented for the mass dispersion cases. The individual flows and weighting matrices follow accordingly. (Note that if ϵ_{bed} is not measured but instead determined from the data of Leva and Grummer 1947b $dp=d/4$ should be used to calculate Dt/dp in using their graphs--but not in AFM equations--since that is the manner in which their data are presented.)

Determination of Film Coefficients

The previous section established that h_p should be proportional to the square root of (G/d_p) (equation (41)) with h_p for cylindrical pellets excess h_p for spherical pellets under equal conditions. This in turn implies that if h_p is known at one G/d_p or "base case" for a given packing (e.g., smooth spheres, rough spheres, smooth cylinders, etc.) the h_p at any other G/d_p combination can be determined from

$$h_p = h_{p_{\text{base}}} \left[\frac{G_{\text{int}}}{G_{\text{int, base}}} \frac{d_{p, \text{base}}}{d_p} \right]^{0.5} \quad (48)$$

where

$$G_{\text{int}} = \frac{\rho Q}{\epsilon_{\text{bed}} A_{\text{tube}}}$$

It was also established that h_w should vary as G^m where m depends on system variables such as tube diameter, pipe material and degree of turbulence (i.e., range of G). Since turbulence in packed beds cannot be readily defined (refer to earlier discussions of particle- and hydraulic-Re in the mass dispersion chapter), the value of m cannot be specified a priori but must be fit to data for a given set of system variables (D_t , pipe material) over the desired range of flow rates. While this may at first seem dissatisfying, note that since h_p is predetermined according to a base case, h_w remains the sole parameter to be correlated. The power-law expression for h_w (equation 45))

is simple to work with. Also recall that no single correlation for h_w exists even for forced-convection in empty tubes due to the complex nature of turbulence. (This may also be the reason that so many correlations exist for the h_w used in conjunction with the Fickian analogy.)

To adequately fit these parameters several types of data are desired:

1. bulk-average outlet fluid temperature, T_b , out--to indicate the total amount of heat transferred,
2. radial temperature profiles--to indicate radial dispersion of heat; temperature at one radial position other than wall (e.g., tube centerline) should suffice if used in conjunction with T_b , out,
3. axial temperature profiles--to support the argument that h_w should be constant for packed beds since the turbulence never dies out.

These data types are listed in order of preference. That is, T_b , out is the most preferred because its measurement is accurate and straightforward. And, since the AFM will most likely be unable to attain a "perfect fit," radial temperature profiles cannot be used without knowledge of the flow distribution at the measurement point to determine T_b , out. Most of the flow within a packed bed channels towards the tube wall so that fluid temperatures closest to the wall should be weighted most heavily. But if the temperature profiles are measured in the empty tube some distance beyond the packed section judgment must be used in weighting the individual radial temperatures to determine

Tb, out. (Recall from earlier discussion that the radial distribution of flow rate changes as the fluid exits the packing.) And, axial temperature gradients at a single radial position alone provide too little information to correlate hw.

To correlate hp and hw for the AFM a base case must first be chosen. The system should contain the fewest possible unknowns. It should have spherical packing to eliminate uncertainties regarding flow and porosity profiles and pellet shape. The pellets should be smooth to eliminate uncertainties regarding surface roughness. The tube should be made of a smooth material so that the exponent m (equation 45)) will be constant over a large range of flow rates. Within this system, a single experiment is designated as base case for which hp and hw are determined by trial and error to give the best Tb, out and radial and axial temperature profiles. This value of hp is used as hp, base in equation (48) and the corresponding flow rate, bed porosity and pellet size yield Gint, base and dp, base.

After the base case has been established, the functional forms of equations (48) and (45) can be verified by changing dp and G. Note that changes in Dt/dp may effect ϵ_{bed} which must then be incorporated in the value of Gint. The coefficient hp is predetermined by equation (48) but hw must be best-fit to each new experiment.

If the tube is hydraulically smooth (e.g., glass or brass, Bennett and Myers, 1982) one can verify the heat transfer/friction factor analogy implied in equation (45) by comparing the value of m predicted for empty tubes to that needed by the AFM in equation (45). For smooth

empty tubes, m should be constant over a wide range of Re (flow rates) (see, for example, Greenkorn and Kessler, 1972, pg. 226). Curve-fitting the empty tube value of f at $Re=60,000$ and $250,000$ leads to

$$4f = 0.184 Re^{-.202}$$

(These values of Re have no significance other than convenience in reading the $f-Re$ graph.) Thus, $n=0.2$ and $m=0.8$ (equation (45)) so that

$$hw = hw_{base} \left(\frac{G_{int}}{G_{int, base}} \right)^{0.8} \quad (49)$$

should hold for smooth tubes. Stretching the analogy further would imply that experiments carried out in rough tubes should lead to $m>0.8$.

The hypothesis that pellet shape would effect the magnitude, but not functional form of hp can be tested by letting

$$\begin{aligned} hp &= \gamma hp, \text{ sphere} \\ &= \gamma hp, \text{ base} \left(\frac{G_{int}}{G_{int, base}} \frac{dp, \text{ base}}{dp} \right)^{0.5} \end{aligned} \quad (50)$$

where γ is a constant that accounts for enhanced heat transfer due to increased turbulence from non-smooth or asymmetric pellets. For cylindrical pellets, then, a new base case must be selected and the coefficients hp and hw again fit by trial and error. The constant γ can then be back-calculated from equation (50). For the hypothesis

to be valid, γ should exceed one but should remain constant for all systems employing cylindrical pellets.

Comparison with Experimental Data

This section presents AFM heat dispersion results for beds packed with uniformly sized spherical or cylindrical pellets. Model parameters are related to the framework within which they were developed--submerged object form for h_p (equations (48) and (50)) and friction factor analogy for h_w (equation (45)). In general, AFM results are not compared to the Fickian analogy because the large number of correlations available for pertinent parameters (as discussed at the beginning of this chapter) would yield a wide range of solutions to equation (19). However, where appropriate, comparisons with back-fit Fickian model may be made.

It should be noted in reading this section that the AFM uses interstitial mass fluxes, G_{int} , to account for the effect of overall bed voidage on velocity. Any G 's attributed to other researchers represent superficial values.

Yagi and Wakao (1959) give both centerline and bulk-average outlet temperatures for their experiments in a (smooth) brass tube packed with smooth, uniformly sized glass pellets. They used one tube size with two different pellet sizes over a range of particle-Reynolds numbers $100 < Re_p < 700$. For their "F-1" run ($G=2740 \text{ kg/hr-m}^2$, $D_t=3.6\text{cm}$, $d_p=.6 \text{ cm}$) they also give the axial variation in centerline temperature. This was therefore selected as the base system with run F-1 as the base case.

Figure 23 compares AFM results ($h_p, \text{base} = .002 \text{ cal/s-cm}^2\text{-K}$, $h_w, \text{base} = .002 \text{ cal/s-cm}^2\text{-K}$) and best-fit Fickian profile and T_b , out to data for the base case. Table 7 compares AFM and best-fit Fickian results to outlet centerline and bulk-average temperature data for all other "E" ($dp=0.26\text{cm}$) and "F" ($dp=0.6$) runs with h_p determined from equation (48) and h_w from equation (49), i.e. equation (45) with $m=0.8$. In predicting bulk outlet values, the AFM surpasses the Fickian analogy in all but three of the cases (in two of these, it differs from the Fickian back-fit by only 0.2°C). In predicting outlet centerline temperatures, the AFM again surpasses the Fickian back-fit in all but three cases (in two of these, the AFM prediction of the corresponding T_b , out is within 0.2°C of the Fickian back-fit). The worst AFM fit is for the centerline temperature of the $Re_p=106$ case. But, recall from earlier discussion that the relationship given by equation (48) is a simplified version of equation (40); it presumes that flow rate is high enough to dominate the RHS of equation (40). If the flow rate, or Re_p , is low, the constant term may begin to assert itself, i.e., the h_p based on the complete version (equation (40)) would be larger than h_p determined from the simpler version (equation (48)) (For example, the AFM can better fit the data with the same h_w and higher h_p --at 1.2 times the value used in Table 7 -- to give: (1) centerline temperature of 63.4°C (AFM) versus 65.3°C (data); and (2) T_b , out of 78.8°C (AFM) versus 77.3°C (data).) Further, Table 7 notes that the AFM must distribute the flow according to the laminar/transition, rather than turbulent, hydraulic resistances. The mass dis-

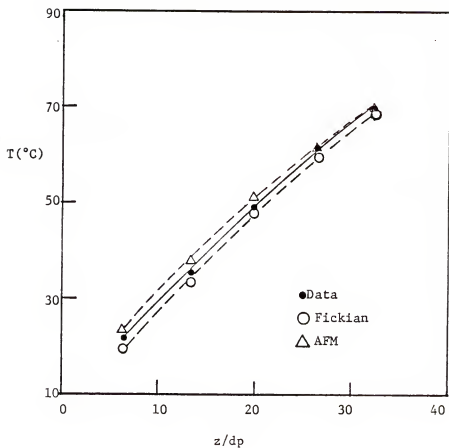


Figure 23: Axial Temperature Profiles for $Re = 234$, $Dt/dp = 6.0$, Data of Yagi and Wakao^P(1959)

Table 7

AFM for Heat Dispersion in Smooth Brass Tube Packed With Glass Spheres

d_p (cm)	Re_p	Item (at exit)	Data	AFM ^a	Fickian ^b
0.6	234	t_c	69.8	69.9	68.5
		T_b	78.8	78.1	77.9
0.6	382	t_c	63.6	62.3	62.1
		T_b	74.8	71.7	73.8
0.6	691	t_c	56.1	57.8	54.1
		T_b	69.2	67.9	67.7
0.26	106 ^c	t_c	65.3	60.2	64.0
		T_b	77.3	77.8	76.4
0.26	183	t_c	51.3	49.4	50.1
		T_b	69.7	70.4	69.0
0.26	238	t_c	52.1	48.8	49.7
		T_b	68.1	69.9	66.5
0.26	323	t_c	50.1	48.2	47.9
		T_b	67.1	69.3	65.5

-
- AFM predictive; used $\epsilon_{bed} \sim 0.40$ in all calculations
 - Fickian back-fit; parameters specified in Table 8
 - AFM used laminar/transition hydraulic resistances to radially distribute flows.

All data from Yagi and Wakao (1959); air at inlet near $T_{in}=20^\circ\text{C}$; $T_{wall}=100^\circ\text{C}$, $Dt=3.6\text{cm}$ in all cases.

Table 8

Fickian Parameters for Table 7 Experiments of Yagi and Wakao (1959)

(cm)	Re_p	$(1000hw)(\text{cal/s-cm}^2\text{-K})$		$(1000\lambda_{e,r})/(\text{cal/s-cm-K})$	
		back-fit ^a	correlated ^b	back-fit	correlated ^b
0.6	234	1.81	1.65	1.52	1.53
0.6	382	2.52	2.44	2.00	2.22
0.6	691	3.61	3.92	3.04	3.68
0.26	106	2.02	2.02	1.25	1.03
0.26	183	2.85	3.13	1.41	1.48
0.26	238	2.88	3.86	1.93	1.79
0.26	323	3.66	4.93	2.35	2.29

a. Back-fit by Yagi and Wakao (1959); assume $K_{\text{air}} \sim 70 \times 10^{-6} \frac{\text{cal}}{\text{s-cm-K}}$

b. From correlation given by Yagi and Wakao (1959); $\text{Pr}_{\text{air}} = 0.75$
 The correlation for $\lambda_{e,r}$ (Their equations 4 and 5) suggests $(\alpha\beta)_{\text{H}} = 0.09$ for $\text{Cp} = 0.6$ and 0.11 for $\text{dp} = 0.26$

persion chapter states that this is necessary at $Re_p < 150$, implying that Re_p --while not the sole parameter dictating packed bed turbulence--must give some indication as to flow regime. It is therefore possible that at this low $Re_p = 106$ the hw exponent m (equation 45)) may not be 0.8. Even for smooth pipes, the f - Re curve has distinct regions for laminar and turbulent flow. For this reason and because only one heat dispersion data set was available at $Re_p < 150$, the h_p values were not fit to the complete form (equation (40)).

According to these arguments, then, the use of equation (48) to determine h_p is justified. And the fact that $m=0.8$ for hw correlates the data so well justifies not only the form of hw given by equation (45) but also the friction factor analogy. Recall from the previous section that $m=0.8$ was predicted solely from arguments relating heat to friction factors in empty tubes (equation (49)). It should be noted that Yagi and Wakao also found hw to vary as $G^{0.8}$ in correlating the Fickian analogy to their experiments.)

Other systems for which the literature provides the actual temperature data needed to correlate AFM parameters are summarized in Table 9. This table excludes any systems containing pellets of high thermal conductivity (e.g., Baumeister and Bennett, 1958; Colburn, 1931; Kwong and Smith, 1957) since the AFM presumes no conduction between pellets, and it excludes any systems of highly irregular geometry, i.e., annular or other non-circular tubes (e.g., Wakao and Kato, 1969; Yagi and Kunii, 1960) or packing made up of anything but uniformly

Table 9 Available Temperature Data

Source	shape ^a	Pellet ^b		Tube	Re _p range
		dp	material	Dt material	
Yagi and Wakao (1959) ^{c,d}	s	0.26cm -0.6cm	glass	3.6cm brass	100 -1.700
Leva (1947) ^{c,d}	s	0.172cm - .388cm	glass	2cm and $\frac{1}{4}$ cm standard	2 -850
Leva and Grummer (1948) ^{d,e}	s,c	varied	glass and rough	2cm and 3/4cm standard	n.a. ^j
Plautz and Johnstone (1955) ^f	s	1.82cm	glass	20.6cm ?	n.a. ^j
Bunnell et al. (1949) ^{f,g}	c	1/8cm	alumina	2cm ?	n.a. ^j
Hall and Smith (1949) ^{f,g}	c	1/8cm	alumina	2cm ?	n.a. ^j
Calderbank and Pogorski (1957) ^h	c,s	1/8cm -1/2cm	various	4cm ?	n.a. ^j

Table 9--continued

Source	Pellet		Tube	Re _p range
	shape ^a	dp ^b material	Dt material	
Lerou and Froment (1977) ^{d,i}	c	0.95cm V ₂ O ₅ catalyst	9.9cm ?	120-500
deWash and Froment (1972) ⁱ	c	0.57cm "	15.75cm ?	n.a. ^j
Schortz and Bischoff (1969) ^{h,i}	s	0.3cm stoneware	4cm ?	n.a. ^j
Coberly and Marshall (1951) ^d	c	3/8cm x 1/2cm celite	5cm ?	360-1300

a. s=spherical; c=cylindrical

b. If cylindrical, see individual reference for definition of dp

c. other shapes and materials; centerline profile for one run; centerline and T_b at outlet for all other runs.

d. authors also studied other Re_p and/or pellets of other shapes, sizes, or materials but these additional data not used, for comparison here.

e. beds packed with mixtures of pellet sizes; thus, data not compared herein because of uncertainty in bed porosity characteristics.

Table 9-continued

- f. non-uniform inlet temperature profile (radial) which was not clearly specified; not enough data to back-out full $T_{in}(r)$ description;
- g. screens located at several axial positions to guide thermowells; thermowells inserted through entire bed length at several radial positions; natural packing pattern disturbed and porosity profiles $\varepsilon(r,z)$ unknown;
- h. unclear which systems correspond to data presented;
- i. temperatures measured more than 1dp beyond packed section
- j. not applicable; data not used for comparison.

sized spheres or cylinders (e.g., Leva and Grummer, 1948). Some systems of the desired geometry were also rejected for purposes of AFM correlation for other experiment-related reasons as noted in Table 8.

Whereas Yagi and Wakao (1959) used smooth brass tubing, the other researchers listed in Table 8 used "standard" pipe, which is probably rougher than brass (e.g., Bennett and Myers, 1982). Thus, these systems should yield higher m values in the hw correlation and may exhibit several flow rate regimes over which m can be considered constant. Only Tb , out data are available for the spherical systems (other than Yagi and Wakao, 1959), as noted in Table 8. While Tb , out provides sufficient information with which to correlate hw (recall discussion in previous section) the absence of radial or axial temperature profiles prevents double-checking the goodness of fit. But, the form of equation (45) implies that a log-log plot of hw versus G should provide a straight line of slope m . The degree of scattering over small segments of G should indicate the adequacy of the correlation. A distinct change in slope at high or low G would indicate that the system has moved from one f -versus- Re regime to another.

Such log-log plots of AFM hw versus flow rate for smooth glass spherical packing in standard pipe (Leva 1947a) are shown in Figure 24 for the smaller tube ($Dt=1.58\text{cm}$, $Dt/dp=4.95$, runs 100a-e) and in Figure 25 for the larger tube ($Dt=5.26\text{cm}$, $Dt/dp=5.33$, runs 9a-h). Each plot shows a definite straight line segment with the expected change in slope (m not constant for all G in rough tubes) and with essentially no scatter in the constant slope segment. The values of $m=1.0$ for the

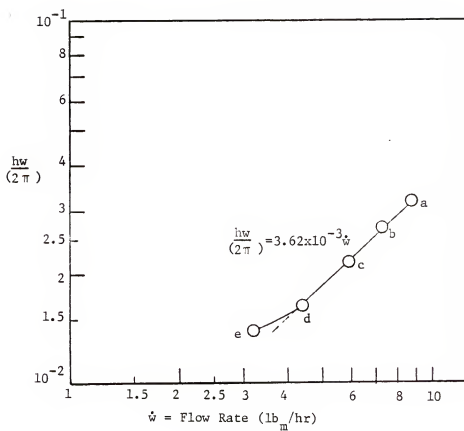


Figure 24: AFM Wall Film Coefficients for Data of Leva (1947b), Runs 100a-e, $D_t/d_p=4.95$, $D_t=1.6\text{cm}$

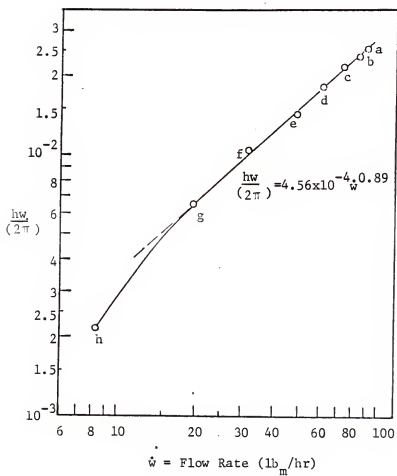


Figure 25: AFM Wall Film Coefficients for Data of
Leva (1947b), Runs 9a-h, $D_t/d_p=5.33$, $D_t=5.3\text{cm}$

tube and $m=0.89$ for the larger tube are consistent with the friction factor analogy discussed earlier: for tubes of the same material, m should be inversely proportional to Dt .

The available literature data for cylindrical pellets provide only radial temperature profiles (albeit at several bed depths for Coberly and Marshall, 1951) without corresponding T_b , out values. Fitting h_w to data of this type presents some difficulty as the distance between temperature measurement point and bed exit increases. Unless the temperatures are actually measured inside the packed section, the difficulty in fitting h_w would also increase as the bed length increases. Consider the following arguments.

As the fluid exits the packed section it mixes radially as it expands from the packing interstices into the empty tube. As the fluid moves further into the empty section, its flow tends to redistribute from the maximum-near-wall profile characteristic of packed beds to the maximum-near-wall profile characteristic of empty tubes. Thus, at the bed exit, mixing occurs because of bulk fluid motion in the radial direction. This bulk mixing should in turn effect the temperature profile as the hotter fluid near the wall mixes with the cooler fluid near the centerline. This effect would be most dramatic when temperature profiles just inside the bed exit are the sharpest, i.e. for short beds. This exit effect may also cause difficulty in determining h_p since it is the AFM's instigator of radial temperature gradients.

Furthermore, Lerou and Froment (1977) and deWasch and Froment (1972) observed "humps" in their measured radial temperature profiles. These humps were most pronounced for short beds and tended to disappear as bed length was increased. That these humps may be results of the measurement exit effect is further supported by the ability of deWasch and Froment to find a point for temperature measurement beyond the packed section after which the humps disappeared.

Coberly and Marshall (1951) ran their experiments with the thermowells "...nearly touching the packing." They also measured radial profiles at several bed depths, keeping all other system variables constant. Thus, if h_w and h_p are fit to their data at maximum bed depth, the corresponding AFM predicted axial-radial temperature profiles can be compared to data to provide added insight into the goodness of fit. These researchers studied several system geometries, but the system of $3/8" \times 1/2"$ cylinders packed in a 5" tube was selected for AFM comparison since it provided the smallest D_t/d_p . The geometric mean d_p (equation (46)) for cylinders of this aspect ratio is 0.44" so that $D_t/d_p=11.3$.

Figure 26 shows the log-log plot of AFM h_w versus flow rate for this system and Figure 27 compares the corresponding AFM axial temperature profiles (at several radial positions) to experimental data. In Figure 26 note the constant slope segment breaking off at low flow rates, in accordance with the friction factor analogy. The high value of $m=2$ cannot, however, be explained within that framework. Note from

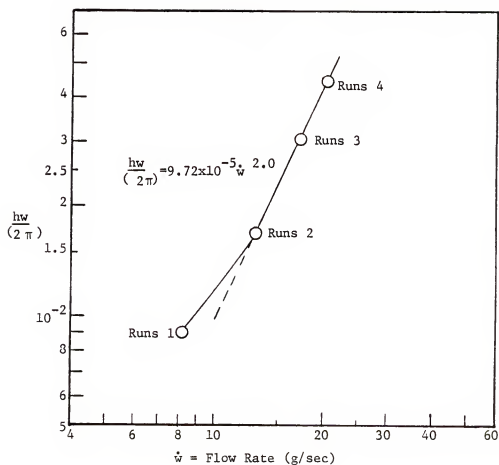


Figure 26: AFM Wall Film Coefficients for Data of Coberly and Marshall (1951), 3/8"x1/2" Cylindrical Pellets

Figure 27 how closely AFM results follow the axial temperature profiles. The largest deviations are at small r near $z=0$. But, as indicated on the Figure, the flow rates at these inner radii are small proportions of the total stream. Thus, those points with the largest absolute error in temperature will have the smallest relative contribution to the overall system. This factor becomes especially important in extending the AFM to include catalytic reactions.

In fitting h_p and h_w to temperature profiles for all four flow rates (at maximum bed depths, i.e., sequence number six in each run set) some judgment was needed in weighting the temperatures closest to the wall more heavily than others, as discussed in the previous section. Thus h_w was fit for each case by trial and error BEFORE any plots were made to avoid bias towards the functional form of equation (45).

The constant, γ used to determine h_p via equation (50) was determined from run 1-6 to be 1.33. This value of $\gamma > 1$ is consistent with the idea that cylindrical pellets increase turbulence and enhance heat transfer over what would be expected for spherical pellets.

Figure 28 shows the log-log plot of AFM h_w versus flow rate for the data of Lerou and Froment (1977) ($D_t=9.9\text{cm}$, cylindrical pellets with $d=l=d_p=0.95\text{cm}$, bed length= 48.8cm). This plot also shows consistency with the friction factor analogy as the constant slope of $m=0.66$ at low flow rate. The magnitude of $m < 0.8$ cannot, however, be explained within the framework of the friction factor analogy. Since neither

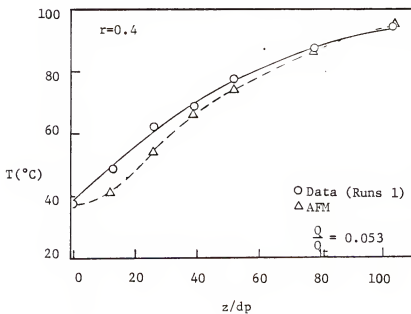
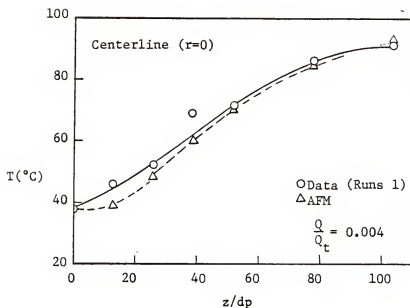


Figure 27: Axial Temperature Profiles for Data of Coberly and Marshall (1951), 3/8"x1/2" Cylindrical Pellets, at two Radial Positions

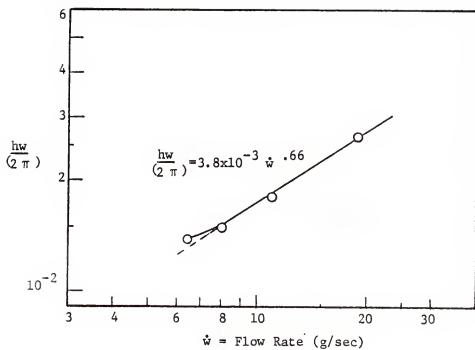


Figure 28: AFM Wall Film Coefficients for Data of Lerou and Froment

Tb, out values nor axial temperature profiles are available for these experiments, no further checking via data can be done. Here, as above, h_p was calculated from equation (50) with $\gamma=1.33$ and h_w was determined by more heavily weighting the outermost temperatures with the same precautions to avoid bias towards equation (45).

Note the slight scattering of points about the straight segment in Figure 28. The scattering may indicate deviation from the friction factor analogy or h_w . Recall, however, the effect of thermowell placement on data accuracy when Tb, out is unavailable. Although Lerou and Froment give no specific axial location of thermowells, they state that their apparatus is similar to that used by deWasch and Froment (1972). In their experiments, deWasch and Froment located their thermocouples "...slightly above the packing, at a distance of one particle diameter. From this distance onwards, the radial temperature profile was completely smooth." In light of the earlier discussion regarding humps in the radial temperature profiles, this may imply that the flow redistribution causing the exit effect may already be complete by the time the measurement is taken. Thus, the AFM may have been fit to a temperature profile that is flatter than the one just before the end of the packed section. A flatter-than-actual profile would imply that the fluid had extra "time" to gain heat, i.e., that the effective flow rate was lower than actual. This may explain the low value of $m=0.66$ obtained for these experiments. For this reason, the AFM was not fit to the data of deWasch and Froment (1972).

Summary of AFM for Heat Dispersion

The Alternating Flow model presumes that heat disperses radially in packed beds through a film resistance at the tube wall and then through a series of pellet film resistances and that heat disperses axially as the fluid repeatedly splits and merges as it traverses many pellet layers. The AFM focuses on fundamental system parameters such as turbulence, pellet size and shape and tube characteristics. Of those AFM parameters needed for heat but not mass dispersion, only one, h_w , must be back-fit for each new set of tube-related variables (e.g., tube material and diameter). This back-fitting is necessary because of the complex nature of forced-convection film heat transfer. The wall coefficient, h_w , follows a friction factor analogy well, giving some insight as to how, in general, it will depend on other system variables. The friction factor/heat transfer analogy gained credibility as h_w versus flow rate correlations took on the expected form. (Indeed, for the case of smooth tube material, the exponent n of equation (45) could be predicted solely from empty tube arguments.) The pellet heat transfer areas are determined from packing geometry (equation (22)). The pellet film coefficient, h_p , correlated well to system variables via equation (48). This supports the presupposition that h_p for pellets would correlate in the same general form as h_p for a single pellet submerged in an infinite fluid.

In addition, the AFM gave good results for both cylindrical and spherical pellets. This justifies the correlation of h_p by equation (50) (with $\gamma=1$ for spheres and 1.33 for cylinders). The good fit of

AFM to data for cylindrical pellets also justifies using a geometric mean pellet diameter (equation (46)) and the lower ϵ_{bed} expected for cylindrical packing in the porosity relationships for spherical packing. These relationships in turn determine flow distribution and mixing characteristics.

CHAPTER IV REACTION

Previous chapters demonstrated the applicability of the Alternating Flow model to simple cases of heat and mass dispersion in packed beds. This chapter, therefore, extends the AFM to include catalytic reaction within the packing material. AFM equations for both adiabatic and wall-cooled reactors are developed and applied to example problems so that general AFM trends can be demonstrated. First-order intrinsic kinetics in the diffusion-limited regime are used. Unlike previous chapters, however, no comparison to actual data is made here. The intent of this chapter is to point out differences between the AFM and the Fickian analogy, thus laying the foundation for future work.

Model Development

The AFM views cases involving catalytic reaction as a combination of mass and heat dispersion steps. As the fluid moves through each radial plug, its reactant concentration decreases because of reaction to the surrounding solid plugs and its temperature increases due transfer of heat of reaction across a film from the solids. In general, the AFM obtains fluid concentrations and temperatures from the plug flow equation for each fluid plug and obtains solid temperatures from steady-state pellet heat balances. The AFM uses heat and mass

dispersion parameters developed in previous chapters and any required reaction-diffusion parameters (e.g., intrinsic kinetics and effective pellet diffusivity). In addition, the AFM also employs the assumptions customarily applied to reaction-diffusion problems (e.g., Lee, 1985; Carberry, 1976; Froment and Bischoff, 1979):

1. dominating external heat transfer resistance--isothermal pellet with all of the temperature drop across the external film,
2. negligible external mass transfer resistance--concentration at pellet surface equal to surrounding fluid concentration.

Any previously-stated AFM assumptions also carry over.

As in the heat dispersion chapter, each plug type must be treated separately:

1. main solid plug (e.g., plugs A3, A5, B2, and B4 of Figure 2)--each side subjected to a different concentration, thus a "two-sided" rate expression must be used; solid temperature obtained via steady-state film heat balance;
2. main fluid plug (e.g., plugs A2, A4, B3, and B5 of Figure 2)--surrounding solids at different temperatures, thus radial loss of reactants at two different rates; temperature rise due to heat transfer from both films;
3. center solid plug (e.g., plug A1 of Figure 2)--surrounded by single fluid annulus, so no need for "two-sided" rate expression; steady-state heat balance yields solid temperature;

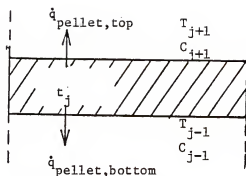
4. center fluid plug (e.g., plug B1 of Figure 2)--surrounded by single solid annulus, thus only one rate needed; temperature rise due to heat transfer from film;
5. wall solid plug (e.g., plug B6 of Figure 2)--wall on one side and fluid on the other implies rate into fluid and no reaction at the wall; in wall-cooled reactor, heat transfer at wall requires inclusion of stagnant film wall coefficients h^* , $a(s,w)$ of Heat Dispersion chapter); adiabatic reactor implies symmetric boundary conditions and provides an expression similar to the one for the center solid plug;
6. wall fluid plug (e.g., plug A6 of Figure 2)--rate of reaction into solid below but not to wall above; heat transfers in across a pellet film resistance (h_p) from below; and, for a wall-cooled reactor, out across a wall film resistance (h_w) as described for the simple heat dispersion case; no wall heat transfer in the adiabatic reactor.

Throughout the following development, lower case t refers to solid temperature and upper case T to fluid temperature.

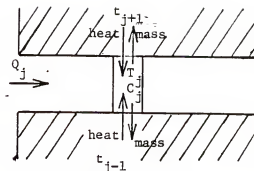
Main Solid Plug

Consider a solid plug with each face subjected to different conditions (Figure 29-a). For a catalyst with unsymmetrical concentration boundary conditions, the work of Tan and Smith (1980) for first order intrinsic kinetics

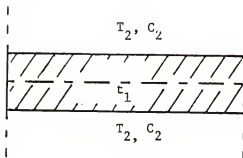
$$r_c = C k(t) = C k_o \exp(-g/t) \quad (51)$$



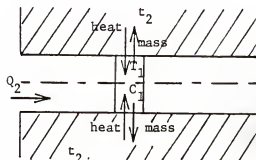
a. Main Solid Plug



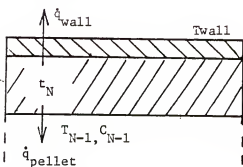
b. Main Fluid Plug



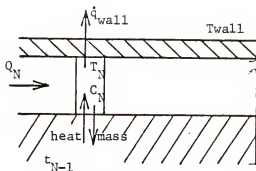
c. Center Solid Plug



d. Center Fluid Plug



e. Wall Solid Plug



f. Wall Fluid Plug

Figure 29: Plug Types for AFM Reaction Analysis

can be applied to give the molar flux, J_i , for diffusion-limited cases ($\phi > 3$, $\phi = L(k/De)^{0.5}$):

$$J_i = C_i [De k(t)]^{0.5} \quad (52)$$

where i = top or bottom, J_i is the molar flux (mol/cm^2) out the i -th face, C_i is the concentration of the key component (mol/cm^3) at the i -th face, De is the effective diffusivity of the key component in the catalyst and k is the rate constant evaluated at the pellet temperature. (Appendix H develops the rate expression for unsymmetric boundary conditions and more general intrinsic kinetics.) In the steady-state any heat generated by reaction is transferred across the pellet film resistance to give

$$\begin{aligned} & hp a(j,j-1) [t_j - T_{j-1}] + hp a(j,j+1) [t_j - T_{j+1}] \\ & = (-\Delta H) Sp [C_{j-1} + C_{j+1}] [De k(t_i)]^{0.5} \end{aligned} \quad (53)$$

where hp is the pellet film heat transfer coefficient (defined in the heat dispersion chapter), $a(j,j+1)$ and $a(j,j-1)$ are the corresponding heat transfer areas (also previously defined, equation (22)) and $(-\Delta H)$ is the heat of reaction. The heat dispersion chapter assumes that half of the pellet surface area faces up and half down (equation (22)) so that $a(j,j+1) = a(j,j-1) = Sp$. Because the fluid temperatures are "known" at any position within the half-cell (e.g., at inlet from mixing calculations or elsewhere from integration of fluid

equations) equation (53) contains only one unknown: the pellet temperature. But, the exponential form of the rate constant prevents direct solution for t , so that "trial and error" must be used. If no solution is possible, i.e., the heating curve (RHS of equation (53)) does not intersect the cooling curve (LHS of equation (53)), the reaction is unstable.

For convenience, however, the rate constant can be linearized via a Taylor series (following Lee, 1981). Rearranging equation (53) gives

$$(t_j - T^*) = X' (k_0)^{0.5} \exp(-g/2t_j) \quad (54)$$

where

$$X' = (-\Delta H) [De]^{0.5} C^* / hp$$

$$T^* = (T_{j+1} + T_{j-1}) / 2$$

$$C^* = (C_{j+1} + C_{j-1}) / 2$$

since $a(j, j+1) = a(j, j-1) = S_p$. Then, expanding the exponential in a Taylor series about T^* and dropping quadratic and higher order terms gives

$$(t_j - T^*) = X [1 + (t_j - T^*) / 2(T^*)^2] \quad (55)$$

where

$$X = X' k(T^*)$$

or

$$t = T^* + \left[\frac{1}{\frac{hp}{(-\Delta H) C^* (De k(T^*))^{0.5}} - \frac{g}{2(T^*)^2}} \right] \quad (56)$$

Instability would be indicated by a negative RHS of equation (55).

Main Fluid Plug

A fluid element as shown in Figure 29-b can be described by

$$Q_j \frac{dC_j}{dz} = -[(S_p' J)_{j+1} + (S_p' J)_{j-1}] \quad (57)$$

and

$$\begin{aligned} \rho C_p Q_j \frac{dT_j}{dz} = & h_p a(j, j+1) [t_{j+1} - T_j] \\ & + h_p a(j, j-1) [t_{j-1} - T_j] \end{aligned} \quad (58)$$

where z is the distance into the half-cell, C_j is the key component concentration in the j -th radial plug, Q_j is the flow rate through the j -th radial plug, ρ is the fluid density, and C_p is the fluid heat capacity. The area parameters and pellet film coefficients were defined in the heat dispersion chapter. From equation (52)

$$\begin{aligned} (J S_p')_{j+1} &= S_{p,j+1}' C_j [De k(t_{j+1})]^{0.5} \\ (J S_p')_{j-1} &= S_{p,j-1}' C_j [De k(t_{j-1})]^{0.5} \end{aligned} \quad (59)$$

where S_p' is the catalyst surface area available for reaction at one face of a given solid plug. These areas were defined for heat transfer in Chapter III so that

$$\begin{aligned} S_{p,j+1}' &= a(j, j+1) \\ S_{p,j-1}' &= a(j, j-1) \end{aligned} \quad (60)$$

The solid temperatures are determined via equation (56). The complexity of equations (57) and (58) requires numerical integration from plug inlet to plug outlet.

Center Solid Plug

Figure 29-c shows that the center solid plug can be treated as

a single pellet surrounded by a fluid of concentration C_2 . Thus, a symmetric effectiveness factor (e.g., Carberry, 1976) can be applied to give

$$J = C_2 [De k(t_1)]^{0.5} \quad (61)$$

A steady-state film balance leads to

$$hp(t_1 - T_2) = (-\Delta H) C_2 [De k(t_1)]^{0.5} \quad (62)$$

if it is again assumed that $a(1,2) = Sp_1$. Linearizing the exponential about T_2 yields

$$t_1 - T_2 = \left[\frac{1}{\frac{hp}{(-\Delta H) C_2 (De k(T_2))^{0.5}} - \frac{g}{2T_2^2}} \right] \quad (63)$$

Again, instability would be indicated by a negative RHS of equation (63).

Center Fluid Plug

The description of the center fluid plug (Figure 29-d) contains only one reaction term:

$$Q_1 \frac{dC_1}{dz} = -Sp_2 C_1 [De k(t_2)]^{0.5} \quad (64)$$

and

$$\rho C_p Q_1 \frac{dT_1}{dz} = hp a(1,2) [t_2 - T_1] \quad (65)$$

where, again it is assumed that $Sp_2 = a(1,2)$. Both equations (64) and (65) must be integrated numerically with t_2 evaluated at each step via equation (56).

Wall Solid Plug

A solid plug adjacent to the tube wall (Figure 29-e) of an adiabatic reactor can be treated as half of a symmetric pellet (since there is no temperature gradient at the wall). In this case, the analysis follows that for the center solid plug to give

$$t_N - T_{N-1} = \frac{1}{\frac{hp}{(-\Delta H)C_{N-1}(De k(T_{N-1}))^{0.5}} - \frac{0.5 g}{(T_{N-1})^2}} \quad (66)$$

For a wall-cooled reactor, a stagnant film heat transfer resistance at the wall must be included:

$$\begin{aligned} & (-\Delta H)S_{p,N}C_{N-1}[De k(t_N)]^{0.5} \\ & = hp a(N,N-1)[t_N - T_{N-1}] + h^* a(s,w)[t_N - T_{wall}] \end{aligned} \quad (67)$$

Dividing both sides by $[hp a(N,N-1)]$ and using equation (60) gives

$$(-\Delta H)C_{N-1}[De k(t_N)]^{0.5} = [t_N - T_{N-1}] + \alpha [t_N - T_{wall}] \quad (68)$$

where

$$\alpha = h^* a(s,w) / hp a(N,N-1) \quad (69)$$

The heat dispersion chapter showed that $h^* a(s,w) = 0.1 hp a(N,N-1)$ gave good results for the cases studied there. Thus, taking $\alpha = 0.1$ and linearizing the exponential of equation (68) about T_{N-1} gives

$$t_N = \frac{(X''Y - 1)T_{N-1} - 0.1 T_{wall} - X''}{X''Y - 1.1} \quad (70)$$

where

$$Y = g / [2 T_{N-1}^2]$$

$$X'' = (-\Delta H)C_{N-1}[De k(T_{N-1})]^{0.5} / hp$$

Here, instability should be suspected if calculations lead to $t_N < t_{N-1}$ or to $t_N < T_{wall}$. (If T_{wall} is low enough, cooling may cause t_N to be lower than T_{N-1} .)

Wall Fluid Plug

A fluid plug adjacent to the tube wall (Figure 29-f) of an adiabatic reactor is analogous to the center fluid plug. Thus

$$Q_N \frac{dC_N}{dz} = - a(N, N-1) C_N [De k(t_{N-1})]^{0.5} \quad (71)$$

$$\rho C_p Q_N \frac{dT_N}{dz} = hp a(N, N-1) [t_{N-1} - T_N] \quad (72)$$

where the solid temperature is obtained via equation (56) at each numerical integration step.

In a wall-cooled reactor, equation (72) must also include a wall film heat transfer resistance:

$$\begin{aligned} \rho C_p Q_N \frac{dT_N}{dz} = & hp a(N, N-1) [t_{N-1} - T_N] \\ & - hw \pi Dt [T_N - T_{wall}] \end{aligned} \quad (73)$$

The solid temperature is again obtained via equation (56).

Condensation of Equations and Solution Technique

The solution technique here is analogous to the procedure outlined earlier for heat dispersion. Description of the complete concentration and temperature profiles at any given z within an A-half-cell requires solid plug equations (56) ($j=3,5,\dots,N-1$) and (63), fluid plug equations (57) and (58) ($j=2,4,\dots,N-2$), (71) and (72) for adiabatic reactors or (73) for wall-cooled reactors. (In this section, $N=N_{rad}$, or the total number of plugs in any half-cell.) Solid plug equations (56) ($j=2,4,\dots,N-2$), and (66) for adiabatic reactors or (70) for wall-cooled reactors, fluid plug equations (57) and (58) ($j=3,4,\dots,N-1$), (64), and (65) are required for a B-half-cell. Since both temperature and concentration vary with z , each fluid plug equation must be integrated numerically from plug inlet to outlet, with solid temperatures calculated at each step. Only then can mixing calculations be made. The cells and plugs must be sized and the flows subdivided according to ϵ_{bed} and Dt/dp as outlined in the mass dispersion chapter. The heat transfer areas and film coefficients, h_p and h_w , must be determined as outlined in the heat

dispersion chapter. Then, given all necessary kinetic (rate) data (e.g., rate constant, heat of reaction, effective pellet diffusivity), the radial profiles can be obtained via the procedure below. (The following outlines a wall-cooled reactor; for an adiabatic reactor, substitute equation (66) for (70) and (72) for (73).)

1. set all inlet temperatures (solid and fluid) to T_{in} and all inlet concentrations to C_{in} ;
2. within the A-half-cell, numerically integrate equations (57) and (58) ($j=2,4,\dots,N-2$), (71) and (73). At each integration step, obtain new solid temperatures via equations (56) ($j=3,5,\dots,N-1$) and (63). The outlet fluid temperatures (T_2, T_4, \dots, T_N) and concentrations (C_2, C_4, \dots, C_N) become elements of the $(N/2)$ -long vectors $\underline{TA}(out,n)$ and $\underline{CA}(out,n)$, respectively, where n is the current cell number;
3. calculate B-half-cell inlet temperatures and concentrations from the previously-defined mixing matrix, \underline{R} via

$$\begin{aligned}\underline{TB}(in,n) &= \underline{R} \underline{TA}(out,n) \\ \underline{CB}(in,n) &= \underline{R} \underline{CA}(out,n)\end{aligned}\tag{74}$$

where

$$\begin{aligned}\underline{TB}(in,n)^T &= [T_1 \ T_3 \ \dots \ T_{N-1}]_n \\ \underline{CB}(in,n)^T &= [C_1 \ C_3 \ \dots \ C_{N-1}]_n\end{aligned}$$

4. integrate equations (57) and (58) ($j=3,5,\dots,N-1$), (64) and (65) from B-half-cell inlet to outlet, calculating new solid temperatures at each integration step from equations

(56) ($j=2,4,\dots,N-2$) and (70). The outlet fluid temperatures (T_1, T_3, \dots, T_{N-1}) and concentrations (C_1, C_3, \dots, C_{N-1}) become the elements of the $(N/2)$ -long vectors $\underline{TB}(\text{out},n)$ and $\underline{CB}(\text{out},n)$, respectively;

5. calculate the next A-half-cell inlet temperatures and concentrations from the previously-defined mixing matrix, \underline{S} via:

$$\begin{aligned}\underline{TA}(\text{in},n+1) &= \underline{S} \underline{TB}(\text{out},n) \\ \underline{CA}(\text{in},n+1) &= \underline{S} \underline{CB}(\text{out},n)\end{aligned}\quad (75)$$

where

$$\begin{aligned}\underline{TA}(\text{in},n+1)^T &= [T_2 \ T_4 \ \dots \ T_N]_{n+1} \\ \underline{CA}(\text{in},n+1)^T &= [C_2 \ C_4 \ \dots \ C_N]_{n+1}\end{aligned}$$

6. repeat steps 2-5 until the desired number of axial cells has been traversed.

Model Parameters

The only parameters added to describe this combined case of heat and mass dispersion relate directly to the reaction involved and not to the AFM itself. These reaction-diffusion parameters (De , k , r_c , $(-\Delta H)$) must be determined independently as described elsewhere (e.g., Carberry, 1976; Froment and Bischoff, 1979; Lee, 1985; Smith, 1981). Thus, the AFM parameters are completely defined by considering only simple heat and mass dispersion characteristics.

Example Problems

Since this section must compare the AFM and the Fickian analogy for a reacting system, the appropriate Fickian equations are first presented. Then, the results of both models for several cases are compared.

The Fickian analogy equations, excluding axial dispersion, for cases involving heterogeneous or catalytic reaction (e.g., Carberry, 1976), are:

$$U_{int} \frac{\partial c}{\partial z} - Dr \left(\frac{\partial^2 c}{\partial r^2} + \frac{1}{r} \frac{\partial c}{\partial r} \right) = -R_G \left(\frac{1-\epsilon_{bed}}{\epsilon_{bed}} \right) \quad (76)$$

$$U_{int} \frac{\partial T}{\partial z} - \lambda r \left(\frac{\partial^2 T}{\partial r^2} + \frac{1}{r} \frac{\partial T}{\partial r} \right) = \left[\frac{(-\Delta H)}{\rho C_p} \right] R_G \left(\frac{1-\epsilon_{bed}}{\epsilon_{bed}} \right)$$

with

$$z=0: (\text{all } r) \quad c=C_{in}, \quad T=T_{in}$$

$$z>0: (r>0) \quad \frac{\partial c}{\partial r} = \frac{\partial T}{\partial r} = 0$$

$$(r=R_{tube}) \quad \frac{\partial c}{\partial r} = 0$$

$$- \lambda r \frac{\partial T}{\partial r} = 0 \quad , \text{ adiabatic}$$

$$hw(T - T_{wall}), \text{ wall-cooled}$$

where

$$R_G = (S_p/V_p) C [De \, k(t_{solid})]^{0.5} \quad (77)$$

$$(-\Delta H) R_G = h_p (S_p/V_p) [t_{solid} - T_{fluid}] \quad (78)$$

Here, all terms are in a consistent set of dimensions (e.g., CGS, MKS, etc.) as non-dimensionalizing these equations complicates their

numerical solution. The implicit Crank-Nicholson method (e.g., Hornbeck, 1975; Lee, 1985) was used to solve the above equations.

Figures 30 - 36 compare the AFM to Fickian analogy results for the system defined in Table 10. Bulk-averaged values for the Fickian model were determined by

$$P_{\text{bulk}} = 2 \int_0^{R_{\text{tube}}} r P(r) dr / (R_{\text{tube}})^2 \quad (79)$$

and for the AFM by

$$P_{\text{bulk}} = \sum_j Q_j P_j / Q_{\text{tot}} \quad (80)$$

where P is the property (concentration or temperature) and j corresponds to fluid plugs only ($j=2, 4, \dots, N$ for A-half-cells and $j=1, 3, \dots, N-1$ for B-half-cells).

Figures 30 and 31 indicate that the AFM predicts lower conversion and bulk fluid temperature than the Fickian analogy for an adiabatic reactor with a 0.5 second residence time. For a wall-cooled reactor with a 1.0 second residence time (Figures 32 and 33), the AFM conversion trend initially follows the Fickian analogy but then levels off at a lower value. Note that the reaction continues although the bulk fluid temperature remains quite low. For these first two cases neither model predicts steep radial temperature gradients. The Fickian analogy indicates a flat profile with about a 10 K drop at the wall. The AFM gives roughly the same overall temperature drop but indicates more of a profile within the bed itself.

Table 10

Example Reaction Case Parameters

$$r_c = kC \quad \text{mol/cm}^3 \text{cat-s}$$

$$k = 4.58 \times 10^8 \exp(-12000/T) \text{s}^{-1}$$

$$(-\Delta H) = 240 \text{ kcal/mol}$$

$$\rho = 9.47 \times 10^{-4} \text{ g/cm}^3$$

$$C_p = 0.25 \text{ cal/g-K}$$

$$Q = 818 \text{ cm}^3/\text{s}$$

$$De = 0.001 \text{ cm}^2/\text{s}$$

$$dp = 0.6 \text{ cm}$$

$$Dt = 3.6 \text{ cm}$$

$$\epsilon_{bed} = 0.40$$

$$Re_p = 234$$

$$Pr = 0.75$$

$$T_{in} = 600 \text{ K}$$

$$\phi_{in} = 3.07$$

Fickian parameters

$$\lambda = .00152 \text{ cal/s-cm-K}$$

$$Dr = 3.5 \text{ cm}^2/\text{s}$$

(from Smith, 1981)

$$hw = .0025 \text{ cal/s-cm}^2\text{-K}$$

(from Yagi and Wakao, 1959)

$$hp = .0026 \text{ cal/s-cm}^2\text{-K}$$

(from Schlunder, 1978)

$$v = 200.9 \text{ cm/s (interstitial)}$$

Table 10-continued

AFM parameters

$$hw = .002 \text{ cal/s-cm}^2\text{-K}$$

$$hp = .002 \text{ cal/s-cm}^2\text{-K}$$

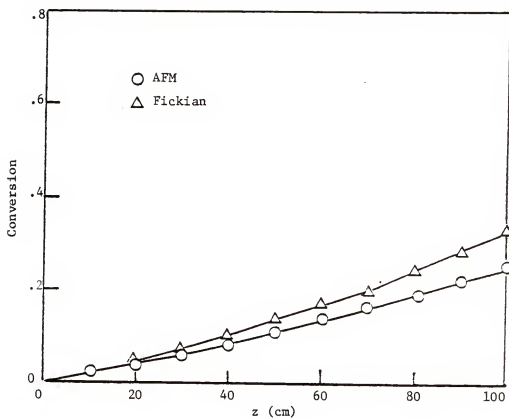


Figure 30: Conversion Profiles for Adiabatic Reactor, $C_{in}=2 \times 10^{-7}$, $T_{in}=600^\circ\text{K}$

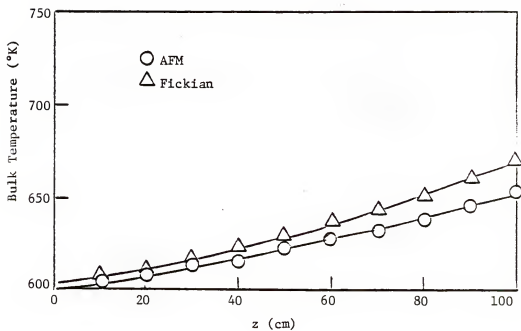


Figure 31: Bulk Temperature Profiles for Adiabatic Reactor,
 $C_{in}=2 \times 10^{-7}$, $T_{in}=600^{\circ}\text{K}$

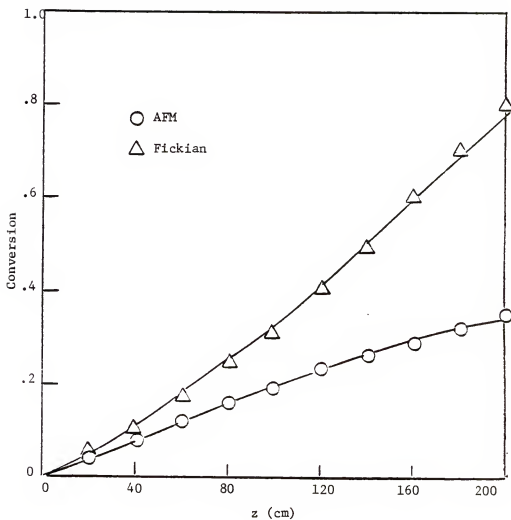


Figure 32: Conversion Profiles for Wall-cooled Reactor,
 $C_{in}=2 \times 10^{-7}$, $T_{in}=T_{wall}=600^{\circ}\text{K}$

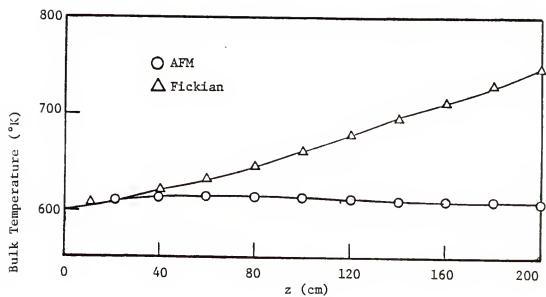


Figure 33: Bulk Temperature Profiles for Wall-cooled Reactor,
 $C_{in}=2 \times 10^{-7}$, $T_{in}=T_{wall}=600^{\circ}\text{K}$

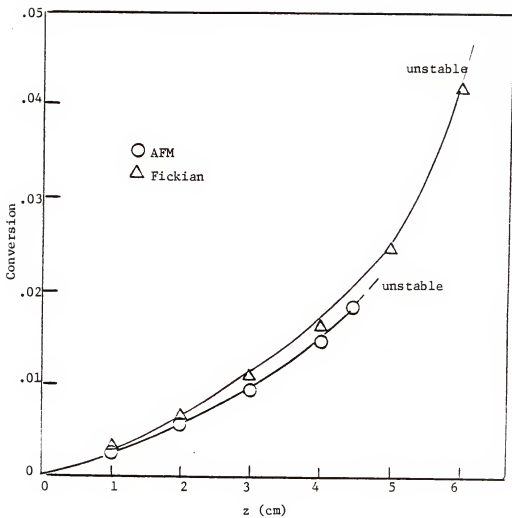


Figure 34: Conversion Profiles for Wall-cooled Reactor, Severe
 Inlet Conditions, $C_{in}=3 \times 10^{-6}$, $T_{in}=T_{wall}=600^\circ\text{K}$,
 (at 4cm, Bulk Temperatures: AFM=639°K, Fickian=646°K)

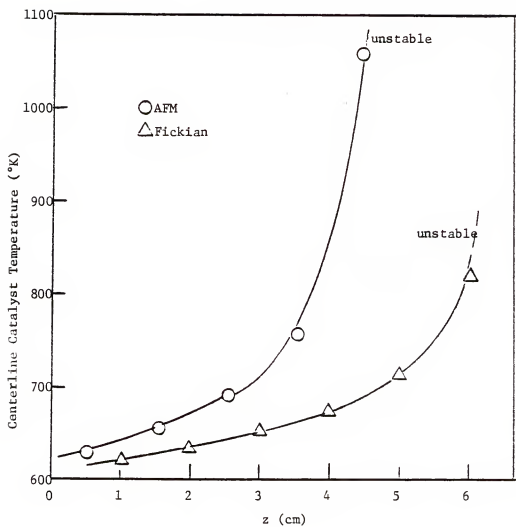


Figure 35: Centerline Catalyst Temperature Profiles for Wall-cooled Reactor with Severe Inlet Conditions

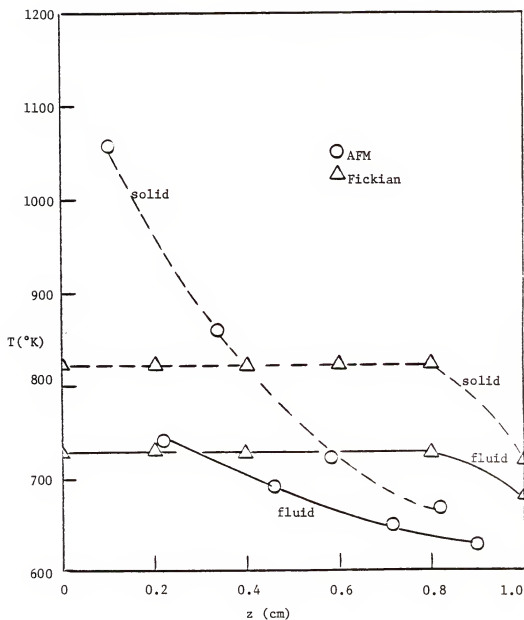


Figure 36: Radial Temperature Profiles for Wall-cooled Reactor, with Severe Inlet Conditions (at $z=4.5$ cm for AFM, at $z=6$ cm for Fickian Analogy)

More severe reaction conditions magnify these differences (Figures 34-36). In this case, the AFM predicts instability after only 4.5cm (0.023 sec) into the bed whereas the Fickian analogy shows the reaction to be stable until 6cm (0.03 sec) even at the low conversions predicted by both models. Although the bulk fluid temperatures at 4cm differ by only 7 K (639 K for the AFM vs. 646 K for the Fickian), the AFM indicates a much higher centerline catalyst temperature than the Fickian analogy (Figure 35). The AFM also indicates a steeper radial temperature profile and a greater difference between fluid and catalyst temperatures (Figure 36).

The AFM's distribution of flows can account for the steeper radial temperature profile. The slower flow rates near the centerline (Table 11) prolongs the residence time there thus allowing for more extent of reaction and larger temperature rise. Numerically, equations (57) and (58) support this argument since smaller Q_j implies larger axial gradients. Smaller Q_j , however, also implies minimal effect on bulk values (equation (80)) so that instability can be predicted even at seemingly low T_{bulk} . The splitting/merging at each half-cell exit eventually propagates this higher temperature radially outward.

The AFM is also more sensitive to wall conditions than the Fickian analogy. Comparison of Figure 31 (residence time of 0.5 sec) to the first 0.5 sec residence time of Figure 33 shows that, for the less severe reaction conditions, changing from a wall-cooled ($T_{wall}=600$ K) to an adiabatic reactor causes a negligible change in the Fickian predictions but a dramatic change in the AFM results. The AFM maximum-

near-wall flow distribution (Table 11) accounts for the model's sensitivity to wall conditions. Any change in the outer plugs will dominate bulk values (equation (80) and will rapidly propagate inward due to the mixing at each half-cell exit.

Figure 37 shows the effect of changing Dt/dp to 3 ($Dt=3.6\text{cm}$, $dp=1.2\text{cm}$, $hp=0.0014\text{cal/s-cm}^2\text{-K}$ for AFM, $0.0018\text{ cal/s-cm}^2\text{-K}$ for Fickian) for the severe reactions of Figures 34-36. Because the increased pellet size slows the overall reaction rate, both models' predicted instabilities move farther into the reactor. However, in this case, the Fickian analogy is more conservative, i.e., it predicts the instability sooner. The AFM flow profiles (Figure 38) can explain this shift. Although the low centerline flow ($Q_1 < .01 Q_{tot}$) should induce large axial concentration and temperature gradients within that plug, its effect is offset by the influence of the large wall plug flow upon mixing at the half-cell exit. (The AFM parameters in Figure 38 required $\epsilon_b=0.23$ (equation (13)) to give $\epsilon_{bed}=0.40$.)

Figures 39 and 40 compare the AFM and Fickian analogy for an example system which yields a Fickian-predicted hot-spot, i.e., maximum in the temperature profile. The system parameters are as given in Table 10, with a lower heat of reaction and higher wall coefficients as noted on the figures. The AFM predicts essentially no reaction after about 10cm into the vessel, whereas the Fickian analogy shows 95% conversion at 100cm. The AFM's sensitivity to wall conditions accounts for the contrast.

Table 11

AFM Flow Distribution
for $Dt/dp=6$, $\epsilon_{bed} = .40$

<u>Half-cell</u>	<u>Plug</u>	<u>Q/Qtot</u>	<u>u/u'</u>
A	2	.044	1.90
	4	.159	2.28
	6	.277	2.38
	8	.520	2.67
B	1	.012	.532
	3	.093	1.33
	5	.197	1.69
	7	.697	3.57

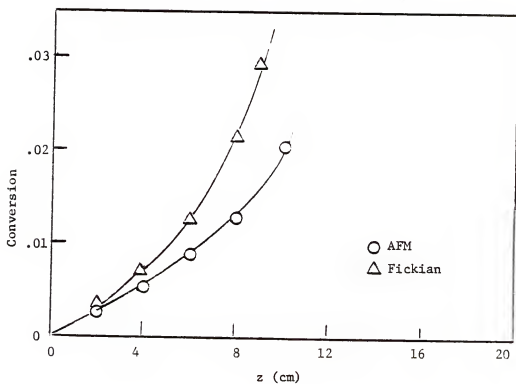
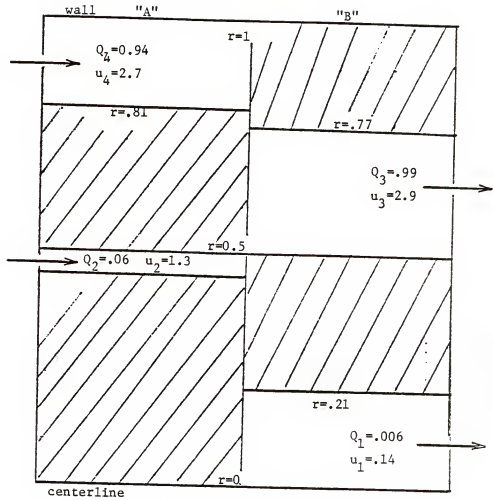


Figure 37: Conversion Profiles for Wall-cooled Reactor,
 $Dt/dp=3.0$, $\epsilon_{bed}=0.40$, $T_{in}=T_{wall}=600^{\circ}\text{K}$, $C_{in}=2 \times 10^{-7}$



NOTE: Given $Q_j=Q_j/Q_{tot}$ and $u_j=u_j/u'$

Figure 38: AFM Parameters for $Dt/dp=3.0$, $\epsilon_{bed}=0.40$

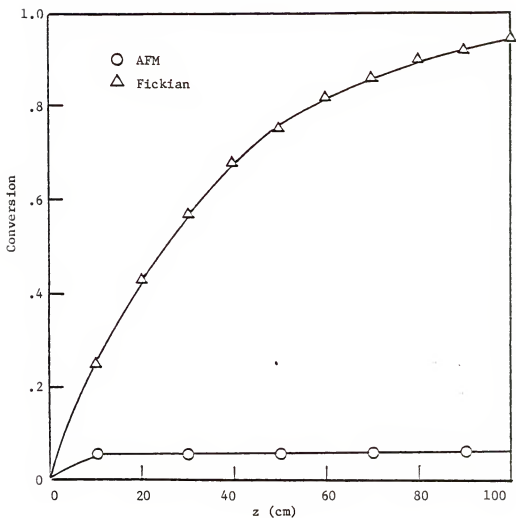


Figure 39: Conversion Profiles for Wall-cooled Reactor, $Dt/dp=6.0$, $\epsilon_{bed}=0.40$, $T_{in}=800^{\circ}\text{K}$, $T_{wall}=400^{\circ}\text{K}$, $C_{in}=2 \times 10^{-8}$, $(-\Delta H)=24 \text{ kcal/mol}$, $hw = 100$ (hw of Table 10)

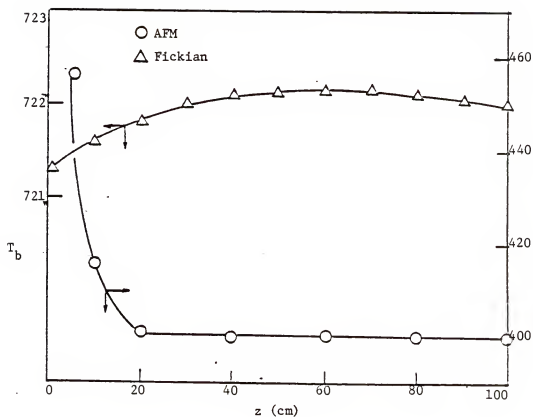


Figure 40: Temperature Profiles for Wall-cooled Reactor, $Dt/dp=6.0$, $\epsilon_{bed}=0.40$, $T_{in}=800^\circ\text{K}$, $T_{wall}=400^\circ\text{K}$, $C_{in}=2 \times 10^{-8}$, $(-\Delta H)=24\text{kcal/mol}$, $hw=100$ (hw of Table 10)

Summary of AFM for Reaction

The Alternating Flow model views reaction in packed beds as a combination of the simple mass and heat dispersion mechanisms with reaction in the packing material, or pellets. Mass disperses axially due to bulk flow and radially because of reaction within the packing and because of mixing at each half-cell outlet. Heat disperses axially with the bulk flow, radially through pellet film resistances (to cool the heat of reaction) and from mixing at each half-cell outlet, and out at the wall through a wall film resistance. The only parameters needed for the combined, but not individual, dispersion case relate directly to reaction within the catalyst pellets and are independent of the AFM itself.

For the examples presented here, the AFM predictions differed significantly from the Fickian analogy. The AFM showed more sensitivity to wall conditions than the Fickian analogy, probably because of the AFM's maximum-near-wall flow distribution. The difference in the models' predictions for instabilities can also be explained in terms of flow patterns.

CHAPTER V CONCLUSIONS

The Alternating Flow Model is a viable alternative to the traditional Fickian analogy approach for modeling dispersion in packed beds. Not only does the AFM require fewer correlated parameters than the Fickian analogy, but it also meets all the dispersion model acceptability set forth in the Introduction. The AFM can also predict, solely from system geometry, the experimentally observed velocity profiles for packed beds.

The AFM equalled or surpassed the Fickian analogy in following the experimental data of the simple mass dispersion cases examined in Chapter II. For simple mass dispersion, the AFM is totally predictive: all model parameters are determined a priori from bed voidage, ϵ_{bed} , and relative size of tube to pellet, D_t/d_p .

For most of the heat dispersion cases studied in Chapter III, the AFM followed experimental data at least as closely as the Fickian analogy. For simple heat dispersion, the AFM requires back-fitting one parameter, the wall film coefficient (h_w), to each new system. The complexity of turbulent heat convection explains this need for back-fitting h_w . A friction factor analogy sheds light on the observed h_w vs. G^m relationship (equation (45)) and can even predict the exponent, m , for smooth tubes. The pellet film coefficient correlation

(equation (50)) can be applied to either spherical or cylindrical pellets without loss of generality. The flow rate dependence was developed from single submerged object considerations.

As a descriptor of reaction in packed beds, the AFM exhibits high sensitivity to reactor wall conditions and may predict instability (even at seemingly low bulk fluid temperatures) where the Fickian analogy does not. These differences can be explained in terms of the AFM's radial flow distribution. Thus, the AFM's ability to correctly predict packed bed velocity profiles suggests that the AFM may more closely follow reaction data. Further, the AFM's ability to predict hot spots should also be examined.

The Fickian analogy with axial dispersion predicts back-mixing where none is observed experimentally, but the AFM cannot predict the diffusion-like behavior expected in the limit of zero velocity. Thus, neither model can adequately cover all possible cases. However, the AFM should better describe cases in which ordered flow can be expected (e.g., low D_t/dp) and has the added advantage of a priori determination of all mass dispersion parameters.

The merits of the AFM discussed here warrant the further studies outlined in Appendix J.

APPENDIX A
HYDRAULIC RESISTANCES

Empty Tubes

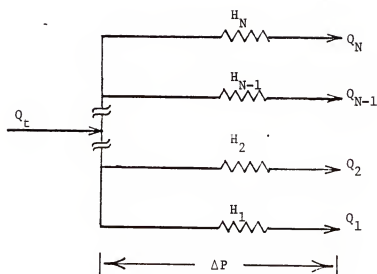
In general, the pressure drop through an empty tube can be expressed as

$$\Delta P = f \left(\frac{L}{R_h} \right) \left(\frac{Q}{A} \right)^2 / 2g_c \quad (A-1)$$

where f is the friction factor, L is the tube length, R_h is the hydraulic radius ($R_h = 4 \text{ cross-sectional area} / \text{wetted perimeter}$), Q is the volumetric flow rate, and A is the cross-sectional area. Equation (A-1) can be rearranged to give

$$Q = a(A^2 R_h / f)^{0.5} (\Delta P)^{0.5} \quad (A-2)$$

where a is constant. If one makes an analogy to Ohm's Law then $(\Delta P)^{0.5}$ becomes the hydraulic "voltage," $a(A^2 R_h / f)^{0.5}$ the inverse of hydraulic resistance, H and Q the current flow. The total flow through a network of resistances will then subdivide according to these hydraulic resistances (Figure 41) whose form depends on pipe shape (because of R_h) and on flow regime (because of f).



$$\frac{Q_j}{Q_t} = \frac{(1/H_j)}{\sum_{j=1}^N (1/H_j)}$$

Figure 41: Flow Subdivision via Hydraulic Resistances

For turbulent flow, f is constant and the hydraulic resistance is given by Equation (A-4a). But, in the transition of laminar regime, f is proportional to $1/Re$ or $Av/Q Rh$ so that Equation (A-2) becomes

$$Q^2 = b A^2 Rh^2 (\Delta P) (Re)$$

or

$$Q = b A Rh^2 (\Delta P) \quad (A-3)$$

where b is constant. The corresponding hydraulic resistance is given by Equation (A-4b).

$$A(Rh)^{0.5} \quad \text{turbulent} \quad (A-4a)$$

$$(1/H) = A Rh^2 \quad \text{laminar} \quad (A-4b)$$

For tubes of circular cross-section, Rh =diameter; for empty annuli, $Rh=2(\text{outer radius} - \text{inner radius})$.

Packed Beds

The corresponding pressure drop relationship for packed beds includes some function of bed voidage. While the literature provides several forms of this function (e.g., Froment and Bischoff, 1979; Coulson, 1949; Ergun, 1952; Ergun and Orning, 1949; Lapin, 1962; Leva, 1947a,b) the one developed by Leva (1947b) will be used here for simplicity:

$$\Delta P = a(1-\epsilon) U_s^2 / \epsilon^3 \quad (A-5)$$

where a is constant and U_s is the superficial velocity based on empty tube cross-section. This can be converted to actual interstitial velocity, U_i based only on the void area, Av , as $U_s = U_i \epsilon_{bed}$, where $U_i = Q/Av$. Thus, (A-5) becomes

$$\Delta P = b(1-\epsilon) \left(\frac{Q}{A_v} \right)^2 / \epsilon \quad (A-6)$$

so that the hydraulic resistance for a packed tube is

$$1/H = (A_v \epsilon / (1-\epsilon))^{0.5} \quad (A-7)$$

and will be referred to as the "Ergun type" resistance. Note that (A-7) implies that the resistance to flow decreases as voidage increases, thus predicting the observed channelling effect of high flow at maximum voidage near the wall.

APPENDIX B
REFERENCE LIST FOR DISPERSION COEFFICIENT
STUDIES

The following is a list of some works regarding axial and radial dispersion from the Fickian analogy point of view, as mentioned in the main text. No claim of completeness is made here. For complete bibliographic information, see the Bibliography.

Carberry, (1958), Chang (1982, 1983), Chung and Wen (1968), Dorweiler and Fahien (1959), Evans and Kenney (1966), Fahien and Smith (1955), Gunn (1969), Gunn and England (1971), Gunn and Pryce (1969), Klinkenberg et al. (1953), Klinkenberg and Sjeniter (1956), Kramers and Alberda (1953), Liles and Geankoplis (1960), McHenry and Wilhelm (1957), Mears (1971), Oliveros and Smith (1982), Plautz and Johnstone (1955), Roemer et al. (1962), Strang and Geankoplis (1958), Suzuki and Smith (1970), Wolff et al. (1979), Awasthi and Vasudeva (1983), Cairns and Prausnitz (1960), Carberry and Bretton (1958), Danckwerts (1953), Ebach and White (1958), Edwards and Richardson (1968), Grabmuller and Schadlich (1983), Hibilaro (1979), Hsiang and Haynes (1977), Jacques and Vermeulen (1957), Liles (1959), Miller and King (1966), Turner (1971, 1983).

APPENDIX C
AXIAL VOIDAGE VARIATION DETERMINATION

If the packed bed is considered to be a perfect cylinder filled with uniformly sized perfect spheres, and the position (coordinates) of each sphere within the cylinder is known then void fractions can be theoretically calculated. If such information is unavailable, the void fraction must be measured experimentally. Each technique is discussed below.

Experimental Measurement

Consider a cylinder marked off in equal increments along its height. Let V_{ol} be the volume of liquid required to raise the level from one height, z_1 , to the next, z_2 , when the cylinder is empty and v be the amount of liquid required to raise the level from z_1 to z_2 when the cylinder is packed with pellets. Then, v is the void volume between z_1 and z_2 and v/V_{ol} is the average void fraction between z_1 and z_2 , as indicated by the dashed step-wise plot in Figure 4.

Experiments leading to Figure 4 were carried out with glass spheres ($d_p=1.56\text{cm}$) in a 1000ml beaker ($D_t=10.3\text{cm}$) whose 25ml increments were 0.3cm apart. This yields $D_t/d_p=6.6$ with axial markings every $d_p/5$ units. Since axial voidage frequencies on the order of

less than one dp are desired, this axial increment must be small enough to achieve the desired sensitivity. Pellet diameter, dp , was determined by measuring the volume of water displaced by a set number of spheres and then calculating dp via the formula for spherical volume. The tube diameter, Dt , was calculated from the formula for cylindrical volume (volume=25ml, length= 0.3cm). The beaker was packed in several steps of pouring in a few spheres and shaking the beaker to attain the densest packing arrangement. Incremental void volumes were measured by introducing water into the packed beaker from a buret.

Theoretical Calculation

Consider a cylindrical coordinate system with its origin at the center of the lowest plane of a vertical cylinder, or tube, which is packed with uniformly sized spheres, or pellets. The tube is bounded within this coordinate system by

$$0 < z < \text{height of cylinder}$$

$$0 < r < Dt/2 \quad (C-1)$$

$$0 < \theta < 2\pi$$

The position of each sphere within the tube is then defined by the location of its center (r_1, θ_1, z_1) and each sphere occupies the space radiating outward from its center ($dp/2$) in all directions. The voidage at any given axial position, z , can be determined by examining the cross-section obtained by cutting the system with a horizontal plane at that z . This would yield a circle of diameter Dt which

surrounds several smaller circles with diameters ranging from $0+$ to $dp/2$ as shown in Figure 42. The unshaded area within the large circle represents the void area, Av . Mathematically, the void volume is given by $(Av)dz$ and the average void volume between two axial positions z_1 and z_2 is found by integrating $(Av)dz$ from z_1 to z_2 .

Care must be taken at each axial position to include all spheres in the system which may be cut by such a plane. This is accomplished by including all spheres whose centers are not more than $(dp/2)$ units away from the plane of interest, i.e., $\Delta z = |z_i - z| < dp/2$. Figure 43 illustrates this point. The area cut out of each eligible sphere by the plane in question is given by

$$A_i = \pi b_i^2 \quad (C-2)$$

where

$$b_i^2 = dp^2/4 - (\Delta z)^2 \quad (C-3)$$

The void fraction at this point is then

$$Z_v/Atube = 1 - 4\epsilon A_i / Dt^2 \quad (C-4)$$

As an example, consider the case of $Dt/dp=3$. The calculated void fractions for Dt/dp were given in Figure 5. Earlier, this case was described as having several layers each containing seven spheres (one at the center and six tangent to the tube wall). These layers were said to build up with the center spheres stacked and successive outer rings rotated 30 degrees. Within our system, this translates to the coordinates shown in Table 12. Figure 44 corresponds to the horizontal plane $z=dp/2$ while Figure 45 corresponds to the plane at $z=1.5dp$.

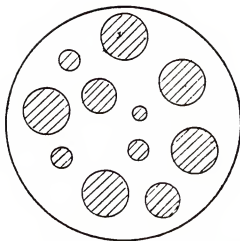
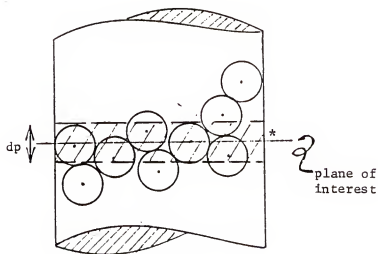


Figure 42: Horizontal Plane through Packed Tube



* pellet center

* include only those pellets
whose centers fall within
shaded region

Figure 43 : Inclusion of Spheres for Axial Voidage Calculations

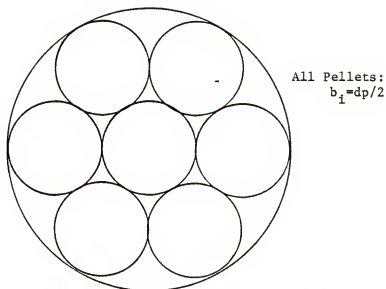


Figure 44: Horizontal Plane at $z=dp/2$ for $Dt/dp=3$

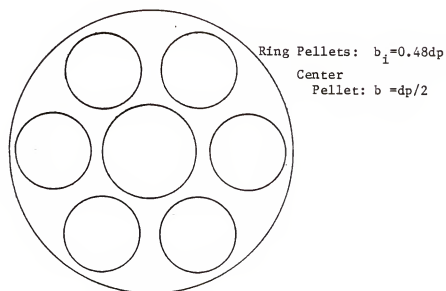


Figure 45 : Horizontal Plane at $z=1.5dp$ for $Dt/dp=3$

APPENDIX D
REFERENCE LIST FOR VOID FRACTION STUDIES

Following is a list of void fraction and pellet packing study references as mentioned in the main text.

Benenati and Brosilow (1962), Bennett (1979), Cohen and Metzner (1981), Dodds (1980), Fedors (1979), Galloway et al. (1957), Hirai (1954), Haughey and Beveridge (1966), Leva and Grummer (1947b), LeGoff et al. (1985), Ouichiyama and Tanaka (1981, 1984), Pillai (1977), Ridgway and Tarbuck (1968), Roblee et al. (1958), Sloane (1984), Standish and McGregor (1978), Stanek and Eckert (1979), Wieckowski and Strek (1966).

APPENDIX E

TRANSIENT SIMULATION TECHNIQUE

The AFM prediction radial concentration profiles at any given time and axial position can be represented in the Laplace domain in equation (12) given in the main text. The motivation for such a matrix formulation was conciseness. However, the AFM transient cases were actually simulated in the time domain plug by plug and cell by cell to properly account for the radial and axial distribution of delay times. In concept, the simulation technique is straightforward, but it does require some careful "bookkeeping" at the actual computer programming stage.

The general procedure below outlines the real-time simulation of an "F-curve" experiment. All time units are assumed to be non-dimensionalized in terms of bed hold-ups. The steps are as follows:

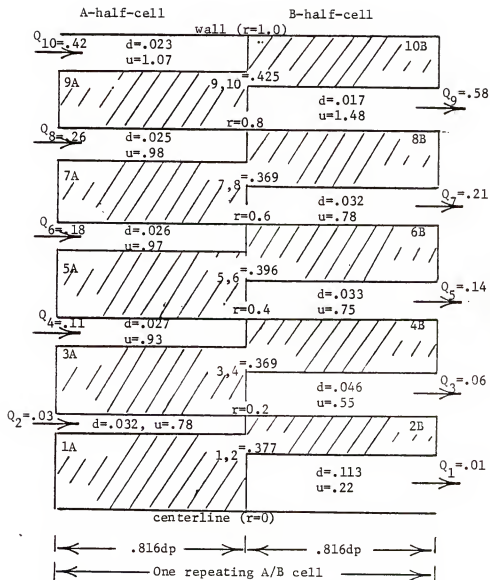
1. Determine size and distribution of radial plugs, number of axial cells, flow distribution, and split/merge matrices (\underline{R} and \underline{S} , equation (12)) as for the steady-state case.
2. After choosing Δt , subdivide each plug into elements as discussed below.
3. Set time=0.
4. Initialize concentration profile by setting all elements inside the bed at $C=0$.

5. Let time = time + Δt .
6. Set the "bottom" (or inlet) elements of the plugs in the first half-cell at $C=1$. (Any convenient number may be used since the calculation of $F(t)$ is independent of this value).
7. Determine concentration in outlet elements of all plugs as discussed below.
8. Determine concentration to be deposited in inlet elements of all plugs by the split/merge calculations, i.e.

$$\underline{B}_{in} = \underline{R}_{A-out} \text{ or } \underline{A}_{in} = \underline{S}_{B-out}$$
9. Determine value of $F(\text{time})$ as $\sum C_j(Qj/Q_t)$ over all j in the outlet elements of the void plugs in the last half-cell ($j=2,4,6,\dots$ for A-half-cell or $j=1,3,5,\dots$ for B-half-cell).
10. Repeat steps 5 through 8 until desired time has elapsed.

Consider as an example the case $Dt/dp=8$, $z/dp=32$ and $\epsilon_{bed}=0.39$ (Jacques and Vermeulen, 1957) which gives $Nz=32/1.632=19.6$ or 20 (A/B) cells with each half-cell containing 5 void-full regions radially distributed as shown in Figure 46 (If $(z/dp)/1.632$ were, say, 19.2, the AFM would require 39 half-cells. That is, round Nz up to the nearest half.) Table 13 gives the corresponding delay times which are used to subdivide each plug into M elements where

$$M_j = d_j / \Delta t \quad (E-1)$$



NOTE: given values are scaled by overall amounts
 $Q_i = Q/Q_t$, $u_i = u/u'$, $r = r/R_{tube}$

Figure 46: Radius, Flow, and Velocity Distribution,
 $Dt/dp=8.0$, overall bed voidage = 0.39

for $j=1,2,3,\dots,N_{rad}$. (The time interval, Δt , is analogous to the step-size one would use with the Euler or Runge-Kutta integration techniques and should be small enough to produce significantly different M_j 's.)

Since each plug consists of a certain number of time elements, the outlet concentration from the j -th plug "now" is what its inlet concentration was M_j time steps ago. In terms of real-time simulation, this translates into shifting elements within an M_j -long array as illustrated in Figure 47. At each time step, then, the "top" element is removed as the current outlet concentration (into C_{out} , all other elements are moved up one slot, and the current inlet concentration is put into the "bottom" element (from C_{in}). This shifting operation must be carried out at each time step for each plug. Note that if the inlet concentration to any given plug remains constant (as for the first half-cell) then all elements of the array will be the same after M_j time steps.

For the example case stated above, there are $(20)(10)=200$ arrays (one per plug) varying in length from 2 to 11 elements if $\Delta t=0.01$. One of the 20 repeating (A/B) cells is shown in Figure 48. Such a large time step was used for illustration purposes only. The actual value used to simulate this case was $\Delta t=0.00125$.

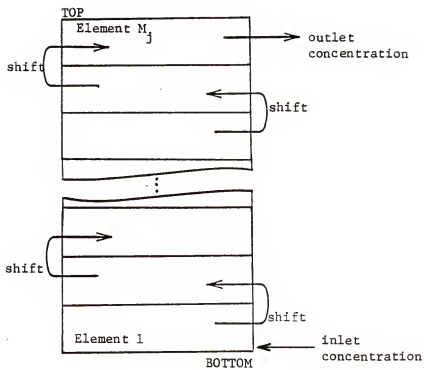
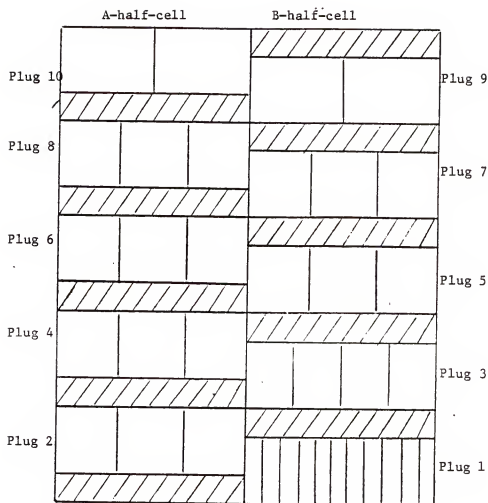


Figure 47: Shifting Procedure for Simulation of Delay Times (Real-time)



NOTES: (a) Radial divisions not to scale
 (b) Each vertical division corresponds to one time step (in void plugs)

Figure 48: Time-step Subdivision of Plugs , $Dt/dp=8.0$,
 overall bed voidage = 0.39

TABLE 13

Delay Times for $Dt/dp=8$, $z/dp=32$, $\epsilon_{bed} = 0.39$

<u>A-half-cell</u>		<u>B-half-cell</u>	
<u>plug</u>	<u>delay</u>	<u>plug</u>	<u>delay</u>
2	.0321	1	.1132
4	.0270	3	.0457
6	.0259	5	.0334
8	.0254	7	.0320
10	.0234	9	.0169

Delay times calculated from equation (17).

For ease of programming, a single three-dimensional array $C(I,J,K)$ was used to hold concentration values for all plugs, the "I" subscript defines radial plug number, "J" the axial cell number, and "K" the time step length, M_j . This array was dimensioned so that K was at least as large as the maximum M_j . Another array, $NSUB(I)$ (I same as above), stored the M_j 's so that inlet concentration values were put into $C(I,J,NSUB(I))$ and shifting for each plug defined by (I,J) occurred only $NSUB(I)$ times at each real-time interval. Thus, some elements of the $C(I,J,K)$ array were unused, but efficient storage usage was overridden by ease in programming.

APPENDIX F
COMPARISON OF AFM FLOW PROFILES BASED ON
EMPTY ANNULUS AND ERGUN-TYPE HYDRAULIC RESISTANCES

The basic premise of the Alternating Flow Model (AFM) is that the bulk fluid passes through the hydraulic resistances presented by a number of (A/B) cells each consisting of a set pattern of void-full annular regions (Figure 2, main text). The empty annulus hydraulic resistances (Appendix A) are then used to determine the radial profile. But, Ergun type resistances also indicate an increase in flow with porosity. Hence, velocity and flow profiles predicted by using both types of hydraulic resistances should be compared.

Consider the case of $Dt/dp=8$, $\epsilon_{bed}=0.39$ (Jacques and Vermeulen, 1957) as discussed in Appendix E. The void annuli in half-cell A are defined by the radii listed in Table 14. Equation (A-7) for the Ergun type resistance requires a void cross-sectional area, A_v , and average void fraction, ϵ , for each plug. A_v is calculated directly from the plug radii and ϵ is taken as the average value over the evenly spaced radii as defined by equation (15), main text; Table F.1 also shows A_v and ϵ for each plug. Table 15 gives the corresponding velocities calculated from empty annulus and Ergun type hydraulic resistances. The only noticeable difference is in the plug 2 velocities. However, because this plug represents such a small fraction of the total throughput, this difference would not significantly affect the F-curve simulation.

TABLE 14

A-Plug Size Parameters for $Dt/dp=8$, $\epsilon_{bed} = 0.39$

<u>plug</u>	<u>r(in)</u>	<u>r(out)</u>	<u>Av</u>	<u>ϵ_{bed}</u>
2	.158	.200	.015	.377
4	.340	.400	.044	.369
6	.535	.600	.074	.369
8	.733	.800	.103	.369
10	.891	1.0	.153	.425

TABLE 15

Flow and Velocity Profiles by Two Types of Resistances

	<u>Empty annulus</u>		<u>Ergun type</u>	
<u>plug</u>	<u>Qi/Qt</u>	<u>u/u'</u>	<u>Qi/Qt</u>	<u>u/u'</u>
2	.0301	.778	.038	.969
4	.106	.928	.109	.954
6	.183	.966	.180	.952
8	.261	.984	.252	.952
10	.421	1.07	.421	1.07

 $z/dp=32 \Rightarrow Nz=20.$

APPENDIX G
FICKIAN HEAT DISPERSION PARAMETER REFERENCES

The studies listed below give values and/or correlations for Fickian heat dispersion parameters in terms of other system variables. No claim regarding completeness of a literature survey is made here. For complete bibliographic information, see the Bibliography.

Baumeister and Bennett (1958), Botterill and Denolye (1978), Bunnell et al. (1949), Calderbank and Pogorski (1957), Clement and Jorgensen (1983), Coberly and Marshall (1951), Colburn (1931), Crider and Foss (1965), Duarte et al. (1985), deWasch and Froment (1972), Froment and Bischoff (1979), Gunn and Khalid (1975), Hall and Smith (1949), Hanratty (1954), Hughmark (1972, 1980), Kunii and Smith (1960), Kunii et al. (1968), Kwong and Smith (1957), Lerou and Froment (1977), Leva (1947a), Leva and Grummer (1948), Li and Finlayson (1977), Patterson and Carberry (1983), Plautz and Johnstone (1955), Reilly (1957), Schertz and Bischoff (1969), Schlunder (1978), Schotte (1960), Scott et al. (1974), Smith (1981), Vortmeyer and Winter (1982), Wakao (1976), Wakao et al. (1979), Wakao and Kato (1968), Whitaker (1972), Yagi and Kunii (1960), Yagi and Wakao (1959), Yoshida et al. (1962).

APPENDIX H TWO-SIDED EFFECTIVENESS FACTOR FOR GENERAL INTRINSIC KINETICS

Consider a catalyst subjected to unequal concentrations on either face (Figure 49). Tan and Smith (1980) derived a rate expression for such unsymmetric boundary conditions (with an isothermal pellet) and first-order intrinsic kinetics. Here, their idea is extended to more general intrinsic kinetics of the form:

$$r_c = k(T)f(C) \quad (H-1)$$

where $k(T)$ is the rate constant (dependent on catalyst temperature) and $f(C)$ is the dependence of rate on concentration of a key component (e.g. $f(C)=C$ for first-order, $f(C)=C^n$ for n -th order, $f(C)=KC/(1+KC)$ for Langmuir-type, etc.). It is assumed that $f(C)$ can be expressed solely in terms of one key component (e.g., Lee, 1985). If the pellet (slab) is isothermal then

$$\frac{d^2C}{dz^2} = \phi^2 f(C) \quad (H-2)$$

with

$$C=C_2 \text{ at } z=-1 \text{ and } C=C_1 \text{ at } z=+1$$

where $z=x/L$, ϕ is the Thiele modulus, $\phi^2=L^2k(T)/De$, L is the slab half-thickness (or V_p/S_p for other shapes) and De is the effective

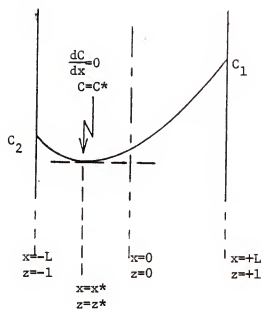


Figure 49: Catalyst Pellet (Slab) with
Unsymmetric Boundary Conditions

diffusivity of the key component in the pellet. Integrating equation (H-2) from the inflection point, z^* , to each face gives the concentration gradient at that face. Then, equating flux at the surface to reaction into the pellet at that face gives

$$(R_G)_1 = Sp[2 k(T) De \int_{C^*}^{C_1} f(C) dC]^{0.5} \quad (H-3)$$

or

$$(R_G/Vp)_1 = \frac{1}{2(Vp/Sp)} [2k(T)De \int_{C^*}^{C_1} f(C) dC]^{0.5} \quad (H-4)$$

Note the appearance of C^* (the concentration at inflection point) in these equations. For first-order kinetics, C^* can be obtained directly from the analytical solution of equation (H-2) to be

$$C^* = (C_1/C_2)^{0.5} / \cosh(\phi) \quad (H-5)$$

No analytical solution is available for more general kinetics. However, some approximations can be made. First, under certain conditions, $C^* \rightarrow 0$. Let $P = C_2/C_1$ so that $C^* = P^{0.5} C_1 \cosh(\phi)$. If, for example, $0.2 < P < 5.0$ and $\phi_G = 3$, then $0.04 < C^*/C_1 < 0.22$ where ϕ_G , the generalized Thiele modulus, is defined as

$$\phi_G = \frac{L(k/De)^{0.5} f(C_1)}{[2 \int_0^{C_1} f(C) dC]^{0.5}} \quad (H-6)$$

But, such a large concentration difference ($P=5$) seems unlikely in AFM calculations, thus setting $C^*=0$ for $\phi_G > 3$ is probably a reasonable approximation (e.g., if $P=2$ and $\phi_G = 3$, $C^*/C_1 = 0.14$). And, as ϕ_G increases, C^* rapidly approaches zero regardless of P . Next, if these conditions are not met (i.e. ϕ_G small or P large), C^* can be approximated by substituting ϕ_G for ϕ in equation (H-5). If $\phi_G < 0.1$ the reaction is considered free of diffusion and $R_G = r_c$ (Lee, 1985).

The exact solution to equation (H-2) should be used for first-order intrinsic kinetics.

APPENDIX I
PACKING ARRANGEMENT FROM POTENTIAL ENERGY
MINIMIZATION

Packed bed voidage profiles, axial and radial, can be calculated if the exact placement of each pellet within the tube is known. Experimentally, locating the exact position of each pellet would seem unnecessary since voidage profiles can be measured directly, thus overriding the need to know individual pellet locations. If, however, the packing arrangement can be determined a priori, solely from the tube and pellet sizes, there is no need to measure voidage profiles from experiments or to determine them from correlations.

Consider, then, the problem of locating N spherical pellets of diameter d_p within a cylindrical tube of diameter D_t and infinite height. If the tube is filled from the top (Figure 50) each pellet will fall to the minimum possible height. The densest packing (lowest bed voidage) is attained when all pellets within the system reach their minimum height or gravitational potential. Thus, the location of each sphere within the tube can be determined by minimizing the overall system potential, Z , subject to several constraints:

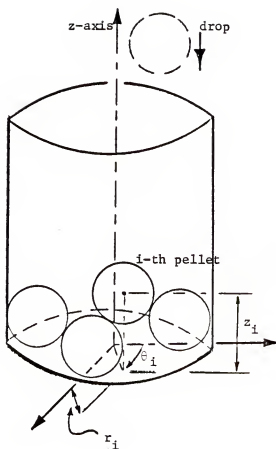


Figure 50: Spherical Pellets within Cylindrical Coordinate System

$$\text{minimize } Z = \sum_{i=1}^N z_i \quad (\text{I-1})$$

$$z_i \geq dp/2 \quad (\text{I-2})$$

$$0 \leq r_i \leq 0.5(Dt-dp) \quad (\text{I-3})$$

$$0 \leq \theta_i \leq 2\pi \quad (\text{I-4})$$

$$d_{i,j} \geq dp \quad (\text{I-5})$$

(Note that the only physical parameters contained in the problem statement are tube and pellet size). Here (r_i, θ_i, z_i) locates the position of the center of the i -th sphere (in cylindrical coordinates) and $d_{i,j}$ is the distance between the centers of the i -th and j -th spheres (Figure 50). The restrictions (I-2) and (I-3) imply that each pellet can neither fall below the bottom of the tube nor extend past the tube wall, while (I-5) prevents pellets from overlapping. Constraint (I-4) defines the angular coordinate range. Note that the only nonlinearity appears in constraint (I-5) since:

$$d_{i,j}^2 = r_i^2 + r_j^2 - 2r_i r_j \cos(\theta_i - \theta_j) + (z_i - z_j)^2 \quad (\text{I-6})$$

And, while there are only N restrictions of types (I-2) through (I-4), there are $N(N-1)/2$ of type (I-5). Thus, the problem is to minimize a linear objective function (I-1) of $3N$ variables N times

(r_i, θ_i, z_i) with $3N$ linear and $N(N-1)/2$ nonlinear constraints. While the constraints could be handled using Lagrangian multipliers and slack (Beveridge and Schechter, 1970) the resulting system would contain a prohibitive number of equations and unknowns. However, the problem can be simplified by modifying the objective function.

Consider the objective function

$$J = \sum_{i=1}^N z_i + \sum_{i=2}^N \sum_{j=1}^{i-1} f(d_{i,j}) \quad (\text{I-7a})$$

where

$$f(d_{i,j}) = \begin{cases} 0 & , d_{i,j} > dp \\ A(dp - d_{i,j})^{0.5} & , d_{i,j} < dp \end{cases} \quad (\text{I-7b})$$

$$(\text{I-7c})$$

and A is some known (positive) constant. The effect of the double summation is to increase the objective function for packing arrangements which cause pellets to overlap. Although a simple constant (instead of equation (I-7c)) would affect elimination of an overlap situation, the square-root functionality will allow a numerical search to differentiate "bad" from "worse". Restrictions (I-2)-(I-4) still apply.

Hence, the problem has been converted to minimization of a nonlinear objective function (equations (I-7)) of $3N$ variables subject to $3N$ linear constraints (equations (I-2)-(I-4)). The problem can be

further simplified by fixing the position of one sphere (e.g. at (0, 0, 0.5dp) since only relative positions are needed. The limits of the summations of equation (I-7) would remain the same, but the number of unknowns and restrictions would each be reduced by 3 (one less each equations (I-2)-(I-4).

Once the system of equations has been solved (i.e., all pellets located), bed voidage profiles can be calculated. At any axial position, z , the average voidage over the entire tube cross-section AT THAT z is

$$\epsilon(z) = 1 - 4 \sum_{j=1}^N b_j^2 / d_t^2 \quad (\text{I-8})$$

where

$$b_j = \begin{cases} 0 & \text{if } |z_i - z| \geq dp/2 \\ [0.25dp^2 - (z_i - z)^2]^{0.5} & \text{if } |z_i - z| \leq dp/2 \end{cases} \quad (\text{I-9})$$

Around any cylindrical shell of radius r the average voidage over the increment $z_1 - z_2$ is

$$\epsilon(r) = 1 - \int_{z_1}^{z_2} \left(\sum_{i=1}^N \alpha_i \right) dz / 2\pi \quad (\text{I-10})$$

where

$$\alpha_i = \begin{cases} 0 & , \text{ if } |r_i - r| \geq dp/2 \\ \arccos \frac{r_i^2 - r^2 - (dp^2/4)}{2rr_i} & , \text{ if } |r_i - r| < dp/2 \end{cases} \quad (\text{I-11})$$

The integration of equation (I-11) must be numerical.

For a system with $Dt/dp=1.5$ the relative positions of the spheres can be intuitively determined as shown in Figure 51. If the above minimization theory holds, then solution to the corresponding set of equations should yield the desired arrangement.

The minimization technique of Luus and Jaakola (1973) was applied to a system of two pellets with $Dt/dp=1.5$. With one pellet fixed at $(0,0,0.5dp)$ and an initial guess on the second pellet's position at $(0.25 \pm 0.125)dp, \pi + \pi, (1.5 \pm 1.0)dp$ their method gave $(r, \theta, z)_2 = (0.25dp, 0.994\pi, 1.366dp)$. The minimization technique of Luus and Jaakola worked equally well for other initial guesses and for two pellets with $Dt/dp=2.0$. But, the technique failed for more complex systems (e.g., $Dt/dp=3.0$ with 7 spheres, one fixed, and hence 18 unknowns). A FORTRAN program for two pellets follows.

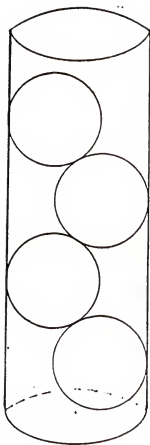


Figure 51: Stacked Arrangement of Spherical Pellets, $D_t/d_p=1.5$

FILE: KKP Emin FORTRAN A1 NORTHEAST REGIONAL DATA CENTER VM/SP RELEASE 3 CMS

```

C THIS PGM FINDS THE MOST DENSE SPHERICAL PELLET PACKING
C CONFIGURATION BY MINIMIZING THE POTENTIAL ENERGY OF THE
C SYSTEM. THAT IS, MINIMIZE THE SUM OF THE HEIGHTS OF
C THE PELLETS, GIVEN THE VARIOUS CONSTRAINTS.
C DIMENSION VARIABLES
C   DIMENSION W(6),R(6),Z(6)
C   COMMON /AA/ X(6),IMAX
C   IMAX = 6
C VARIABLE LIST.
C W-ARRAY--EACH TRIPLET (W(1),W(2),W(3)) REPRESENTS THE
C   R,THETA,Z (RESPECTIVELY) POSITION OF A GIVEN SPHERE
C   W IS THE BEST POINT FROM LAST = START PT. FOR THIS RANGE ITER.
C X-ARRAY--SAME SET-UP AS W-ARRAY; THESE ARE THE TEST VALUES
C Z-ARRAY--SAME SET-UP AS W-ARRAY; THESE ARE THE BEST
C   VALUES AT ANY GIVEN TRIAL WITHIN A GIVEN RANGE ITERATION
C R-ARRAY--RANGES FOR CORRESPONDING W VALUES
C TUBE AND PELLET SIZE DATA
C   DP = 1.0
C   DTP = 2
C   PI = 3.141596
C INITIAL GUESS AT POSITION OF SPHERES
C   W(1) = 0.5*DP
C   W(2) = 0
C   W(3) = DP/2
C   W(4) = 0.25*DP
C   W(5) = PI
C   W(6) = 1.5*DP
C INITIAL RANGES
C   R(1) = 0
C   R(2) = 0
C   R(3) = 0
C   R(4) = 0.25*DP*(DTP-1.)
C   R(5) = PI
C   R(6) = DP
C INITIALIZE OPTIMIZATION PARAMETERS
C JU==>NO. OF TIMES TO REDUCE RANGE SIZE
C KP==>NO. OF POINTS TO TRY WITHIN EACH RANGE ITERATION
C E==>AMOUNT BY WHICH TO REDUCE RANGE IN SUBSEQUENT ITERATIONS
C READ(5,1000)JU,KP,E
C IF(JU.LT.1)GOTO 5000
C WRITE(6,2040)JU,KP,E
C SEED RANDOM NO. GENERATOR
C CALL RSEED(0)
C WRITE HEADINGS AND INITIAL GUESS
C   N = IMAX/3
C   WRITE(6,2000)N
C   WRITE(6,2010)
C   WRITE(6,2020)(W(I),I=1,IMAX)
C CALC FUNCTION AT INITIAL GUESS
C   DO 5 I=1,IMAX
C     X(I) = W(I)
C     CALL FUN(F0)
C WRITE FUNCTION AT INITIAL GUESS
C   WRITE(6,2030)F0
C NOW, CALCULATION AND COMPARISON
C   DO 300 J=1,JU
C     DO 400 K=1,KP
C       PICK TRIAL POINT VIA RANDOM POSITION WITHIN PARAM. RANGES
C       DO 300 I=1,IMAX
C         V = RNDMF(1.0)
C         V = V-0.5
C         X(I) = W(I) + V*R(I)
C CHECK INEQUALITY CONSTRAINTS--ELIMINATE POINT IF DOESN'T WORK.
C   DO 310 I=1,IMAX,3
C     MAX RADIAL POSITION IS (DT-DP)/2...
C     TEST = DP*(DTP-1)/2
C     IF(X(I).LT.0)GOTO 400
C     IF(X(I).GT.TEST)GOTO 400
C     THETA SHOULD BE BETWEEN +/- PI...
C     IF(X(I+1).LT.0)GOTO 400
C     IF(X(I+1).GT.2.0*PI)GOTO 400
C MIN Z POSITION IS DP/2...
C     IF(X(I+2).LT.DP/2.) GOTO 400
C   CONTINUE
C CHECK DISTANCE BETWEEN PELLET CENTERS (CANNOT BE CLOSER THAN TOUCHING)
C   DO 330 L=1,IMAX,3

```

FILE: KAPEMIN FORTRAN A1 NORTHEAST REGIONAL DATA CENTER VM/SP RELEASE 3 CMS

```

      DO 320 M=1,IMAX,3
      IF(L.EQ.M)GOTO 320
      DLM = X(L)*X(L) + X(M)*X(M)
      THETA = X(L+1)-X(M+1)
      DLM = DLM - 2.0*X(L)*X(M)*COS(THETA)
      DIFF = X(L+2)-X(M+2)
      DIFF = DIFF*DIFF
      DLM = DLM + DIFF
      DLM = SORT(DLM)
      IF(DLM.LT.DP/2.0)GOTO 400
320  CONTINUE
330  CONTINUE
C    SELECTED POINT MEETS CONSTRAINTS==>EVALUATE FUNCTION
      CALL FUN(F)
C    CHECK FOR MINIMUM
      IF(F.GE.FO)GOTO 400
C    WE HAVE A NEW MIN
      FO = F
      DO 340 I=1,IMAX
340  Z(I) = X(I)
C    SKIP TO HERE IF CONSTRAINT NOT MET OR FUNCTION NOT MIN
400  CONTINUE
C    HAVE BEST ONE AS STARTING POINT FOR NEXT ROUND OF RANGES
      DO 410 I=1,IMAX
410  W(I) = Z(I)
C    DECREASE RANGES
      R(I) = R(I)*(1.0-E)
C    GO BACK FOR ANOTHER ROUND IN THE SMALLER RANGES
500  CONTINUE
C    WE'RE FINISHED!!!
      WRITE(6,2020)(W(I),I=1,IMAX)
      WRITE(6,2030)FO
C
1000  FORMAT(I3,1X,I3,1X,F5.3)
2000  FORMAT(///,' MINIMIZATION OF POTENTIAL ENERGY BY DIRECT SEARCH',
      1,' , NUMBER OF PELLETS = ',I3)
2010  FORMAT(' , R ',12X,' THETA ',8X,' Z ',/,1X,3(10(' - '),3X))
2020  FORMAT(1X,3(E10.4,3X))
2030  FORMAT(' ---FUNCTION VALUE IS ',E10.4,/)
2040  FORMAT(' OPTIMIZATION PARAM...JU=',I3,' KP=',I3,' EPS=',F5.3)
C
5000  GOTO 9
      STOP
      END
      SUBROUTINE FUN(F)
      COMMON /AA/ X(6),IMAX
      F = 0
      DO 10 I=3,IMAX,3
      F = F + X(I)
10    CONTINUE
      RETURN
      END

```

APPENDIX J
SUGGESTIONS FOR FUTURE WORK

Cell Length and Plug Thickness

The AFM uses porosity profile data to determine axial cell length and radial plug distribution. These parameters alone then determine the velocity profile, flow distribution, and all mass dispersion characteristics. The porosity profiles for uniformly sized spherical pellets packed in cylindrical tubes are well-documented (as discussed in the Mass Dispersion chapter), but (as mentioned in the Heat Dispersion chapter) such details are not readily available for cylindrical pellets. Since many applications involve spheres of non-uniform size distributions or non-spherical pellets, the AFM requires the corresponding porosity profiles to adequately describe such applications. And, even for uniformly sized spheres, the Cohen-Metzner radial and HCP axial porosity profiles may not apply below some small Dt/dp . The research proposed below enables the AFM to account for the effect of pellet shape on mass dispersion.

Objectives

The specific objectives are to evaluate axial and radial porosity profiles for cylindrical tubes packed with spherical pellets:

1. uniformly sized, at low Dt/dp . Below some critical Dt/dp , the previously established profiles may not apply (e.g., for $Dt/dp=1.5$ the axial porosity cycle width is 0.866dp vs 0.816dp for HCP);
2. of known size distribution;
and packed with cylindrical pellets (with the added objective of identifying a simple "shape normalization" parameter, i.e., an effective diameter by which irregular shapes can be equated to spheres):
3. uniformly sized, with each pellet at a known position (similar to the Dt/dp numerical calculation case presented in the Mass Dispersion chapter); this will establish a method of calculating $\epsilon(r,z)$ in the theoretical approach to each of the remaining objectives;
4. uniformly sized, with aspect ratio $l/d=1$; this provides the simplest non-spherical shape;
5. uniformly sized, with aspect l/d other than 1;
6. of known size/shape distribution.

Theoretical Approaches

The exact position of each spherical pellet within a cylindrical tube can be determined by minimizing a potential function as outlined in Appendix I. Each approach below suggests modifying the minimization problem to account for shape irregularities. In each case, the resulting overall bed voidage should be checked against experimental values (measured as below or from available literature data, e.g., Leva and Grummer, 1947b).

For the spherical cases (numbers refer to objectives, above):

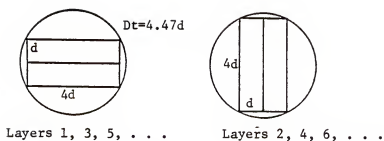
1. optimization as stated in Appendix I since spheres are uniformly sized;
2. modify the minimization problem to include a probability that each pellet will be of certain diameter, e.g., if packing is a mixture of 30% dp_1 and 70% dp_2 then as each pellet is defined select its diameter using a normal distribution and random number. Generate a random number between -1 and +1 at each pellet definition. If the number falls within the $\pm 35\%$ Gaussian limits of zero, then $dp=dp_2$. Otherwise, $dp=dp_1$. Alternatively, define pellets in groups of 10, letting three of them have $dp=dp_1$ and seven have $dp=dp_2$.

For the cylindrical pellet cases:

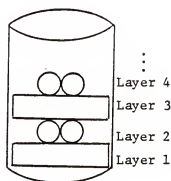
3. develop a procedure for specifying the position of each pellet and for calculating the corresponding $\epsilon(r,z)$. For example, the pellet position may be defined by its centroid and its volume described by the equation for a cylindrical shell surrounding that centroid. Then, axial calculations would involve the intersection of z -planes with the individual cylinders and radial porosity would involve the intersection of a larger cylindrical shell with the individual packing cylinders. Note that, for cylindrical pellets, orientation must also be considered in defining the occupied volume, i.e., the angle between each pellet's axis and the tube axis. In

the simplest cases, all pellets would have the same orientation (e.g., pellet axes perpendicular to tube axis or pellet axes parallel to tube axis). Establish a simple test case, such as pellets with $l/d=4$, with two pellets per layer each in the perpendicular orientation as illustrated in Figure 52. Coordinates can be determined from geometric analysis;

4. including the orientation of each pellet increases the difficulty of the problem--orientation becomes an additional unknown. If pellet shape can be reduced via some effective diameter to a sphere, the problem is greatly simplified. Thus, attempt the minimization in the following steps:
 - a. treat each pellet as a sphere with an effective diameter of $((d^2 + l^2)/2)^{0.5}$. If the overall bed voidage is close to the experimentally measured value, this is a good approximation. If not, try a different normalization (e.g., $dp/4$) until a good match on ϵ_{bed} is attained;
 - b. treat each pellet as a cylinder whose position and volume are defined by the method established in objective 3; note that orientation becomes an additional unknown in the minimization problem. Start with the least complicated case of a 50/50 probability of the parallel or perpendicular orientations. Replace the $f(d_{ij})$ function (used to eliminate packing arrangements which cause two pellets to occupy the same volume) with a volume of overlap function;



TOP VIEWS



SIDE VIEW

Figure 52: Predetermined Packing Geometry for Cylindrical Pellets ($1/d=4$)

- c. include a full distribution of orientation, as opposed to the 50/50 mix. Assign orientations by random numbers within some normal distribution.
- 5. as for objective 4, but with size of each pellet determined from the known distribution as in objective 2;
- 6. as for objective 4;

Experimental Approaches

For each of the objectives listed above, the experimental technique is the same. Care should be taken to pack the tube a few pellets at a time, shaking the tube after each addition to ensure the densest packing. A screen should be placed over the top of the packed section so that pellets do not float during the measurement procedure.

1. Axial profile

- a) water method--described in Appendix C. Pellets must be large enough to allow for accurate reading of the water level.
- b) "wax" method--use cylindrical tubes of disposable material (e.g., commonly available containers for products such as oatmeal or cleanser). Pellets should be of material of known density that can be cut with available tools. Pack the tube as described above, secure top of packed section with screen. Fill container with hot liquid wax (slowly to avoid bubbles) or other material (e.g., epoxy or gelatin) of known density which will not contract on

hardening. Allow filling material to harden and then peel off cardboard container. Cut off ends so that remaining cylinder contains packed section only (no regions of "wax" only). Weigh the entire cylinder and measure its volume. Determine the relative amounts of "wax" and pellet material from density calculations. Cut several discs from cylinder, being sure to record their relative axial position. Each disc should be short enough to give good indication of axial periodicity, e.g., of length $\leq dp/4$. Calculate the porosity of each disc from its density (as for overall bed).

2. Radial profile--use the "wax" method, but instead of cutting discs, shave off smaller annular shells, working from outside inward. After each shaving, weigh the remaining cylindrical core to determine how much mass was lost. The density of the shaved annular shell can then be calculated as the incremental weight loss/incremental volume change. The porosity can be calculated by relating the known densities of the pellet and "wax" materials to the density of that shell.

Packed Section Velocity Profiles

Some question remains as to whether the available velocity profile data truly represent flow within the interstices of the packed section since measurements were taken in the empty tube some distance

beyond the bed exit. The most detailed data are given by Mariovoet et al. (1974) for spherical pellets at a short distance ($0.625d_p$) into the empty tube. AFM predictions closely follow these data, but they are at only one Dt/dp value. Further, such details for cylindrical packing is unavailable. Thus, the following research is proposed to verify the AFM's method for calculating velocity profiles.

Objectives

1. verify AFM method for calculating velocity profiles for spherical and cylindrical pellets;
2. determine effect of pellet roughness on velocity profile;
3. determine range of applicability of AFM method for calculating velocity profiles.

Theoretical Approaches

Objectives 1 and 2--based on the measured (empty tubes) velocity profiles, back out what entrance profile was. Must solve Navier-Stokes (N-S) equations for empty tube. Look to work of Vortmeyer and Winter (1982) as guide; they have solved the N-S equations for set entrance velocity profiles. Or, given exact position and shape of each pellet, solve the N-S equations for velocity profiles in the packed section. (Objective 3--no definitive theoretical approach.)

Experimental Approaches

The technique of Marivoet et al. (1974) can be applied here to achieve all three objectives. Their method uses a revolving point sensor for minimum disturbance to flow pattern during measurement.

1. measure velocity profiles for wide range of Dt/dp and pellet shapes. Compare to AFM predictions;
2. compare measured velocity profiles for smooth and rough pellets of same relative size (i.e., same Dt and same dp). (Should see no difference since roughness will effect all pellets in same way);
3. measure velocity profiles over wide range of flow rates, or Re_p . Look for minimum below which and/or maximum above which the porosity-velocity relationship breaks down. Look for Dt/dp range also (e.g., for $Dt/dp=1.5$, the bulk fluid may "snake" through as one plug, leaving dead spaces, or regions of zero velocity, near the wall).

Applicability of AFM versus Fickian Analogy

The main text of this work shows the AFM to equal or surpass in all mass dispersion and most heat dispersion cases examined here. But, it was also pointed out that while the AFM cannot predict the diffusion-like behavior expected at very low flow rates the Fickian analogy (with axial dispersion) will predict back-mixing where none is observed experimentally. Thus, each model must have a particular range of system variables in which it should be preferred. The degree of turbulence determines whether the AFM will apply to a given situation. Turbulence in packed beds is not well-defined, however, as pointed out in the discussion of Reynolds numbers (Chapter II). The following research is therefore proposed for systems of uniformly-sized spherical packing.

Objectives

1. determine range of flow rates and fluid properties (i.e. some form of Reynolds number) over which AFM best describes dispersion in packed beds;
2. determine range of Dt/dp over which AFM best describes dispersion in packed beds (there may be a maximum above which the Fickian analogy gives satisfactory results).

Experimental Approaches

The same experiments can be used to define dispersion behavior for each of the objectives, above. The simplest experiments are those involving mass dispersion only since the pellets are inert, i.e., they act merely as barriers to flow and do not absorb any mass.

1. The steady-state injection of dye, or tracer material, at some point along the tube centerline can be used to determine the Reynolds number, Re^* , at which back-mixing is observed. Experiments using salt and indicator (as described by Hiby, 1963) should be used as they give visible concentration profiles. Determine Re^* for several Dt/dp values. Then, run steady-state tracer injection experiments for gases (as described by Fahien and Smith, 1955) over range of Re which includes Re^* . Apparatus should be geometrically similar (i.e., same Dt/dp) to system used to determine Re^* . To minimize entrance effects, the tracer injection tube should have a straight section of at least five tube diameters before entering the packed section (as opposed to "angling in" a

- short distance before the packing). Verify the steady-state results with transient F-curve experiments (as described by Danckwerts, 1953) which have no entrance effects. There will probably be some minimum Re (close to Re^*) below which the AFM fails to match experiment (even when the "laminar" hydraulic resistance is used to calculate flow/velocity profiles); in this range, the Fickian analogy with axial dispersion will better describe the observed concentration profiles. And, there will probably be some maximum Re above which both models can describe the observed dispersion behavior. These Re limits, however, probably depend on Dt/dp ;
2. Run both steady-state and transient mass dispersion experiments for low Dt/dp . At very low Dt/dp , the injection tube must be of small size relative to the pellets so that the entrance effect will not obscure meaningful results. Alternatively, at very low Dt/dp , run only the transient experiments since the radial velocity profile determines the shape of the F-curve. There will probably be some minimum Dt/dp below which the Fickian analogy cannot match the data, regardless of Re . There will probably be some maximum Dt/dp above which both the AFM and the Fickian analogy follow the data (given the Re range determined above).

Effect of Pellet Shape on Mass Dispersion

According to the AFM, the only effect pellet shape should have on mass dispersion is via the corresponding porosity-velocity profiles. All systems compared in the Mass Dispersion chapter were for spherical pellets. It is therefore proposed here that both steady-state and transient mass dispersion experiments be carried out for systems of non-spherical pellets for which porosity profiles are known. A wide range of system variables (as described in the previous section) should be examined.

Pellet Heat Transfer Coefficient

Chapter III covered steady-state heating of a packed bed with constant wall temperature. Such cases involve both wall and pellet heat transfer characteristics and any results thus obtained may be coupled. The research proposed here eliminates wall heat transfer to verify the pellet coefficients presented earlier.

Objectives

1. verify the h_p correlation (equation 50)) presented earlier for uniformly sized spherical pellets of low thermal conductivity;
2. verify the shape factor, γ (equation (50)), for cylindrical pellets and determine whether γ depends on aspect ratio of individual pellets;
3. determine effect of mixture of pellet sizes on h_p ;
4. determine the effect of pellet surface roughness on h_p ;

5. determine the effect of fluid properties on h_p ;
6. determine the effect of pellet material properties (e.g., thermal conductivity, specific heat, etc.) on h_p ;
7. verify that tube characteristics do not effect h_p .

Experimental Approaches

Decoupling pellet from wall heat transfer requires an insulated tube. In this case, the simplest heat transfer experiment is analogous to the steady-state injection of tracer material: the steady-state injection of heated fluid at some point along the tube axis. To minimize entrance effects, the injection tube should be small relative to pellet size and should have a straight segment of at least five tube diameters before entering the packed section. Radial temperature profiles should be measured as close as possible to the top of the bed to minimize exit effects. Axial profiles should be obtained by successively adding more packing material (as described by Fahien and Smith, 1955) as opposed to inserting thermowells into the packed section. For each of the objectives, the following details should be observed:

1. run the point-source experiments for a "base case" system (i.e., smooth spherical pellets in smooth tube). The tube material should have a low enough thermal conductivity to be considered insulating (e.g., glass). Otherwise, there will be heat transfer to raise the wall temperature. Examine a wide range of flow rates and pellet sizes to verify the square-root correlation of h_p to (G/d_p) ;

2. run experiments as described for objective 1, using cylindrical pellets;
3. run experiments as described for objective 1 for known size distribution of spherical pellets. Determine whether some additive form of equation (50) can be used or whether new correlation must be developed for each size mixture;
4. run the experiments described for objective 1, but with uniformly sized spherical pellets of varying degrees of surface roughness, e.g., catalyst support material. The value of γ (equation (50)) may be effected by pellet roughness, which can be described--
 - a) visually (qualitative);
 - b) by pellet porosity (an indication of "holes" on the surface;
 - c) by pressure drop relative to smooth tubes of same geometry, i.e., $\text{roughness} = (\Delta P)_{\text{rough}} / (\Delta P)_{\text{smooth}}$ at same Re and Dt/dp ;
5. run experiments for objective 1 with fluids other than air (for which equation (50) was developed). Check correlation with fluid properties such as thermal conductivity, specific heat, etc.;
6. run experiments for objective 1 with materials of increasing thermal conductivity. There will be some maximum at which the

conduction between pellets assumption no longer holds. Below this maximum, however, check correlation of h_p with pellet material properties such as thermal conductivity, specific heat, etc.;

7. run experiments for objective 1 with tubes of different sizes. While materials of varying degrees of surface roughness would be desirable, care should be taken in selecting low thermal conductivity (i.e., insulating) materials for the reasons stated above.

Wall Heat Transfer Coefficient

Once the pellet heat transfer coefficient has been independently verified as described above, the constant wall temperature experiments discussed earlier can be used to verify the AFM h_w correlation. The same results can be used to examine the weighted average for calculating "wall solid plug" temperatures (equation (37)).

Objectives

1. verify h_w correlation form;
2. determine the effect of tube characteristics (e.g., roughness, D_t , D_t/d_p , thermal conductivity, heat capacity, etc.) on h_w ;
3. determine effect of bulk fluid properties (e.g., thermal conductivity, heat capacity, etc.) on h_w ;
4. verify weighted-average calculation of wall solid plug temperatures.

Theoretical Approaches

The complexity of convective film heat transfer precludes strictly theoretical prediction of h_w . However, several alternatives to the "stagnant film" argument leading to the weighted-average temperature should be considered:

1. replace the stagnant film analysis with conduction from wall to solid. Note that not all of wall area would be involved in conduction because of imperfect contact between pellets and tube. The contact area would be determined empirically. This analysis would lead to some constant value for the equivalent of $a(s,w)h^*$, or a weighting that would vary with flow rate, G ;
2. consider conduction (rather than convection) through the stagnant film. Film may not be strictly stagnant, so that its thickness will depend on flow rate, G . This analysis would lead to a flow-dependent equivalent of $a(s,w)h^*$, or a weighting that would remain essentially independent of flow rate. Look to boundary-layer theory as guide to determining film thickness.

Experimental Approaches

Each of the above objectives can be examined by the constant wall temperature experiments described by Yagi and Wakao (1959). Radial and axial temperature profiles and bulk outlet temperatures should be measured for each run. Radial profiles should be measured as close

as possible to the top of bed to avoid exit effects. Axial profiles should be obtained by adding packing, as opposed to inserting thermowells, to avoid disturbances to packing geometry.

3. Select a base case as described in Chapter III (e.g., smooth tube, smooth uniformly sized pellets). Run the experiments, covering a wide range of flow rates. Compare to AFM results using the independently determined h_p (previous section) and the 10%-90% weighting given in Chapter III. If $(\log h_w) - (\log G)$ plot exhibits such scatter, either correlation form is invalid or weighting (for wall solid plug) may be function of flow rate (as described in Theoretical Approaches, above). Run for several pellet sizes;
4. run the experiments as described for objective 1, varying tube size (with constant D_t/d_p), tube size (with changing D_t/d_p), and tube material. Check correlation of h_w with these parameters;
5. run experiments for objective 1 but with fluids other than air (for which all cases discussed in Chapter III were run). Check correlation of h_w with fluid properties;
6. this objective is incorporated into the experiments for objective 1;

AFM as a Reactor Design Tool

The AFM has particular applicability to situations where ordered flow can be expected, such as low Dt/dp . Such situations are common in applications involving highly exothermic catalytic reactions where only a few pellets are placed across the tube diameter to facilitate cooling. It was shown earlier that the AFM and Fickian analogy predict different behavior for catalytic reaction within the pellets of packed beds. Thus, the following research is proposed.

Objectives

1. check the AFM's ability to match laboratory data for reaction in beds packed with spherical catalyst pellets;
2. check the AFM's ability to predict hot spots in wall-cooled reactors;
3. evaluate the AFM as a reactor design tool.

Experimental Approaches

For each of the above objectives, the deoxygenation of ethylene oxide to ethylene is proposed as the test reaction since its kinetics have been previously determined (Hong, 1984; Akella, 1983).

1. run the reaction at concentrations and flow rates that mesh with AFM assumptions (i.e., diffusion-limited, no back-mixing, etc.). First, run adiabatic reactions (if possible without instabilities) so that there is no wall heat transfer effect and some of the AFM assumptions can be verified. Next, run with constant wall temperature so that hw correlations and other related assumptions can be verified. Spherical pellets

should be used since porosity and velocity profiles are well-understood. Radial, axial, and bulk-averaged outlet profiles of concentration and temperature should be measured for each experiment. Radial profiles should be taken as close as possible to the top of the bed (to avoid exit effects) and axial profiles should be measured by successively adding packing (to avoid disturbance to packing geometry). Several values of Dt/dp should be tried to check the effect of flow distribution on conversion;

2. run the reactions as described for objective 1, but at more severe conditions and constant coolant (wall) temperature. Increase bed depth and/or vary reaction conditions until a hot spot (axial peak) in temperature is observed. Check against AFM predictions;
3. the example problems presented in Chapter IV suggest instabilities at the centerline can occur before they occur in the outer regions of the tube. This suggests that, in cases with such severe conditions, it may be advantageous to pack the bed with inert (non-reacting) pellets along the tube axis surrounded by active catalytic pellets. According to the AFM, little conversion would be lost because of the small proportion of the total fluid which flows near the bed center. If the AFM proves successful in following the reaction data described for objectives 1 and 2, above, its ability to suggest such alternatives to normal operating procedure should be exploited.

APPENDIX K
FORTRAN PROGRAM LISTINGS

Steady-state Mass Dispersion

The following program consists of a main calling routine and several subroutines. Program flow is as follows:

1. determine radial subdivisions RA(I) and RB(I) given Dt/dp and porosity about which radial cycles oscillate (EBAR) (subroutine VOID performs numerical integration of porosity function EFUNC);
2. subdivide flows G(I) according to void cross-sectional areas A(I) and hydraulic radii RH(I) (subroutine ANN does this; two versions are included--the first version is for turbulent and the second for laminar hydraulic resistances);
3. calculate velocities;
4. determine weighting factors for mixing W(I) (subroutine MIX1);
5. initialize concentrations C(I);
6. march down reactor from inlet to outlet, transversing NLONG axial cells (NOTE: run cases with NLONG=1 for trial and error on the value of EBAR which gives the desired overall bed voidage, then run for the entire bed length to get concentration profiles).

a) A-to-B transition (subroutine MIX2 with ITRANS=0)

b) B-to-A transition (subroutine MIX2 with ITRANS=1)

Other variables and program steps are commented in the listing.

All flow, area, and radius variables are scaled by total flow, total tube cross-section, and tube radius, respectively.

```

C   PROGRAM NAME 'AAPVJ FORTRAN'
C
C   -----
C   THIS RUN FOR DATA OF LATINEN
C   4-INCR PIPE
C   -----
C   LAST UPDATE/USE ON 19 MAY 85
C   DIMENSION D(10)
C   DIMENSION Q(100),R(100),A(100),VEL(100)
C   DIMENSION W(100),C(100)
C   DIMENSION RA(100),RB(100)
C   THIS PROGRAM CALCULATES FLOWS AND CONCENTRATIONS GIVEN
C   ANNULUS DIMENSIONS.
C
C   DATA NLONG,NPRINT /1,0/
C   DATA C /100*0.0/
C   DATA W0,D /1, 12.8, 11.1, 13.3, 25.6, 6*0.0/
C   DATA R /100*0.0/
C   DATA FUDGE /0.05/
C   CALC AREAS BASED ON DTPD AND EA
C   DTPD = 13.2
C   DO 10 I=1,100
C   W(I) = 20.0
C   Z = DTPD + 0.5
C   NOW, TRY ASSIGNING NO. CELLS BASED ON CORRELATION...
C   Z = DTPD/0.816 + 0.5
C   N = Z
C   Z = N
C   Z = 0.5*Z
C   NB = Z
C   NA = N-NB
C   RESTRICT TO EVEN NO. SEGMENTS
C   IF (NA .GT. NB) NB = NA
C   N = NA+NB
C   WRITE(6,2020) DTPD,N,NA,NB
C   SIZE RADII
C   SET DP TO DO INCREASING EA'S...
C   SIZE EVENLY SPACED RADII
C   ZN = N/2
C   DELB = 1.0/ZN
C   R(2) = DELB
C   DO 80 I=4,N,2
C   R(I) = R(I-2) + DELB
C   CONTINUE
C   DETERMINE EPS FOR EACH SEGMENT...
C   EBAR = 0.3600
C   VOID FRACTION OF FIRST SEGMENT
C   CALL VOID(100,DTPD,0.0,R(2),EBAR,E1)
C   I=2
C   WRITE(6,2010) I,E1
C   100 RA(I) = (1.0-E1)*R(2)*R(2)
C   RA(I) = SQRT( RA(I) )
C   RB(I) = E1*R(2)*R(2)
C   RB(I) = SQRT( RB(I) )
C   NAL = N-1
C   DO 120 I=3,NAL,2
C   VOID FRACTIONS OF RADIAL CELLS BASED ON CORRELATION
C   RHC2 = R(I+1)
C   RHO1 = R(I-1)
C   CALL VOID(100,DTPD,RHO1,RHO2,EBAR,EHAT)
C   IS = I+1
C   WRITE(6,2010) IS,EHAT
C   XI = R(I+1)*R(I+1) - R(I-1)*R(I-1)
C   RA(I) = (1.0-EHAT)*XI
C   RA(I) = R(I-1)*R(I-1) + RA(I)
C   RA(I) = SQRT( RA(I) )
C   RB(I) = EHAT * XI
C   RB(I) = R(I-1)*R(I-1) + RB(I)
C   RB(I) = SQRT( RB(I) )
C   120 CONTINUE
C   NAI = N-1
C   WRITE(6,2150)
C   WRITE(6,2160) (RA(I),R(I+1),I=1,NAI,2)
C   WRITE(6,2160) (RB(I),R(I+1),I=1,NAI,2)
C   CALL ANR(NA,NB,G,B,A,B1,B2,BA,RB)
C   N = NA+NB
C   DO 200 I=1,N
C   VEL(I) = E1*Q(I)/A(I)
C   WRITE RESDLTS

```

```

WRITE(6,2050)
IF (NA .GT. NB) GOTO 390
DO 300 I=2,N,2
J=I-1
WRITE(6,2060) I,A(I),Q(I),VEL(I),J,A(J),Q(J),VEL(J)
300 CONTINUE
WRITE(6,2070) B1,B2
GOTO 410
390 CONTINUE
NAX = N-1
DO 400 I=1,NAX,2
J = I+1
WRITE(6,2060) I,A(I),Q(I),VEL(I),J,A(J),Q(J),VEL(J)
400 CONTINUE
WRITE(6,2060) N,A(N),Q(N),VEL(N)
WRITE(6,2070) B1,B2
410 CONTINUE
WRITE(6,2150)
WRITE(6,2160) (R(I),I=1,N)
CALL MIX1(NA,NB,Q,W)
WRITE(6,2170)
WRITE(6,2160) (W(I),I=1,N)
IF (NA .GT. NB) C(1) = 4.1E-3/Q(1)
IF (NA .EQ. NB) C(2) = 4.1E-3/Q(2)
N = NA + NB
C NOW, CALC CONCENTRATIONS...
WRITE(6,2230)
KCOUNT = 0
500 KOUNT1 = KCOUNT+1
IF (KCOUNT .GT. NLONG) GOTO 1000
IF (KOUNT1 .LT. 2) GOTO 510
CALL MIX2(I,NA,NB,Q,W,C)
510 CALL MIX2(Q,NA,NB,Q,W,C)
IF (KOUNT1 .LT. NPRINT) GOTO 710
WRITE(6,2240) KCOUNT
IF (NA .GT. NB) GOTO 690
C CALC AVG CONC IN EACH HALF-CELL FOR NA>NB (N=>A'S EVEN)
CABAR = 0
CEBAR = 0
DO 520 I=2,N,2
CABAR = CABAR + C(I)*Q(I)
CEBAR = CEBAR + C(I-1)*Q(I-1)
520 CONTINUE
DO 600 I=2,N,2
J = I-1
CA = C(I)/CABAR
CB = C(J)/CEBAR
WRITE(6,2250) I,C(I),CA,J,C(J),CB
600 CONTINUE
GOTO 710
690 CONTINUE
C CALC AVG CONC IN EACH HALF-CELL FOR NA>NB (N=>A'S ODD)
CABAR = 0
CEBAR = 0
NAX = N-1
DO 695 I=2,NAX,2
CABAR = CABAR + C(I-1)*Q(I-1)
CEBAR = CEBAR + C(I)*Q(I)
695 CONTINUE
CABAR = CABAR + C(N)*Q(N)
NAX = N-1
DO 700 I=1,NAX,2
J = I+1
CA = C(I)/CABAR
CB = C(J)/CEBAR
WRITE(6,2250) I,C(I),CA,J,C(J),CB
700 CONTINUE
CA = C(N)/CABAR
WRITE(6,2250) N,C(N),CA
710 CONTINUE
GOTO 500
1000 CONTINUE
C FORMATS. . .
2010 FORMAT(' I =',I4,' EPS =',E11.4)
2015 FORMAT(' ALPHA =',E11.4)
2020 FORMAT(' DTDP =',E11.4,' N =',I3,' NA =',I3,' NB =',I3)
2030 FORMAT(' D1/B =',E11.4)
2040 FORMAT(' F =',E11.4)
2050 FORMAT(20I,'A',43I,'B',/,2X,40(' - '),2X,40(' - '),/,
1 2(2X,'I',7X,'A',11X,'P',9X,'VEL ',5X),/,

```

```

DUM00810
DUM00820
DUM00830
DUM00840
DUM00850
DUM00860
DUM00870
DUM00880
DUM00890
DUM00900
DUM00910
DUM00920
DUM00930
DUM00940
DUM00950
DUM00960
DUM00970
DUM00980
DUM00990
DUM01000
DUM01010
DUM01020
DUM01030
DUM01040
DUM01050
DUM01060
DUM01070
DUM01080
DUM01090
DUM01100
DUM01110
DUM01120
DUM01130
DUM01140
DUM01150
DUM01160
DUM01170
DUM01180
DUM01190
DUM01200
DUM01210
DUM01220
DUM01230
DUM01240
DUM01250
DUM01260
DUM01270
DUM01280
DUM01290
DUM01300
DUM01310
DUM01320
DUM01330
DUM01340
DUM01350
DUM01360
DUM01370
DUM01380
DUM01390
DUM01400
DUM01410
DUM01420
DUM01430
DUM01440
DUM01450
DUM01460
DUM01470
DUM01480
DUM01490
DUM01500
DUM01510
DUM01520
DUM01530
DUM01540
DUM01550
DUM01560
DUM01570
DUM01580
DUM01590
DUM01600

```

```

2 1X,2('---',2X,3('-----',2X))          D0M0 1610
2060 FORMAT(1X,2(I3,2X,3(E10.4,2X))          D0M0 1620
2070 FORMAT(' E1 = ',E11.4,' E2 = ',E11.4)    D0M0 1630
2150 FORMAT(' RADII...')                      D0M0 1640
2160 FORMAT(5(2X,E11.4))                      D0M0 1650
2170 FORMAT(' SLICHO WEIGHT FACTORS. . .')    D0M0 1660
2230 FORMAT(9X,'A',30X,'B',/,2(2X,29('---'))/, D0M0 1670
1 2X,2(1X,'X',BX,'C',7X,3X,'C/CAYG',4X),/,   C0M0 1680
2 2X,2('---',2X,'-----',2X,'-----',2X)) D0M0 1690
C23456789.123456789.123456789.123456789.    D0M0 1700
2240 FORMAT(' CELL NO ',I5)                   D0M0 1710
2250 FORMAT(2X,2(I3,2X,E11.4,2X,E11.4,2X))    D0M0 1720
2260 FORMAT(' NA = ',E11.4,' EBD = ',E11.4)    D0M0 1730
2270 FORMAT(' CALC. INVALID VOID REACT. PGM ABORTED ') D0M0 1740
2290 FORMAT(' F = ',E11.4,' SUM = ',E11.4,' EPS1 = ',E11.4) D0M0 1750
STOP                                           D0M0 1760
END                                           C0M0 1770

C                                           D0M0 1780
SUBROUTINE ANN(NA,NB,Q,R,A,E1,E2,RA,RB)      D0M0 1790
DIMENSION BA(100),BB(100)                  D0M0 1800
DIMENSION Q(100),B(100),BB(100),A(100)     C0M0 1810
C CALC HYDRAULIC RADII, AND AREAS          D0M0 1820
N = NA + NB                                C0M0 1830
C A HALF-CELL                               C0M0 1840
DO 10 I=2,N,2                               C0M0 1850
  RR(I) = B(I) - BA(I-1)                   D0M0 1860
  A(I) = R(I)*R(I) - BA(I-1)*RA(I-1)        D0M0 1870
10 CONTINUE                                 C0M0 1880
C B HALF-CELL                               C0M0 1890
  BB(1) = BB(1)                             D0M0 1900
  A(1) = BB(1)*RB(1)                         C0M0 1910
  MAX = N-1                                 C0M0 1920
  DO 20 I=3,MAX,2                           D0M0 1930
    BB(I) = BB(I) - B(I-1)                   C0M0 1940
    A(I) = BB(I)*RB(I) - B(I-1)*R(I-1)       D0M0 1950
20 CONTINUE                                 C0M0 1960
C NOW, DETERMINE FLOWS AND POROSITIES OF A AND B SEGMS D0M0 1970
C DEPENDS ON NA AND NB                      D0M0 1980
IF (NA .LE. NB) GOTO 500                   D0M0 1990
C THIS SECTION FOR NA GT NB                D0M0 2000
C FLOW DISTRIBUTION AND POROSITY           D0M0 2010
  E1 = 0.0                                  D0M0 2020
  SUM = 0.0                                  D0M0 2030
  DO 100 I=1,N,2                             D0M0 2040
    E1 = E1 + A(I)                            D0M0 2050
    SUM = SUM + A(I)*SQRT(BB(I))              C0M0 2060
    DO 110 I=1,N,2                             D0M0 2070
      Q(I) = A(I)*SQRT(BB(I))/SUM             D0M0 2080
110 CONTINUE                                 C0M0 2090
C B SEGMENT                                C0M0 2100
  E2 = 0.0                                  C0M0 2110
  SUM = 0.0                                  C0M0 2120
  N1 = N-1                                   C0M0 2130
  DO 120 I=2,N1,2                             C0M0 2140
    E2 = E2+A(I)                              C0M0 2150
120 CONTINUE                                 C0M0 2160
    IX = A(I-1)*SQRT(BB(N-1))                 C0M0 2170
    IY = A(N-3)*SQRT(BB(N-3))                 C0M0 2180
    Q(N-1) = Q(N) + Q(N-2)*IX/(IX+IY)          C0M0 2190
    IX = A(2)*SQRT(BB(2))                     C0M0 2200
    IY = A(4)*SQRT(BB(4))                     C0M0 2210
    Q(2) = Q(1) + Q(3)*IX/(IX+IY)              D0M0 2220
    MAX = N-3                                  C0M0 2230
C DON'T NEED FOLLOWING IF N .LE. 5          C0M0 2240
IF (N .LE. 5) GOTO 1000                    C0M0 2250
DO 130 I=4,MAX,2                             C0M0 2260
  IX = A(I)*SQRT(BB(I))                       C0M0 2270
  IY = A(I-2)*SQRT(BB(I-2))                   D0M0 2280
  ZZ = A(I+2)*SQRT(BB(I+2))                   C0M0 2290
  Q(I) = Q(I-1)*IX/(IX+IY) + Q(I+1)*IX/(IX+ZZ) D0M0 2300
130 CONTINUE                                 C0M0 2310
GOTO 1000                                    D0M0 2320
500 CONTINUE                                 D0M0 2330
C THIS SECTION FOR NA=NB                   C0M0 2340
C FLOW DISTRIBUTION AND POROSITY           D0M0 2350
C A-SEGMENT                                C0M0 2360
  SUM = 0.0                                  C0M0 2370
  E1 = 0.0                                  C0M0 2380
  DO 510 I=2,N,2                             D0M0 2390
    E1 = E1 + A(I)                            C0M0 2400

```

```

510  S0N = S0N + A(I)*SQRT(R0(I))
      00 520 I=2,N,2
      Q(I) = A(I)*SQRT(R0(I))/S0N
520  CONTINUE
C  H-SEG
      Z2 = 0.0
      S0N = 0.0
      N1 = N-1
      DO 530 I=1,N1,2
      Z2 = Z2+A(I)
530  CONTINUE
C  TRY SUBDIVIDING BASED ON SQRT(R0)
C  --INSTEAD OF A*SQRT(R0)
      IX = A(N-1)*SQRT(R0(N-1))
      IY = A(N-3)*SQRT(R0(N-3))
      Q(N-1) = Q(N) + Q(N-2)*IX/(IX+IY)
      IX = A(1)*SQRT(R0(1))
      IY = A(3)*SQRT(R0(3))
      Q(1) = Q(2)*IX/(IX+IY)
      N1 = N-3
C  DON'T NEED FOLLOWING IF N .LE. 4
      IF (N .LE. 4) GOTO 1000
      DO 540 I=3,N1,2
      IX = A(I)*SQRT(R0(I))
      IY = A(I-2)*SQRT(R0(I-2))
      ZZ = A(I+2)*SQRT(R0(I+2))
      Q(I) = Q(I-1)*IX/(IX+IY) + Q(I+1)*IY/(IY+ZZ)
540  CONTINUE
1000  RETURN
      END
C
      SUBROUTINE VOID (NDIV,DTDP,R001,R002,EBAR,EPS)
      ZNDIV = NDIV
      DELR = (R002 - R001) / ZNDIV
      ROLD = R001
      FOLD = R001*EFUNC(R001, DTDP, EBAR)
      S0N = 0.0
      DO 100 I=1,NDIV
      RNEW = ROLD + DELR
      FNEW = ENEW + EFUNC(RNEW, DTDP, EBAR)
      FINT = 0.5*DELR*(FNEW + FOLD)
      S0N = S0N + FINT
      FCID = FNEW
      ROLD = RNEW
100  CONTINUE
      VIOT = R002*R002 - R001*R001
      EPS = S0N
      EPS = 2.0*EPS/VIOT
      RETURN
      END
C
      FUNCTION EFUNC(R, DTDP, EBAR)
      PI = 2.0*ABSIN(1.0)
      A1 = 0.3463
      A2 = 0.4273
      A3 = 2.4509
      A4 = 2.2011
      I = 0.5*OTDP*(1.0-R)
      IF (I .LT. 0.25) GOTO 100
      IY = COS( (A3*I-A4)*PI )
      IY = A1*IY/EXP(A2*I)
      EFUNC = (1.0-EBAR)*IY + EBAR
      GOTO 1000
100  CONTINUE
C  THIS SECTION FOR 'WALL' REGION
      IY = 7.0*I*L/9.0
      IY = 4.5*(I-IY)
      IY = (1.0-EBAR)*IY
      EFUNC = 1.0-IY
1000  RETURN
      END
C
      SUBROUTINE FINDP(X,D1R,P)
C  DIRECT SEARCH FOR ROOT OF POLYNOMIAL.
C  WILL LIMIT TO P BETWEEN 1 AND 5
C  WILL SEARCH IN INCREMENTS OF 0.01
      DELP = 0.005
      P = 1.0-DELP
10  P = P + DELP
      IF (P .LE. 5.0) GOTO 20

```

```

C CAN'T FIND ROOT OF EQ'N; ABOUT PROGRAM          C0P03210
WRITE(6,15) N,DIR                                C0M03220
15  FORMAT(' ***** PGM ABORTED IN SUBROUTINE FINDF.',/,
      1 ' NO ROOT TO POLYNOMIAL FOR N=',I3,' D1/R=',E11.4)
      STOP                                          C0C03230
20  SUM = 1.0                                     C0P03240
      TERM = 1.0                                  C0M03250
      DO 30 I=2,N                                C0P03260
      TERM = TERM * F                              C0M03270
      SUM = SUM + TERM                             C0P03280
30  CONTINUE                                       C0M03290
      TEST = 1.0/D18                               C0P03300
      IF (SUM .GE. TEST) GOTO 100                 C0M03310
      GOTO 10                                       C0P03320
100  RETURN                                         C0M03330
      END                                           C0P03340
C                                                    C0M03350
C SUBROUTINE MIX1(NA,NB,Q,W)                      C0P03360
C THIS SUBROUTINE DETERMINES HEIGHT FACTORS FOR  C0M03370
C MIXING AT ANNULUS INLETS                       C0P03380
C DIMENSION Q(100),W(100)                       C0M03390
      N = NA+NB                                    C0P03400
      IF (NA .LE. NB) GOTO 200                    C0M03410
C THIS SECTION FOR NA GT NB                      C0P03420
C ZERO WEIGHTS FOR ODD NUMBERED SEGMENTS         C0M03430
      W(N) = 0.0                                  C0P03440
      W(1) = 1.0                                  C0M03450
      N2 = N-2                                     C0P03460
      DO 10 I=3,N2,2                               C0M03470
      I1 = N2 - I + 3                              C0P03480
      W(I1) = ( Q(I1+1) - (1.0-W(I1+2)) * Q(I1+2) ) / Q(I1)
10  CONTINUE                                       C0M03490
      GOTO 1000                                    C0P03500
200  CONTINUE                                       C0M03510
C THIS SECTION FOR NA = NB                      C0P03520
C ZERO WEIGHTS FOR EVEN NUMBERED SEGMENTS         C0M03530
      W(N) = 0.0                                  C0P03540
      N2 = N-2                                     C0M03550
      DO 300 I=2,N2,2                              C0P03560
      I1 = 2-I+N2                                  C0M03570
      W(I1) = ( Q(I1+1) - (1.0-W(I1+2)) * Q(I1+2) ) / Q(I1)
300  CONTINUE                                       C0P03580
1000  CONTINUE                                       C0M03590
      RETURN                                         C0P03600
      END                                           C0M03610
      SUBROUTINE MIX2(ITRANS,NA,NB,Q,W,C)          C0P03620
      DIMENSION W(100),Q(100),C(100)             C0M03630
C THIS SUBROUTINE DETERMINES ANNULUS INLET CONCENTRATIONS
C ITRANS=0=>A TO B TRANSITION                    C0P03640
C =1=>B TO A TRANSITION                          C0M03650
      N = NA+NB                                    C0P03660
      IF (NA .LE. NB) GOTO 500                     C0M03670
C THIS SECTION FOR NA GT NB                      C0P03680
      IF (ITRANS .NE. 0) GOTO 200                  C0M03690
C A TO B TRANS                                    C0P03700
C B'S ARE EVEN NUMBERED SUBSCRIPTS               C0M03710
      N1 = N-1                                     C0P03720
      DO 100 I=2,N1,2                              C0M03730
      C(I) = (1.0-W(I+1)) * Q(I+1) * C(I+1)
      C(I) = C(I) + W(I-1) * Q(I-1) * C(I-1)
100  CONTINUE                                       C0P03740
      RETURN                                         C0M03750
200  CONTINUE                                       C0P03760
C B TO A TRANS                                    C0M03770
C A'S ARE ODD NUMBERED SUBSCRIPTS                C0P03780
      C(1) = C(2)                                  C0M03790
      C(N) = C(N-1)                                C0P03800
      N2 = N-2                                     C0M03810
      DO 300 I=3,N2,2                              C0P03820
      C(I) = (1.0-W(I)) * C(I-1) + W(I) * C(I+1)
300  CONTINUE                                       C0M03830
      RETURN                                         C0P03840
500  CONTINUE                                       C0M03850
C THIS SECTION FOR NA=NB                         C0P03860
      IF (ITRANS .NE. 0) GOTO 700                  C0M03870
C A TO B TRANS                                    C0P03880
C B'S ODD NUMBERED SUBSCRIPTS                    C0M03890
      C(1) = C(2)                                  C0P03900
      N1 = N-1                                     C0M03910

```

	DO 600 I=3,N1,2	COMQ0010
	C(I) = (1.0-W(I+1))*Q(I+1)*C(I+1)	COMQ0020
	C(I) = C(I) + W(I-1)*Q(I-1)*C(I-1)	COMQ0030
	C(I) = C(I) / Q(I)	COMQ0040
600	CONTINUE	COMQ0050
	RETURN	COMQ0060
700	CONTINUE	COMQ0070
C	O TO A TRANSITION	COMQ0080
C	A'S EVEN NUMBERED SUBSCRIPTS	COMQ0090
	C(N) = C(N-1)	COMQ0100
	N2 = N-2	COMQ0110
	DO 800 I=2,N2,2	COMQ0120
	C(I) = W(I)*C(I+1) + (1.0-W(I))*C(I-1)	COMQ0130
800	CONTINUE	COMQ0140
	RETURN	COMQ0150
	END	COMQ0160

```

      SUBROUTINE ANN(NR,Q,3,A,Z1,Z2,RA,RB)
      DIMENSION RA(100),RB(100)
      DIMENSION Q(100),R(100),RH(100),A(100)
      C CALC HYDRAULIC RADII, AND AREAS
      N = NA + RB
      C A HALF-CELL
      DO 10 I=2,N,2
      RH(I) = R(I) - RA(I-1)
      A(I) = R(I)*RH(I) - RA(I-1)*RA(I-1)
      C CONTINUE
      C B HALF-CELL
      RH(1) = RB(1)
      A(1) = RB(1)*RB(1)
      NAI = N-1
      DO 20 I=3,NAI,2
      RH(I) = RB(I) - R(I-1)
      A(I) = RB(I)*RB(I) - R(I-1)*R(I-1)
      C CONTINUE
      C NOW, DETERMINE FLOWS AND POROSITIES OF A AND B SEGS
      C DEPENDS ON NA AND NB
      C *****
      C ASSUME NA = NB
      C
      C THIS SECTION FOR NA=NB
      C FLOW DISTRIBUTION AND POROSITY
      C A-SEGMENT
      S0A = 0.0
      Z1 = 0.0
      DO 510 I=2,N,2
      Z1 = Z1 + A(I)
      S0A = S0A + A(I)*RH(I)*RB(I)
      DO 520 I=2,N,2
      Q(I) = A(I)*RH(I)*RB(I)/S0A
      C CONTINUE
      C B-SEG
      C USE FACTOR TO ACCOUNT FOR WEIRD RESISTANCES AT WALL AND C.L.
      Z2 = 0.0
      S0B = 0.0
      N1 = N-1
      DO 530 I=1,N1,2
      Z2 = Z2+A(I)
      C CONTINUE
      C ---WALL RESISTANCES---
      FACWR = 1.0
      XI = A(N-1)*RH(N-1)*RH(N-1)
      YI = A(N-3)*RH(N-3)*RH(N-3)
      STOPF = Q(N-2) * XI/(XI + FACTOR*YI)
      Q(N-1) = Q(N) + STOPF
      IX = A(N-3)*RH(N-3)*RH(N-3)
      YI = A(N-5)*RH(N-5)*RH(N-5)
      Q(N-3) = Q(N-2) - STOPF + Q(N-5)*XI/(XI+YI)
      C ---CENTERLINE RESISTANCES---
      FACCLR = 1.0
      XI = A(1)*RH(1)*RH(1)
      YI = A(3)*RH(3)*RH(3)
      Q(1) = Q(2)*XI*FACTOR/(XI*FACTOR + YI)
      IX = A(3)*RH(3)*RH(3)
      YI = A(5)*RH(5)*RH(5)
      Q(3) = Q(2) - Q(1) + Q(5)*XI/(XI+YI)
      NAI = N-5
      C CAN'T HANDLE ANYTHING LESS THAN 8 RADIAL DIVS...
      IF( N .LT. 8)GOTO 550
      DO 540 I=5,NAI,2
      XI = A(I)*RH(I)*RH(I)
      YI = A(I-2)*RH(I-2)*RH(I-2)
      Z2 = A(I+2)*RH(I+2)*RH(I+2)
      Q(I) = Q(I-1)*XI/(XI+YI) + Q(I+1)*XI/(XI+Z2)
      C CONTINUE
      GOTO 1000
      C CONTINUE
      WRITE(6,560)
      560 FORMAT('.....PGM ABORT IN -ANN-. N .LT. 8.....')
      1000 RETURN
      END

```


Transient Mass Dispersion

General program flow builds a time step loop around the steady-state calculations. Concentration becomes a triple-subscripted array as explained in the listing. Additional subroutines are:

1. STEP--shifts delay time arrays;
2. DELTA--determines number of delay elements (time steps)

NSUB (I) corresponding to each radial plug.

Variables (TDEAD(I) correspond to delay times. Additional information is provided by the comments contained within the listing. All time variables are scaled by bed hold-up time (ignore any spurious comment statements in the listing to the contrary).

```

C PROGRAM NAME 'PLSV3 FORTRAN'
C
C -----
C THIS BOX FOR DATA OF CALDS AND FRAUSNITZ
C
C LAST UPDATE/USE ON 30 APR 85
C
C TRANSIENT AAP MODEL
C SUBSCRIPTS ON C(I,J,K)--
C I=RADIAL POSITION
C J=AXIAL POS (A/R CELL NO.)
C K=TIME STEPS (FOR DEAD TIME PURPOSES)
C CORRCN /ONE/ RA(21),RB(21),R(20)
C CORRCN /TWO/ Q(20), A(20), W(20)
C CORRCN /FIVE/ C(20,118,50), CIR(20,118)
C CORRCN /FOUR/ TDEAO(20),NSUB(20)
C DIMENSION DUMMY(20),VHL(20),EPS(20)
C
C IOPT =0--PRINT ONLY AVG CONC AT EACH TPRINT
C =ANYTHING ELSE, PRINT EVERYTHING AT EACH TPRINT
C
C DATA IOPT /0/
C
C -----
C THIS SECTION SIZES ANNULI, CALCS FLOWS, VELOCITIES, ETC.
C
C -----
C CALC AREAS BASED ON OTOP AND EA
C DTEP = 15.9
C DO 10 I=1,20
C   W(I) = 20.0
10 NOW, TRY ASSIGNING NO. CELLS BASED ON CORRELATION...
C   Z = OTDP/0.816 + 0.5
C   N = Z
C   Z = N
C   Z = 0.5*Z
C   NB = Z
C   NA = N-NB
C RESTRICT TO EVEN NO. SEGMENTS
C IF (NA .GT. NB) NB = NA
C N = NA+NB
C WRITE(6,3020) DTEP, N, NA, NB
C SIZE RACII
C SET UP TO DO INCREASING EA'S...
C SIZE EVENLY SPACED RADII
C   ZB = W/2
C   DELB = 1.0/ZB
C   R(2) = DELB
C   DO 80 I=N,2
C   R(I) = R(I-2) + DELB
80 CONTINUE
C DETERMINE EPS FOR EACH SEGMENT...
C   EBAR = 0.360
C VOID FRACTION OF FIRST SEGMENT
C   CALL VOID(100,DTEP,0.0,R(2),EBAR,Z1)
C   I=2
C   WRITE(6,3010) I, Z1
C
C ***** TEST--LOWER VELOCITY BY MULT TIMES POROSITY *****
C   EPS(2) = E1
C   EPS(1) = E1
100 RA(1) = (1.0-E1)*R(2)*R(2)
C   RA(1) = SQRT( RA(1) )
C   RB(1) = E1*R(2)*R(2)
C   RB(1) = SQRT( RB(1) )
C   MAX = N-1
C   DO 120 I=3,MAX,2
C   VOID FRACTIONS OF RADIAL CELLS BASED ON CORRELATION
C   RHC2 = R(I+1)
C   RHO1 = R(I-1)
C   CALL VOID(100,DTEP,RHO1,RHO2,EFAR,EHAT)
C   IW = I+1
C   WRITE(6,3010) IW, EHAT
C   EPS(IW) = EHAT
C   EPS(I) = EHAT

```

```

IX = R(I*1)*R(I*1) - R(I-1)*R(I-1)
RA(I) = (1.0-IRAT)*XI
RA(I) = R(I-1)*R(I-1) + RA(I)
RA(I) = SQRT( RA(I) )
RB(I) = ERAT * XI
RB(I) = R(I-1)*R(I-1) + RB(I)
RB(I) = SQRT( RB(I) )
120 CONTINUE
NAI = N-1
WRITE(6,3150)
WRITE(6,3160) (RA(I),R(I*1),I=1,NAI,2)
WRITE(6,3160) (RB(I),R(I*1),I=1,NAI,2)
CALL ANN(NA,RB,E1,E2)
N = NA+NB
CCC DO 200 I=1,N
C200 VEL(I) = Q(I)/A(I)
C*****
C TEST CALCULATING VELOCITY BY SIMPLE RATIO OF EPS/EDAR...
C*****
DC 210 I=1,N
CCC VEL(I) = EPS(I)/E1
CCC VEL(I) = VEL(I)*VEL(I)
C *---*--- BACK TO OLD WAY *---*---
VEL(I) = E1*Q(I)/A(I)
210 CONTINUE
C WRITE RESULTS
WRITE(6,3050)
IF ( NA .GT. NB)GOTO 390
DO 300 I=2,N,2
J=I-1
WRITE(6,3060) I,A(I),Q(I),VEL(I),J,A(J),Q(J),VEL(J)
300 CONTINUE
WRITE(6,3070) E1,E2
GOTO 410
390 CONTINUE
NAI = N-1
DO 400 I=1,NAI,2
J = I+1
WRITE(6,3060) I,A(I),Q(I),VEL(I),J,A(J),Q(J),VEL(J)
400 CONTINUE
WRITE(6,3060) N,A(N),Q(N),VEL(N)
WRITE(6,3070) E1,E2
410 CONTINUE
WRITE(6,3150)
WRITE(6,3160) (R(I),I=1,N)
CALL MIX1(NA,NB)
WRITE(6,3170)
WRITE(6,3160) (W(I),I=1,N)
C
C -----
C THIS SECTION TAKES CARE OF TIME STEPS, ETC.
C
C -----
C
DTIME = 5.0E-4
TMAX = 1.13
C SET OF PULSE WIDTH
WIDTH = TMAX*DTIME
C ---NOTE THAT ABOVE ENSURES STEP INPUT
TPRINT = 0.005
RPRINT = TPRINT / DTIME
WRITE(6,1015) OTIME
1015 FORMAT(2I,'DTIME =',E11.0)
NZMAI = 117
C
C CALC READ TIMES BASED ON VELOCITIES. NOTE---TRET*BE
C IN INTERVALS OF HOLD-UP TIMES.
C
ITZ = NZMAI
DO 1020 II=1,N
CCC TRET(II) = 1.0 / (2.0 * ITZ * E1 * VEL(II) )
C USE REAL(DIMENSIONAL) TIME...
C TIME IN SEC, DT AND DP IN INCHES
C QTOT IN CO.IN/SEC
CCC QTOT = 11.55 * 2.0/3.0
CCC DP = 0.75
CCC DT = DTDP*DP
CCC CL = 0.816 * CP
CCC AIS = 3.14 * DT * DT / 4.0

```

```

CCC   TDEAD(II) = CL * AIS / ( VEL(II)*QTOT )           FL501610
      IIZ = NZNAI                                         FL501620
      TDEAI(II) = 1.0/( VEL(II)*2.0*IIZ )               FL501630
1020  CONTINUE                                           FL501640
      CALL DELTA(OTIRB, N, NA, NB, JNAI, NCHG)          FL501650
      WRITE(6,1016) (I,TDEAD(I),NSUB(I),I=1,N)          FL501660
1016  FORNAT(15,21,811.4,IS)                          FL501670
      IFLAG = 0                                           FL501680
C     IFLAG=0==>INLET CONC'N = 1.0                      FL501690
C     .NB.0==>INLET CONC'N = 0.0                        FL501700
C                                                     FL501710
      CALL STEP(N,NA,NB,TIME,IFLAG)                     FL501720
      TIME = 0.0                                          FL501730
CCC   NSR = JNAI                                         FL501740
      KOONI = 0                                           FL501750
      IPRIOT = 0                                          FL501760
      JNAI = NZNAI                                         FL501770
1050  CCNTINOZ                                           FL501780
C     FOR TESTING, WRITE BRO INLET CONC'NS             FL501790
C     ASSUME CMI EVEN NO. RADIAL DIVISIONS            FL501800
CCC   WRITE(6,3270)                                       FL501810
CCC   DO 1051 I=2,N,2                                     FL501820
CCC   ISUB = NSUB(I)                                       FL501830
CCC   WRITE(6,3160)CIN(I,1), C(I,1,ISUB)              FL501840
C1051  CCNTINOB                                           FL501850
C     SET OF PULSES ON STEP                             FL501860
      IF (TIME .GT. WIDTH) IFLAG = 10                   FL501870
      DO 1100 J=1,JNAI                                     FL501880
C     B INLETS==>A OUTLETS, ETC.                      FL501890
C     OUTLETS==>SUBSCRIPT=1: INLETS==>SUBSCRIPT=NSUB   FL501900
C     TRANSFER TO DUMMI ARRAY TO USE SOBROUTINE        FL501910
C     A TO E TRANSITION...                             FL501920
      DO 1060 I=1,N,2                                     FL501930
C     THIS PART NA=NB                                   FL501940
      IA = I+1                                           FL501950
      IB = I                                              FL501960
1060  OOBBI(IA) = C(IA,J,1)                             FL501970
      CALL MIX2(0,NA,NB,DUMMI)                          FL501980
C     TRANSFER TO CIN ARRAY                             FL501990
      DO 1070 I=1,N,2                                     FL502000
C     THIS PART NA=NB                                   FL502010
      IA = I+1                                           FL502020
      IB = I                                              FL502030
1070  CIN(IB,J) = DUMMI(IB)                             FL502040
C     B TO A TRANSITION                                FL502050
      DO 1080 I=1,N,2                                     FL502060
C     THIS SCI NA=NB                                   FL502070
      IA = I+1                                           FL502080
      IB = I                                              FL502090
1080  DUMMI(IB) = C(IS,J,1)                             FL502100
      CALL MIX2(1,NA,NB,DUMMI)                          FL502110
C     BACK TO CIN'S                                    FL502120
      DO 1090 I=1,N,2                                     FL502130
C     NA = NB                                           FL502140
      IA = I+1                                           FL502150
      IB = I                                              FL502160
1090  CIN(IA,J+1) = OOBBI(IA)                          FL502170
1100  CONTINUE                                           FL502180
C     SHIFT AFRALS FOR DEAD TIME                      FL502190
C     DON'T FORGET TO CHECK IF WE NEED PULSE INPUT     FL502200
      IF (IFLAG .EQ. 0) GOTO 1110                       FL502210
      CALL STEP(N,NA,NB,TIME,IFLAG)                    FL502220
1110  CCNTINOB                                           FL502230
      DO 1200 J=1,JNAI                                     FL502240
      DO 1200 I=1,N                                       FL502250
      KNAI = NSUB(I) - 1                                  FL502260
      DO 1150 K=1,KNAI                                    FL502270
      KI = K+1                                             FL502280
      C(I,J,K) = C(I,J,K1)                               FL502290
1150  CONTINUE                                           FL502300
C     NOW, INLETS GO INTO LAST POSITION                FL502310
      KI = NSUB(I)                                         FL502320
      C(I,J,KI) = CIN(I,J)                               FL502330
1200  CONTINUE                                           FL502340
C     ONLY WRITE RESULTS AT DESIRED INTERVALS          FL502350
      IPRIOT = IPRIOT + 1                                  FL502360
      IF (IPRIOT .LT. NPRINT) GOTO 1350                 FL502370
      IPRIOT = 0                                           FL502380
C     CHECK IF WE WRITE EVERYTHING OR ONLY AVG.        FL502390
      IF (IOPT .EQ. 0) GOTO 1305                         FL502400

```



```

C A HALF-CELL
DO 10 I=2,N,2
  RH(I) = R(I) - 8A(I-1)
  A(I) = 8(I)*R(I) - 8A(I-1)*RA(I-1)
10 CONTINUE
C B HALF-CELL
  RH(1) = R(1)
  A(1) = RB(1)*RB(1)
  NAI = N-1
  DO 20 I=3,NAI,2
    RH(I) = RB(I) - R(I-1)
    A(I) = RB(I)*RB(I) - R(I-1)*R(I-1)
20 CONTINUE
C NOW, DETERMINE FLOWS AND POROSITIES OF A AND B SEGS
C DEFERES ON RA AND RB
  IF (NA - LB, NB) GOTO 500
C THIS SECTION FOR RA GT NB
C FLUX DISTRIBUTION AND POROSITY
  Z1 = 0.0
  S0R = 0.0
  DO 100 I=1,N,2
    Z1 = Z1 + A(I)
    S0R = S0R + A(I)*SQRT(RH(I))
100 Q(I) = A(I)*SQRT(RH(I))/S0R
110 CONTINUE
C B SEGMENT
  Z2 = 0.0
  S0B = 0.0
  N1 = N-1
  DO 120 I=2,N1,2
    Z2 = Z2 + A(I)
120 CONTINUE
  IX = A(N-1)*SQRT(RH(N-1))
  IY = A(N-3)*SQRT(RH(N-3))
  Q(N-1) = Q(N) + Q(N-2)*IX/(IX+IY)
  IX = A(2)*SQRT(RH(2))
  IY = A(4)*SQRT(RH(4))
  Q(2) = Q(1) + Q(3)*IX/(IX+IY)
  NAI = N-3
C DON'T NEED FOLLOWING IF N - LB, 5
  IF (N - LB, 5) GOTO 1000
  DO 130 I=4,NAI,2
    IX = A(I)*SQRT(RH(I))
    IY = A(I-2)*SQRT(RH(I-2))
    ZZ = A(I+2)*SQRT(RH(I+2))
    Q(I) = Q(I-1)*IX/(IX+IY) + Q(I+1)*IY/(IX+ZZ)
130 CONTINUE
GOTO 1000
500 CONTINUE
C THIS SECTION FOR NA=NB
C FLUX DISTRIBUTION AND POROSITY
C A-SEGMENT
  S0A = 0.0
  Z1 = 0.0
  DO 510 I=2,N,2
    Z1 = Z1 + A(I)
    S0A = S0A + A(I)*SQRT(RH(I))
510 DO 520 I=2,N,2
    Q(I) = A(I)*SQRT(RH(I))/S0A
520 CONTINUE
C B-SEG
  Z2 = 0.0
  S0B = 0.0
  N1 = N-1
  DO 530 I=1,N1,2
    Z2 = Z2 + A(I)
530 CONTINUE
  IX = A(N-1)*SQRT(RH(N-1))
  IY = A(N-3)*SQRT(RH(N-3))
  Q(N-1) = Q(N) + Q(N-2)*IX/(IX+IY)
  IX = A(1)*SQRT(RH(1))
  IY = A(3)*SQRT(RH(3))
  Q(1) = Q(2)*IX/(IX+IY)
  NAI = N-3
C DON'T NEED FOLLOWING IF N - LB, 4
  IF (N - LB, 4) GOTO 1000
  DO 540 I=3,NAI,2
    IX = A(I)*SQRT(RH(I))
    IY = A(I-2)*SQRT(RH(I-2))

```

```

FLS03210
FLS03220
FLS03230
FLS03240
FLS03250
FLS03260
FLS03270
FLS03280
FLS03290
FLS03300
FLS03310
FLS03320
FLS03330
FLS03340
FLS03350
FLS03360
FLS03370
FLS03380
FLS03390
FLS03400
FLS03410
FLS03420
FLS03430
FLS03440
FLS03450
FLS03460
FLS03470
FLS03480
FLS03490
FLS03500
FLS03510
FLS03520
FLS03530
FLS03540
FLS03550
FLS03560
FLS03570
FLS03580
FLS03590
FLS03600
FLS03610
FLS03620
FLS03630
FLS03640
FLS03650
FLS03660
FLS03670
FLS03680
FLS03690
FLS03700
FLS03710
FLS03720
FLS03730
FLS03740
FLS03750
FLS03760
FLS03770
FLS03780
FLS03790
FLS03800
FLS03810
FLS03820
FLS03830
FLS03840
FLS03850
FLS03860
FLS03870
FLS03880
FLS03890
FLS03900
FLS03910
FLS03920
FLS03930
FLS03940
FLS03950
FLS03960
FLS03970
FLS03980
FLS03990
FLS04000

```

```

      ZZ = A(I+2)*SQRT(BR(I+2))
      Q(I) = Q(I-1)*IX/(IX+II) + Q(I+1)*IX/(IX+ZZ)
540  CONTINUE
1000 RETURN
      ENO

C
      SUBROUTINE MII2(ITRANS,NA,NB,C)
      COMMON /TWO/ Q(20),A(20),W(20)
      DIMENSION C(20)
C THIS SUBROUTINE DETERMINES ANNULUS INLET CONCENTRATIONS
C ITRANS=0=>A TO B TRANSITION
C ITRANS=1=>B TO A TRANSITION
      N = NA+NB
      IF (NA .LE. NB) GOTO 500
C THIS SECTION FOR BA GT NB
      IF (ITRANS .NE. 0) GOTO 200
C A TO B TRANS
C B'S ARE EVEN NUMBERED SUBSCRIPTS
      N1 = N-1
      DO 100 I=2,N1,2
      C(I) = (1.0-W(I+1))*Q(I+1)*C(I+1)
      C(I) = C(I) + W(I-1)*Q(I-1)*C(I-1)
      C(I) = C(I) / Q(I)
100  CONTINUE
      RETURN
200  CONTINUE
C B TO A TRANS
C A'S ARE ODD NUMBERED SUBSCRIPTS
      C(1) = C(2)
      C(N) = C(N-1)
      N2 = N-2
      DO 300 I=3,N2,2
      C(I) = (1.0-W(I))*C(I-1) + W(I)*C(I+1)
300  CONTINUE
      RETURN
500  CONTINUE
C THIS SECTION FOR NA=NB
      IF (ITRANS .NE. 0) GOTO 700
C A TO B TRANS
C B'S ODD NUMBERED SUBSCRIPTS
      C(1) = C(2)
      N1 = N-1
      DO 600 I=3,N1,2
      C(I) = (1.0-W(I+1))*Q(I+1)*C(I+1)
      C(I) = C(I) + W(I-1)*Q(I-1)*C(I-1)
      C(I) = C(I) / Q(I)
600  CONTINUE
      RETURN
700  CONTINUE
C B TO A TRANSITION
C A'S EVEN NUMBERED SUBSCRIPTS
      C(N) = C(N-1)
      N2 = N-2
      DO 800 I=2,N2,2
      C(I) = W(I)*C(I+1) + (1.0-W(I))*C(I-1)
800  CONTINUE
      RETURN
      ENO
      SUBROUTINE STEP(N,NA,NB,TIME,IFLAG)
      COMMON /FIVE/ C(20,118,50),CIN(20,118)
      COMMON /FOUR/ I0EA0(20),NSUB(20)
      IF (TIME .GT. 0.0) GOTO 15
      DO 10 I=1,20
      DO 10 J=1,118
      DO 10 K=1,50
      C(I,J,K) = 0.0
10  CONTINUE
15  CONTINUE
C NOW, SET OF STEP-CHANGE (OR PULSE) AT INLET
C IFLAG=0=>INLET CONC AT 1.0
C IFLAG=1=>BACK TO 0.0
      VALUE = 1.0
      IF (IFLAG .NE. 0) VALUE = 0.0

C
C NOTE--ASSUME ONLY EVEN NO. RADIAL DIVISIONS
C
C THIS SECTION FOR NA = NB
100  CONTINUE
      DO 150 I=2,N,2
      ISOR = NSOR(I)

```

FLS04010
 FLS04020
 FLS04030
 FLS04040
 FLS04050
 FLS04060
 FLS04070
 FLS04080
 FLS04090
 FLS04100
 FLS04110
 FLS04120
 FLS04130
 FLS04140
 FLS04150
 FLS04160
 FLS04170
 FLS04180
 FLS04190
 FLS04200
 FLS04210
 FLS04220
 FLS04230
 FLS04240
 FLS04250
 FLS04260
 FLS04270
 FLS04280
 FLS04290
 FLS04300
 FLS04310
 FLS04320
 FLS04330
 FLS04340
 FLS04350
 FLS04360
 FLS04370
 FLS04380
 FLS04390
 FLS04400
 FLS04410
 FLS04420
 FLS04430
 FLS04440
 FLS04450
 FLS04460
 FLS04470
 FLS04480
 FLS04490
 FLS04500
 FLS04510
 FLS04520
 FLS04530
 FLS04540
 FLS04550
 FLS04560
 FLS04570
 FLS04580
 FLS04590
 FLS04600
 FLS04610
 FLS04620
 FLS04630
 FLS04640
 FLS04650
 FLS04660
 FLS04670
 FLS04680
 FLS04690
 FLS04700
 FLS04710
 FLS04720
 FLS04730
 FLS04740
 FLS04750
 FLS04760
 FLS04770
 FLS04780
 FLS04790
 FLS04800

```

      C(I,1,ISUB) = VALUE
      CIB(I,1) = VALUE
      IF (TIME .GT. 0.0) GOTO 145
      I1 = I-1
      ISUB = NSUB(I1)
      C(I1,1,ISUB) = 0.0
      CIN(I1,1) = 0.0
145  CONTINUE
150  CONTINUE
      ENDS
      END

C
      SUBROUTINE DELTA(OTIME, N, NA, NB, JNAI, NCRG)
      COMMON /PCUB/ TCEAO(20), NSUB(20)
C  CALC LINE STEPS/DEAD TIME
      DO 100 I=1,N
        ZZZ = TCEAO(I) / OTIME + 0.5
        NSUB(I) = ZZZ
        IF (NSUB(I) .LT. 1) NSUB(I) = 1
100  CONTINUE
C  NOW, CALC NAI AND MIN NSUB'S IN EACH HALF-CELL
C  ...DEFENDS ON NA=NB OR NA>NB
      IF (NA .LE. NB) GOTO 500
C  THIS SECTION FOR NA>NB
      NAXA = 0
      NAZE = 0
      NINA = 126
      MINB = 126
      DO 200 I=1,N,2
        IF (NSUB(I) .LT. NAXA) GOTO 150
        NAXA = NSUB(I)
150  CONTINUE
        IF (NSUB(I) .GT. NINA) GOTO 160
        NINA = NSUB(I)
160  CONTINUE
        I1 = I+1
        IF (I1 .GT. N) GOTO 200
        IF (NSUB(I1) .LT. NAXB) GOTO 180
        NAXB = NSUB(I1)
180  CONTINUE
        IF (NSUB(I1) .GT. MINB) GOTO 200
        MINB = NSUB(I1)
200  CONTINUE
        GOTO 700
C  THIS SECTION FOR NA=NB
500  CONTINUE
      NAXA = 0
      NAXB = 0
      NINA = 126
      MINB = 126
      DO 600 I=2,N,2
        IF (NSUB(I) .LT. NAXA) GOTO 550
        NAXA = NSUB(I)
550  CONTINUE
        IF (NSUB(I) .GT. NINA) GOTO 560
        NINA = NSUB(I)
560  CONTINUE
        I1 = I-1
        IF (NSUB(I1) .LT. NAXB) GOTO 580
        NAXB = NSUB(I1)
580  CONTINUE
        IF (NSUB(I1) .GT. MINB) GOTO 600
        MINB = NSUB(I1)
600  CONTINUE
C
700  CONTINUE
      WRITE(6,2000) NAXA, NAXB
      WRITE(6,2010) NINA, MINB
C  NOW, ADD UP NAX'S AND MIN'S TO CALC NO AXIAL CELLS (JNAI)
      NCRG = 0
      SNAI = NAXA + NAXB
      SMIN = NINA + MINB
      ZZZ = SNAI/SMIN
      JNAI = ZZZ
      JNAI = JNAI + 1
      NCRG = NAXA + NAZE
      WRITE(6,2020) JNAI, NCRG
      IF (JNAI .LE. (10) ) GOTO 750
      WRITE(6,2040)
      STOP

```

FLS04810
FLS04820
FLS04830
FLS04840
FLS04850
FLS04860
FLS04870
FLS04880
FLS04890
FLS04900
FLS04910
FLS04920
FLS04930
FLS04940
FLS04950
FLS04960
FLS04970
FLS04980
FLS04990
FLS05000
FLS05010
FLS05020
FLS05030
FLS05040
FLS05050
FLS05060
FLS05070
FLS05080
FLS05090
FLS05100
FLS05110
FLS05120
FLS05130
FLS05140
FLS05150
FLS05160
FLS05170
FLS05180
FLS05190
FLS05200
FLS05210
FLS05220
FLS05230
FLS05240
FLS05250
FLS05260
FLS05270
FLS05280
FLS05290
FLS05300
FLS05310
FLS05320
FLS05330
FLS05340
FLS05350
FLS05360
FLS05370
FLS05380
FLS05390
FLS05400
FLS05410
FLS05420
FLS05430
FLS05440
FLS05450
FLS05460
FLS05470
FLS05480
FLS05490
FLS05500
FLS05510
FLS05520
FLS05530
FLS05540
FLS05550
FLS05560
FLS05570
FLS05580
FLS05590
FLS05600


```

      IFLAG = 0
      DO 800 I=1,N
      IF( NSOB(I) .GT. (50) ) IFLAG = 10
800  CONTINUE
      IF( IFLAG .LT. 1) GOTO 900
      WRITE(6,2030)
      STCF
900  RZTUBN
2000  FORMAT( ' NAXA = ',I5, ' NAXB = ',I5)
2010  FORMAT( ' MINA = ',I5, ' MINB = ',I5)
2020  FORMAT( ' JMAX = ',I5, ' NCRG = ',I5)
2030  FORMAT( ' ...PGM ABOBT IN SUBR DELTA.  NSUB GT (15) ')
2040  FORMAT( ' ...PGM ABOBT IN SUBR DELTA.  JMAX GT (10) ')
      ENB
      FL505750

C
      SUBROUTINE VOID(NCIV,DTDP,BBC1,BHO2,EBAR,EFS)
      ZNDIV = NDIV
      DELB = (BHO2 - BBC1) /ZNDIV
      ROLD = BHO1
      FOLD = BHO1*EFONC(BHO1, DTDP, EBAR)
      SON = 0.0
      DO 100 I=1,NDIV
      RNEW = ROLD + DELB
      FNEW = RNEW * EFONC(RNEW, DTDP, EBAR)
      FINT = 0.5*DELB*(FNEW + FOLD)
      SON = SON + FINT
      FOLD = FNEW
      ROLD = RNEW
100  CONTINUE
      VTOT = BHO2*BHO2 - BHO1*BHO1
      EFS = SON
      EFS = 2.0*EFS/VTOT
      RETURN
      ENC
      FL505950

C
      FORCON EFONC(N, DTDP, EBAR)
      PI = 2.0*ASIN(1.0)
      A1 = 0.3463
      A2 = 0.4273
      A3 = 2.4509
      A4 = 2.2011
      I = 0.5*OTOP*(1.0-B)
      IF( I .LT. 0.25) GOTO 100
      IY = COS( (A3*I-A4)*PI )
      IY = A1*IY/EXP(A2*I)
      EFONC = (1.0-EBAR)*IY + EBAR
      GOTO 1000
100  CCATINUZ
C THIS SECTION FOR 'WALL' REGION
      IY = 7.0*I*I/9.0
      IY = 4.5*(I-IY)
      IY = (1.0-EBAR)*IY
      EFONC = 1.0-IY
1000 RETURN
      ENC
      FL506150

C
C
      SUBROUTINE MIX1(NA,NB)
C THIS SUBROUTINE DETERMINES WEIGHT FACTORS FOR
C MIXING AT ANNOLOS INLETS
      CORRCN /TWC/ Q(20),A(20),W(20)
      N = NA*NB
      IF(NA .LE. NB) GOTO 200
C THIS SECTION FOR NA GT NB
C NEED WEIGHTS FOR ODD NUMBERED SEGMENTS
      W(N) = 0.0
      W(1) = 1.0
      N2 = N-2
      DO 10 I=3,N2,2
      I1 = N2 - I + 3
      W(I1) = ( Q(I1+1) - (1.0-W(I1+2)) *Q(I1+2) )/Q(I1)
10  CONTINUE
      GOTO 1000
200  CONTINUE
C THIS SECTION FOR NA = NB
C NEED WEIGHTS FOR EVEN NUMBERED SEGMENTS
      W(N) = 0.0
      N2 = N-2
      DO 300 I=2,N2,2
      FL506400

```

```

      I1 = 2-I*N2
      W(I1) = ( Q(I1+1) - (1.0-W(I1+2)) *Q(I1+2) )/Q(I1)
300  CONTINUE
1000 CONTINUE
      RETURN
      END

```

```

PLS06410
PLS06420
PLS06430
PLS06440
PLS06450
PLS06460

```

Steady-state Heat Dispersion

General program flow follows that for steady-state mass dispersion, but with added steps of numerical integration along the length of each half-cell (subroutine CELLIN) between mixing calculations. As for mass dispersion, two versions of subroutine ANN are given. Other programming details are commented in the listing.

```

C PROGRAM NAME 'TEMPV3 FORTRAN'
C
C-----
C THIS RUN FOR DATA OF LEROU AND FROMENT--CYLINDERS
C-----
C
C LAST UPDATE/USE ON 28 JUNE 85
C DIMENSION EPS(100),AIS(100)
C DIMENSION TIN(100)
C DIMENSION Q(100),B(100),A(100),VEL(100)
C DIMENSION W(100),C(100),I(100)
C DIMENSION RA(100),SB(100)
C COMMON /ONE/ TOLD(100), ER(100), LASTDR
C COMMON /B1/ NP,BE,DT,DP,CP,TWALL,G,HEIGHT,ISHAPE,APELL
C DATA TIN /100*20.5/
C DATA NLONG,NPRINT /49,0/
C THIS PROGRAM CALCULATES FLOWS AND TEMPERATURES GIVEN
C AROUNDLOS DIMENSIONS.
C
C DATA C /100*0.0/
C DATA E /100*0.0/
C NOTE---THE VARIABLE 'ISHAPE' DEOTES SHAPE OF PARTICLES
C DIMENSION PSIP(5),PSIW(5)
C DATA PSIP / 1.0 , 1.0, 3*1.0 /
C DATA PSIW /1.0, 1.0, 3*1.0/
C (EFFECT HEAT TRANSFER CASES)
C IF ISHAPE = 1 ==> SPHERES
C PSIP = 2 ==> CYLINDERS
C IT IS THE SUBSCRIPT OF THE 'SHAPE FACTOR' VECTOR, PSI
C TO BE USED IN THE J-FACTOR ANALOGY. . .
C N = CONST * PSI * N(SPHERE)
C PSIP==PELLET R; PSIW==WALL R
C ISHAPE = 2
C
C*****
C WRITE(6,2370)
C DT = 3.6
C ZDE = 0.26
C ZLP = ZDP
C DP = ZDP*ZDP + ZLP*ZLP
C DP = SQRT(0.5*DP)
C DON'T FORGET THAT ZLP=ZDP FOR SPHERICAL PELLETS
C ALSO, FORM OF SORF AREA/VOL (APELL) CHANGES WITH SHAPE...
C APELL = 6.0/ZDP
C DTD = DT/DP
C UC TO I=1,100
10 W(I) = 20.0
C NOW, TRY ASSIGNING NO. CELLS BASED ON CORRELATION...
C Z = DTD/0.816 + 0.5
C N = 2
C Z = N
C Z = 0.5*Z
C NB = Z
C NA = N-NB
C RESTRICT TO EVEN NO. SEGMENTS
C IF (NA -GT. NB) NB = NA
C N = NA+NB
C WRITE(6,2020) DTD,N,NA,NB
C SIZE RADII
C SET UP TO DO INCREASING RA'S...
C SIZE EVENLY SPACED RADII
C ZN = N/2
C DELB = 1.0/ZN
C B(2) = DELB
C DO 80 I=4,N,2
C B(I) = B(I-2) + DELB
80 CONTINUE
C DETERMINE EPS FOR EACH SEGMENT...
C EBAF = 0.32
C VOID FRACTION OF FIRST SEGMENT
C CALL VOID(DTD,0.0,R(2),SBAR,E1)
C I=2
C WRITE(6,2010) I,E1
100 CONTINUE
C EPS(1) = E1
C EPS(2) = E1
C IX = B(2)*R(2)
C AIS(1) = IX
C AIS(2) = IX
C RA(1) = (1.0-E1)*IX

```

```

      RA(1) = SQRT( RA(1) )
      RB(1) = E1*IX
      RE(1) = SQRT( RE(1) )
      RA(2) = R(2)
      RB(2) = R(2)
      MAX = N-1
      DO 120 I=3,MAX,2
C      YOU FRACTIONS OF RADIAL CELLS BASED ON COBBELIATION
      RUC2 = R(I+1)
      RHG1 = R(I-1)
      CALL VOIC(UTDF, RHG1, RHG2, REAR, ERAT)
      IW = I+1
      WRITE(6,2010) IW, ERAT
      IX = R(I+1)*R(I+1) - R(I-1)*R(I-1)
      AXS(I) = IX
      AIS(IW) = IX
      EPS(I) = ERAT
      EPS(IW) = ERAT
      RA(I) = (1.0-ERAT)*IX
      RA(I) = R(I-1)*R(I-1) + RA(I)
      RA(I) = SQRT( RA(I) )
      RB(I) = ERAT * IX
      RB(I) = R(I-1)*R(I-1) + RB(I)
      RB(I) = SQRT( RB(I) )
      RA(IW) = R(IW)
      RB(IW) = R(IW)
120  CONTINUE
      MAX = N-1
      WRITE(6,2150)
      WRITE(6,2160) (RA(I), R(I+1), I=1, MAX, 2)
      WRITE(6,2160) (RB(I), R(I+1), I=1, MAX, 2)
      CALL ANB(HA, NB, Q, R, A, B1, B2, RA, RB)
      CALL E1X(HA, NB, Q, B)
C      *****DON'T FORGET REAT X-FER GOCCIES*****
C      REAT I=REB DATA GOES REUB
C      --- C.G.S. UNITS---
C
CCC  TIR = 30.0
      DO 1 I=1,100
1    TOL0(I) = TIR(I)
      TRALL = 100.0
      CP = 0.25
C      NOTE--USING SYMBOL 'G' TO SIGNIFY MASS FLOW RATE
C      (G/SEC) AND 'H01' MASS FLOW (G/SEC-CM**2)!!!!
C      ---GDOT=MASS FLOW; GBASE=BASE CASE MASS FLOW
C      ----- INTERSTITIAL VALUES -----
      IX = 0.4*3600.0
      GBASE = 274.0/IX
      GWALL = 7.17 * 454.0 / 3600.0
      MW = 1.80
      G = GW
      XI = 3.1816*0.25*CT*DT*E1
      GDOT = G/IX
C      TRY AT CORRELATION FOR HP AND HW. . .
C      INCLUDE TEMP DEPENDENCE OF DENSITY FOR VELOCITY PURPOSES
      TBASE = 60.0+273.15
      TEMP = (TIR(1)+TRALL)/2. + 273.15
      RP = 1.0E-3 * SQRT( TEMP*GDOT*0.6/(GBASE * TBASE * DP) )
      RP = RP*1.0
CCC  HW = 2.40E-3
      HW = 2.0E-3*( GDOT/GBASE )**0.8
      WEIGHT = 0.10
      WRITE(6,2360) HW, RP, WEIGHT, TEMP
      STUFF = G * CP * DDP
      STOFF = 4.0*SQRT(2.0/3.0) / STUFF
      STUFF = STUFF/Q(N)
      DO 200 I=1,N
      VEL(I) = E1*Q(I)/A(I)
200  CONTINUE
      WRITE(6,2050)
      DO 300 I=2,N,2
      J = I-1
      WRITE(6,2060) I, A(I), Q(I), VEL(I), J, A(J), Q(J), VEL(J)
300  CONTINUE
      WRITE(6,2070) E1, E2
      WRITE(6,2150)
CCC  W = RA + RB
      W = RA + RB
C      INITIALIZE PROFILE.
      DO 420 I=1,N

```

```

00E00810
CUM00820
CUM00830
CUM00840
CUM00850
CUM00860
CUM00870
CUM00880
CUM00890
CUM00900
CUM00910
CUM00920
CUM00930
CUM00940
CUM00950
CUM00960
CUM00970
CUM00980
CUM00990
CUM01000
CUM01010
CUM01020
CUM01030
CUM01040
CUM01050
CUM01060
CUM01070
CUM01080
CUM01090
CUM01100
CUM01110
CUM01120
CUM01130
CUM01140
CUM01150
CUM01160
CUM01170
CUM01180
CUM01190
CUM01200
CUM01210
CUM01220
CUM01230
CUM01240
CUM01250
CUM01260
CUM01270
CUM01280
CUM01290
CUM01300
CUM01310
CUM01320
CUM01330
CUM01340
CUM01350
CUM01360
CUM01370
CUM01380
CUM01390
CUM01400
CUM01410
CUM01420
CUM01430
CUM01440
CUM01450
CUM01460
CUM01470
CUM01480
CUM01490
CUM01500
CUM01510
CUM01520
CUM01530
CUM01540
CUM01550
CUM01560
CUM01570
CUM01580
CUM01590
CUM01600

```

```

      T(I) = TINI(I)
420  CONTINUE
C NOW, CALC TEMPERATURES...
CCC  WRITE(6,2230)
      ACOUNT = 0
500  ACOUNT = ACOUNT+1
      WRITE(6,2240) ACOUNT
      IF (ACOUNT .GT. 5000) GOTO 1000
C RECALC FLOW DISTRIBUTION BASED ON T PROFILE
C USE LAST CELL'S TEMP TO CALC HW
CCC  HW = HWALL( T(N), 234.0, DP)
CCC  BE = 234.0
CCC  HP = HPCELL( T(I), BE, DP)
CCC  ALP = STOFF*BW
CCC  ALF = 0.0
CCC  WRITE(6,2310) HP,HW
C -----
C NUMERICAL INTEGRATION ALONG THE LENGTH OF EACH HALF-CELL
CCC  WRITE(6,2320)
CCC  WRITE(6,2400) (I,T(I),I=1,N)
      CALL CELLIN(I,N,Q,T,RA,RS,R,EPS,AIS)
      WRITE(6,2330)
      WRITE(6,2400) (I,T(I),I=1,N)
      CALL SIX2(0,NA,NB,Q,U,T,TWALL,0.0)
CCC  WRITE(6,2340)
CCC  WRITE(6,2400) (I,T(I),I=1,N)
      CALL CELLIN(0,N,Q,T,RA,RS,R,EPS,AIS)
      WRITE(6,2350)
      WRITE(6,2400) (I,T(I),I=1,N)
C CALC AVG TEMPS AND WRITE RESULTS
C ASSUME EVEN NO. RADIAL DIVISIONS
      TABAR = 0.0
      TBAR = 0.0
      DO 520 I=2,N,2
        J=I-1
        TABAR = TABAR + Q(I)*T(I)
        TBAR = TBAR + Q(J)*T(J)
CCC  WRITE(6,2250) I,Q(I),T(I),J,Q(J),T(J)
520  CONTINUE
      TABAR = TABAR/2
      TBAR = TBAR/2
C CALC A-INLETS...
      CALL SIX2(1,NA,NB,Q,U,T,TWALL,0.0)
      GOIC 500
1000 CONTINUE
C FORNALS. . .
2010 FORNAT(' I = ',I4,' EPS = ',E11.4)
2015 FORNAT(' ALPHA = ',E11.4)
2020 FORNAT(' DTP = ',E11.4,' N = ',I3,' NA = ',I3,' NB = ',I3)
2030 FORNAT(' D1/B = ',E11.4)
2040 FORNAT(' F = ',E11.4)
2050 FORNAT(20I,'A',4X,'B',/,2X,40(' '),2X,40(' '),/,
      1 2(2X,'I',7X,'A',11X,'P',9X,'VEL ',5X),/,
      2 1X,2('---',2X,3('-----',2X)))
2060 FORNAT(1X,2(13,2X,3(E10.4,2X)))
2070 FORNAT(' E1 = ',E11.4,' E2 = ',E11.4)
2150 FORNAT(' RADII...')
2160 FORNAT(5(2X,E11.4))
2170 FORNAT(' RISING HEIGHT FACTORS. . .')
2230 FORNAT(9I,'A',30X,'B',/,2(2X,29('---'),/,
      1 2X,2(1X,'I',8X,'G',7X,3X,' T ',4X),/,
      2 2X,2('---',2X,'-----',2X,'-----',2X)))
C23456789.123456789.123456789.123456789.123456789.
2240 FORNAT(' CELL NO ',I5)
2250 FORNAT(2X,2(13,2X,E11.4,2X,E11.4,2X))
2260 FORNAT(' WA = ',E11.4,' EBBD = ',E11.4)
2270 FORNAT(' CALC. INVALID VOID FRACT. FOR ASCRBTED ')
2290 FORNAT(' F = ',E11.4,' SDR = ',E11.4,' EPS1 = ',E11.4)
2300 FORNAT(' AVG TEMPS ',2X,E11.4,10X,E11.4)
2310 FORNAT(' ---HP = ',E11.4,' HW = ',E11.4)
2320 FORNAT(' A INLETS...')
2330 FORNAT(' A OUTLETS...')
2340 FORNAT(' B INLETS...')
2350 FORNAT(' B OUTLETS...')
2360 FORNAT(' QH = ',E11.4,' HP = ',E11.4,' WEIGHT = ',E11.4,
      ' T(DENSITY,K)=',E11.4)
2370 FORNAT(5(' **'),TEMP3J,5(' **'))
2400 FORNAT(' Q(I4,2X,E11.4) )
      STOP
      END

```

```

D0M01610
D0M01620
D0M01630
D0M01640
D0M01650
D0M01660
D0M01670
D0M01680
D0M01690
D0M01700
D0M01710
D0M01720
D0M01730
D0M01740
D0M01750
D0M01760
D0M01770
D0M01780
D0M01790
D0M01800
D0M01810
D0M01820
D0M01830
D0M01840
D0M01850
D0M01860
D0M01870
D0M01880
D0M01890
D0M01900
D0M01910
D0M01920
D0M01930
D0M01940
D0M01950
D0M01960
D0M01970
D0M01980
D0M01990
D0M02000
D0M02010
D0M02020
D0M02030
D0M02040
D0M02050
D0M02060
D0M02070
D0M02080
D0M02090
D0M02100
D0M02110
D0M02120
D0M02130
D0M02140
D0M02150
D0M02160
D0M02170
D0M02180
D0M02190
D0M02200
D0M02210
D0M02220
D0M02230
D0M02240
D0M02250
D0M02260
D0M02270
D0M02280
D0M02290
D0M02300
D0M02310
D0M02320
D0M02330
D0M02340
D0M02350
D0M02360
D0M02370
D0M02380
D0M02390
D0M02400

```

```

C
C
      SORSCUTINE ANN (NA, NR, Q, R, A, E1, E2, RA, RB)
      DIMENSION RA(100), RR(100)
      DIMENSION Q(100), B(100), RH(100), A(100)
C  CALC  HYDRAULIC RADII, AND AREAS
      N = NA + NR
C  A BALF-CELL
      DO 10 I=2, N, 2
      RH(I) = R(I) - RA(I-1)
      A(I) = R(I)*R(I) - RA(I-1)*RA(I-1)
10  CONTINUE
C  B BALF-CELL
      RH(1) = RR(1)
      A(1) = RB(1)*RB(1)
      N1 = N-1
      DO 20 I=3, N1, 2
      RH(I) = RR(I) - R(I-1)
      A(I) = RB(I)*RR(I) - R(I-1)*R(I-1)
20  CONTINUE
C  NOW, DETERMINE FLOWS AND POROSITIES OF A AND B SEGMS
C  DEPENDS ON NA AND NR
      IF (NA .LE. NR) GOTO 500
C  THIS SECTION FOR NA GT NR
C  FLOW DISTRIBUTION AND POROSITY
      E1 = 0.0
      SUM = 0.0
      DO 100 I=1, N, 2
      E1 = E1 + A(I)
      SUM = SUM + A(I)*SQRT(RH(I))
100  DO 110 I=1, N, 2
      Q(I) = A(I)*SQRT(RH(I))/SUM
110  CONTINUE
C  B SEGMENT
      E2 = 0.0
      SUM = 0.0
      N1 = N-1
      DO 120 I=2, N1, 2
      E2 = E2 + A(I)
120  CONTINUE
      IX = A(N-1)*SQRT(RH(N-1))
      IY = A(N-3)*SQRT(RH(N-3))
      Q(N-1) = Q(N) + Q(N-2)*IX/(IX+IY)
      IX = A(2)*SQRT(RH(2))
      IY = A(4)*SQRT(RH(4))
      Q(2) = Q(1) + Q(3)*IX/(IX+IY)
      N1 = N-3
C  DON'T NEED FOLLOWING IF N .LE. 5
      IF (N .LE. 5) GOTO 1000
      DO 130 I=4, N1, 2
      IX = A(I)*SQRT(RH(I))
      IY = A(I-2)*SQRT(RH(I-2))
      ZZ = A(I+2)*SQRT(RH(I+2))
      Q(I) = Q(I-1)*IX/(IX+IY) + Q(I+1)*IY/(IY+ZZ)
130  CONTINUE
      GOTO 1000
500  CONTINUE
C  THIS SECTION FOR NA=NR
C  FLOW DISTRIBUTION AND POROSITY
C  A-SEGMENT
      SUM = 0.0
      E1 = 0.0
      DO 510 I=2, N, 2
      E1 = E1 + A(I)
      SUM = SUM + A(I)*SQRT(RH(I))
510  DO 520 I=2, N, 2
      Q(I) = A(I)*SQRT(RH(I))/SUM
520  CONTINUE
C  B-SEG
      E2 = 0.0
      SUM = 0.0
      N1 = N-1
      DO 530 I=1, N1, 2
      E2 = E2 + A(I)
530  CONTINUE
C  TEST SUBDIVIDING BASED ON SQRT(RB)
C  --INSTEAD OF A*SQRT(RB)
      IX = A(N-1)*SQRT(RH(N-1))
      IY = A(N-3)*SQRT(RH(N-3))
      Q(N-1) = Q(N) + Q(N-2)*IX/(IX+IY)
      EUN02410
      EUN02420
      EUN02430
      EUN02440
      EUN02450
      EUN02460
      EUN02470
      EUN02480
      EUN02490
      EUN02500
      EUN02510
      EUN02520
      EUN02530
      EUN02540
      EUN02550
      EUN02560
      EUN02570
      EUN02580
      EUN02590
      EUN02600
      EUN02610
      EUN02620
      EUN02630
      EUN02640
      EUN02650
      EUN02660
      EUN02670
      EUN02680
      EUN02690
      EUN02700
      EUN02710
      EUN02720
      EUN02730
      EUN02740
      EUN02750
      EUN02760
      EUN02770
      EUN02780
      EUN02790
      EUN02800
      EUN02810
      EUN02820
      EUN02830
      EUN02840
      EUN02850
      EUN02860
      EUN02870
      EUN02880
      EUN02890
      EUN02900
      EUN02910
      EUN02920
      EUN02930
      EUN02940
      EUN02950
      EUN02960
      EUN02970
      EUN02980
      EUN02990
      EUN03000
      EUN03010
      EUN03020
      EUN03030
      EUN03040
      EUN03050
      EUN03060
      EUN03070
      EUN03080
      EUN03090
      EUN03100
      EUN03110
      EUN03120
      EUN03130
      EUN03140
      EUN03150
      EUN03160
      EUN03170
      EUN03180
      EUN03190
      EUN03200

```

```

      IX = A(1)*SQRT(RR(1))
      YI = A(3)*SQRT(RR(3))
      Q(I) = Q(2)*IX/(IX+II)
      BAI = B-3
C    DON'T NEED FOLLOWING IF N .LT. 4
      IF ( N .LT. 4) GOTO 1000
      UO 540 I=3,MAX,2
      IX = A(I)*SQRT(RR(I))
      YI = A(I-2)*SQRT(RR(I-2))
      ZI = A(I+2)*SQRT(RR(I+2))
      Q(I) = Q(I-1)*IX/(IX+II) + Q(I+1)*IX/(IX+ZI)
540  CONTINUE
1000 RETURN
      ENC
C
C
      SUBROUTINE VOID(DTUP,RHO1,RHO2,ZBAR,EPS)
      PI = 2.0*ABSIN(1.0)
      A1 = 0.3463
      A2 = 0.4273
      A3 = 2.4509
      A4 = 2.2011
      ALP = 0.5*UTUP*A2
      B = (A3 - A4)*PI*UTUP/2.0
      C = A3 * PI * UTUP / 2.0
      A = A1 * (1.0-ZBAR) * ZIF(-1.0*ALP)
CCC  WRITE(6,2000) A,ALP,B,C,UTUP
      R2 = RHO2
      R1 = RHO1
      VACD = 0.0
      V = 0.0
      TEST = 1.0-0.5/UTUP
      IF(RHO2 .LT. TEST) GOTO 100
C  THIS SECTION TREATS OUTERMOST ANNULUS. VOID BETWEEN
C  WALL AND 0.250P HAS DIFFERENT FUNCTION....
      VACD = 0.5 - 0.28479*(1.0-ZBAR)
      VACD = VADD*DTUP - 0.125
      VACD = VADD/(DTUP*DTUP)
      B2 = TEST
      IF(RHO1 .GE. TEST) GOTO 200
100  CONTINUE
      V = 0.5*ZBAR*(B2*B2-B1*R1)
      ARG = B-C*B2
      F2 = ALP*COS(ARG) - C*SIN(ARG)
      F2 = F2 * EXP( ALP*B2 )
      ARG = B-C*B1
      F1 = ALP*COS(ARG) - C*SIN(ARG)
      F1 = F1*EXP( ALP*B1 )
      V = V + (F2-F1)*A/(ALP*ALP + C*C)
200  VVICU = 2.0*(V + VACU)
      VVICI = RHO2*RHO2 - RHO1*RHO1
      EPS = VVICU/VVICI
C2000 FORMAT(' A, ALP, B, C, DTUP . . .',/,4(21,H11.4) )
      RETURN
      END
C
C
      SUBROUTINE SIX1(NA,NB,Q, W)
C  THIS SUBROUTINE DETERMINES WEIGHT FACTORS FOR
C  RAILING AT ANNULUS INLETS
      DIMENSION Q(100),W(100)
      N = NA+NB
      IF(NA .LT. NB) GOTO 200
C  THIS SECTION FOR NA GT NB
C  NEED WEIGHTS FOR ODU NUMBERSU SEGMENTS
      W(N) = 0.0
      W(1) = 1.0
      N2 = N-2
      DO 10 I=1,N2,2
        I1 = I2 - 1 + 3
        W(I1) = ( Q(I1+1) - (1.0-W(I1+2))*Q(I1+2) )/Q(I1)
10  CONTINUE
      GOTO 1000
200  CONTINUE
C  THIS SECTION FOR NA = NB
C  NEED WEIGHTS FOR EVEN NUMBERSU SEGMENTS
      W(N) = 0.0
      N2 = N-2
      DO 300 I=2,N2,2

```

```

CUM03210
CUM03220
CUM03230
CUM03240
CUM03250
CUM03260
CUM03270
CUM03280
CUM03290
CUM03300
CUM03310
CUM03320
CUM03330
CUM03340
CUM03350
CUM03360
CUM03370
CUM03380
CUM03390
CUM03400
CUM03410
CUM03420
CUM03430
CUM03440
CUM03450
CUM03460
CUM03470
CUM03480
CUM03490
CUM03500
CUM03510
CUM03520
CUM03530
CUM03540
CUM03550
CUM03560
CUM03570
CUM03580
CUM03590
CUM03600
CUM03610
CUM03620
CUM03630
CUM03640
CUM03650
CUM03660
CUM03670
CUM03680
CUM03690
CUM03700
CUM03710
CUM03720
CUM03730
CUM03740
CUM03750
CUM03760
CUM03770
CUM03780
CUM03790
CUM03800
CUM03810
CUM03820
CUM03830
CUM03840
CUM03850
CUM03860
CUM03870
CUM03880
CUM03890
CUM03900
CUM03910
CUM03920
CUM03930
CUM03940
CUM03950
CUM03960
CUM03970
CUM03980
CUM03990
CUM04000

```



```

      I1 = 2-I+*2
      W(I1) = ( Q(I1+1) - (1.0-W(I1+2))*Q(I1+2) ) /Q(I1)
300  CONTINUE
1000 CONTINUE
      RETURN
      END
      SUBROUTINE MIX2(ITRANS,NA,NB,Q,W,C,TWALL,ALP)
      DIMENSION W(100),Q(100),C(100)
C THIS SUBROUTINE DETERMINES AMMUIUS INLET CONCENTRATIONS
C ITRANS=0==>A TO B TRANSITION
C      =1==>B TO A TRANSITION
      N = NA+NB
C ASSURE NA = NB
C NOTE--USING C ARRAY TO HOLD T-VALUES
500  CONTINUE
C THIS SECTION FOR NA=NB
      IF (ITRANS .NE. 0) GOTO 700
C A TO B TRANS
C B'S ODD NUMBERED SUBSCRIPTS
      C(1) = C(2)
      N1 = N-1
      DO 600 I=3,N1,2
      C(I) = (1.0-W(I+1))*Q(I+1)*C(I+1)
      C(I) = C(I) + W(I-1)*Q(I-1)*C(I-1)
      C(I) = C(I) / Q(I)
600  CONTINUE
      RETURN
700  CONTINUE
C B TO A TRANSITION
C A'S EVEN NUMBERED SUBSCRIPTS
C USE HEAT BAL TO CALC OUTERMOST TEMP
CCC  IZ = BIP( -1.0 * ALP )
CCC  C(N) = TWALL + ( C(N-1)-TWALL ) * IZ
      C(N) = C(N-1)
      N2 = N-2
      DO 800 I=2,N2,2
      C(I) = W(I)*C(I+1) + (1.0-W(I))*C(I-1)
800  CONTINUE
      RETURN
      END
      FUNCTION HWALL(T,BE,DP)
C ----- I IS IN DEGREES CELSIUS -----
C USE Y & W CORRELATION
      FACTOR = 0.18 * BE**0.80
      ZKAIR = 0.1663*(T+273.15) + 12.493
      ZKAIR = ZKAIR*1.0E-6
      HWALL = 0.1*FACTOR * ZKAIR/DP
      RETURN
      END
C
      FUNCTION HPCELL(T,BE,DP)
C USE S.S.L. CORREL...
      ZKAIR = 0.1663*(T+273.15) + 12.493
      ZKAIR = ZKAIR * 1.0E-6
      CFNU = 4.4385E-5
      PR = CFNU/ZKAIR
      PR = 0.66
      FACTOR = PR**0.33333
      FACTOR = 2.0 * 0.6*SQRT(BE)*FACTOR
      HPCELL = FACTOR * ZKAIR/DP
      RETURN
      END
      SUBROUTINE CELLIN(ITRANS,N,Q,T,RA,RR,R,EPS,AIS)
      DIMENSION EPS(100),AXS(100),I(100),Q(100)
      DIMENSION ISHAPE(5)
      DIMENSION RA(100),RB(100),R(100)
      COEFFCN /RZ,RP,RW,DT,DP,CF,TWALL,G,HEIGHT,ISHAPE,APCELL
      DATA ISHAPE /1.0, 0.6667, 3*1.0/
C
C ITRANS .EQ. 1==>BE*BE IN A
C      .EQ. 0==>BE*BE IN B
C DEFINE NUMERICAL INTEGRATION PARAMETERS
      DIV = 1.0
      FI = 3.1416
      DZ = 0.816*DP/DIV
      IZRAI = DIV
      IF (ITRANS .EQ. 0) GOTO 500
C THIS SECTION FOR A=HALF-CELL
C ALREADY HAVE INLET TEMPS...
      DO 100 IZ=1,IZRAI

```

```

C CALC SOLID TEMPS AS AVG OF SURROUNDING FLOIDS
  T(1) = T(2)
  NAI = N-1
  DO 50 I=3,NAI,2
    T(I) = 0.5*( T(I+1) + T(I-1) )
50 CONTINUE
C NOW FLUID TEMPS
C WALL AND PLUG 2 DIFFERENT
  DT0Z = HW*PI*DI*(TWALL-T(N))
  AP = (1.0-EPS(N))*AIS(N)
  AP = ISHAPE(ISHAPE)*0.25*APELL*PI*DT*DT*AP
  DT0Z = DT0Z - HP*AP*( T(N)-T(N-1) )
  IX = Q(N)*CP*G
  T(N) = T(N) + EZ*DT0Z/IX
  IX = Q(2)*CP*G
  AP = (1.0-EPS(2))*AIS(2)
  AP = ISHAPE(ISHAPE)*0.25*APELL*PI*DT*DT*AP
  DT0Z = HP*AP*( T(3)-T(2) )
  T(2) = T(2) + 0Z*DT0Z/IX
  I=2
  NAI = N-2
  DO 60 I=4,NAI,2
    IX = Q(I)*CP*G
    APTOP = ISHAPE(ISHAPE)*(1.0-EPS(I+1))*AIS(I+1)
    APBOT = ISHAPE(ISHAPE)*(1.0-EPS(I-1))*AIS(I-1)
    DT0Z = APTOP*( T(I+1)-T(I) ) - APBOT*( T(I)-T(I-1) )
    DT0Z = DT0Z*HP*0.25*APELL*PI*DT*DT/IX
    T(I) = T(I) + DZ*DT0Z
60 CONTINUE
100 CONTINUE
C NOW, HAVE OUTLET FLOID TEMPS, BOT
C MOST CALC NEW SOLID TEMPS.
  T(1) = T(2)
  NAI = N-1
  DO 110 I=3,NAI,2
    T(I) = 0.5*(T(I+1)+T(I-1))
110 CONTINUE
  GOTC 1000
C THIS SECTION FOR B-HALF-CELL
500 CONTINUE
  DO 600 I2=1,IZMAX
C CALC SOLID TEMPS
    T(N) = WEIGHT*TWALL + (1.0-WEIGHT)*T(N-1)
    NAI = N-2
    DO 550 I=2,NAI,2
      T(I) = 0.5*( T(I+1)+T(I-1) )
550 CONTINUE
C NOW, FIND FLOID TEMPS...
C CENTER FLOID DIFFERENT
    IX = Q(1)*CP*G
    AP = (1.0-EPS(2))*AIS(2)
    AP = ISHAPE(ISHAPE)*PI*0.25*APELL*DT*DT*AP
    DT0Z = HP*AP*( T(2)-T(1) )
    DT0Z = DT0Z/IX
    T(1) = T(1) + 0Z*DT0Z
    NAI = N-1
    DO 560 I=3,NAI,2
      IX = Q(I)*CP*G
      APTOP = ISHAPE(ISHAPE)*(1.0-EPS(I+1))*AIS(I+1)
      APBOT = ISHAPE(ISHAPE)*(1.0-EPS(I-1))*AIS(I-1)
      DT0Z = APTOP*( T(I+1)-T(I) ) - APBOT*( T(I)-T(I-1) )
      DT0Z = DT0Z*HP*0.25*APELL*PI*DT*DT/IX
      T(I) = T(I) + DZ*DT0Z
560 CONTINUE
600 CONTINUE
C NOW, FEED OUTLET SOLID TEMPS...
C SEE NOTE ABOVE RE: COTERNOST FLOID
    T(N) = WEIGHT*TWALL + (1.0-WEIGHT)*T(N-1)
    NAI = N-2
    DO 610 I=2,NAI,2
      T(I) = 0.5*(T(I+1)+T(I-1))
610 CONTINUE
C THAT'S IT!!!
1000 RETURN
  END

```

```

D0N08810
D0N08820
D0N08830
D0N08840
D0N08850
D0N08860
D0N08870
D0N08880
D0N08890
D0N08900
D0N08910
D0N08920
D0N08930
D0N08940
D0N08950
D0N08960
D0N08970
D0N08980
D0N08990
D0N09000
D0N09010
D0N09020
D0N09030
D0N09040
D0N09050
D0N09060
D0N09070
D0N09080
D0N09090
D0N09100
D0N09110
D0N09120
D0N09130
D0N09140
D0N09150
D0N09160
D0N09170
D0N09180
D0N09190
D0N09200
D0N09210
D0N09220
D0N09230
D0N09240
D0N09250
D0N09260
D0N09270
D0N09280
D0N09290
D0N09300
D0N09310
D0N09320
D0N09330
D0N09340
D0N09350
D0N09360
D0N09370
D0N09380
D0N09390
D0N09400
D0N09410
D0N09420
D0N09430
D0N09440
D0N09450
D0N09460
D0N09470
D0N09480
D0N09490
D0N09500
D0N09510
D0N09520
D0N09530
D0N09540
D0N09550

```

```

SUBROUTINE ARB (NA, NB, Q, N, A, N1, E2, RA, RB)
  DIMENSION RA(100), RB(100)
  DIMENSION Q(100), R(100), RH(100), A(100)
  C CALC HYDRAULIC RADII, AND AREAS
  N = NA + NB
  DD05560
  DD05570
  DD05580
  DD05590
  DD05600
  DD05610
  DD05620
  DD05630
  DD05640
  DD05650
  DD05660
  DD05670
  DD05680
  DD05690
  DD05700
  DD05710
  DD05720
  DD05730
  DD05740
  DD05750
  DD05760
  DD05770
  DD05780
  DD05790
  DD05800
  DD05810
  DD05820
  DD05830
  DD05840
  DD05850
  DD05860
  DD05870
  DD05880
  DD05890
  DD05900
  DD05910
  DD05920
  DD05930
  DD05940
  DD05950
  DD05960
  DD05970
  DD05980
  DD05990
  DD06000
  DD06010
  DD06020
  DD06030
  DD06040
  DD06050
  DD06060
  DD06070
  DD06080
  DD06090
  DD06100
  DD06110
  DD06120
  DD06130
  DD06140
  DD06150
  DD06160
  DD06170
  DD06180
  DD06190
  DD06200
  DD06210
  DD06220
  DD06230
  DD06240
  DD06250
  DD06260
  DD06270
  DD06280
  DD06290
  DD06300
  DD06310
  DD06320
  DD06330
  DD06340
  DD06350
  DD06360
  DD06370
  DD06380
  DD06390
  DD06400

  C A HALF-CELL
  DO 10 I=2, N, 2
    RH(I) = R(I) - RA(I-1)
    A(I) = R(I)*RH(I) - RA(I-1)*RA(I-1)
  10 CONTINUE
  C B HALF-CELL
  RH(1) = RB(1)
  A(1) = RB(1)*RH(1)
  MAX = N-1
  DO 20 I=3, NA1, 2
    RH(I) = RB(I) - R(I-1)
    A(I) = RB(I)*RH(I) - R(I-1)*R(I-1)
  20 CONTINUE
  C NOW, DETERMINE FLOWS AND POROSITIES OF A AND B SEGS
  C DIFFERES ON RA AND RB
  IF (N .LE. NB) GOTU 500
  C THIS SECTION FOR RA GT NB
  C FLOW DISTRIBUTION AND POROSITY
  E1 = 0.0
  SUM = 0.0
  DO 100 I=1, N, 2
    E1 = R1 + A(I)
  100 SUM = SUM + A(I)*RH(I)*RH(I)
    DO 110 I=1, N, 2
      Q(I) = A(I)*RH(I)*RH(I)/SUM
    110 CONTINUE
  C B SEGMENT
  E2 = 0.0
  SUM = 0.0
  N1 = N-1
  DO 120 I=2, N1, 2
    E2 = E2 + A(I)
  120 CONTINUE
    IX = A(N-1)*RH(N-1)*RH(N-1)
    IY = A(N-3)*RH(N-3)*RH(N-3)
    Q(N-1) = Q(N) + Q(N-2)*IX/(IX+IY)
    XX = A(2)*RH(2)*RH(2)
    IY = A(4)*RH(4)*RH(4)
    Q(2) = Q(1) + Q(3)*IX/(IX+IY)
    MAX = N-3
  C DON'T NEED FOLLOWING IF N .LE. 5
  IF (N .LE. 5) GOTU 1000
  DO 130 I=0, NA1, 2
    IY = A(I)*RH(I)*RH(I)
    IY = A(I-2)*RH(I-2)*RH(I-2)
    ZZ = A(I+2)*RH(I+2)*RH(I+2)
    Q(I) = Q(I-1)*IX/(IX+IY) + Q(I+1)*IX/(IX+ZZ)
  130 CONTINUE
    GOTU 1000
  500 CONTINUE
  C THIS SECTION FOR NA=NB
  C FLOW DISTRIBUTION AND POROSITY
  C A-SEGMENT
  SUM = 0.0
  E1 = 0.0
  DO 510 I=2, N, 2
    E1 = R1 + A(I)
  510 SUM = SUM + A(I)*RH(I)*RH(I)
    DO 520 I=2, N, 2
      Q(I) = A(I)*RH(I)*RH(I)/SUM
    520 CONTINUE
  C B-SEG
  E2 = 0.0
  SUM = 0.0
  N1 = N-1
  DO 530 I=1, N1, 2
    E2 = E2 + A(I)
  530 CONTINUE
  C TRY SUBDIVIDING BASED ON SORT(RH)
  --INSTEAD OF A+SORT(RH)
  C
    IX = A(N-1)*RH(N-1)*RH(N-1)
    IY = A(N-3)*RH(N-3)*RH(N-3)
    Q(N-1) = Q(N) + Q(N-2)*IX/(IX+IY)
    XX = A(1)*RH(1)*RH(1)
    IY = A(3)*RH(3)*RH(3)
    Q(1) = Q(2)*IX/(IX+IY)
    MAX = N-3
  C DON'T NEED FOLLOWING IF N .LE. 4
  IF (N .LE. 4) GOTU 1000
  DO 540 I=3, NA1, 2

```

```

AA = A(I)*BB(I)*BB(I)
YY = A(I-2)*BB(I-2)*BB(I-2)
ZZ = A(I+2)*BB(I+2)*BB(I+2)
Q(I) = Q(I-1)*XX/(XX+YY) + Q(I+1)*XX/(XX+ZZ)
540 CONTINUE
1000 RETURN
END

```

```

DUM06310
DUM06320
DUM06330
DUM06340
DUM06350
DUM06360
DUM06370

```

Steady-state Reaction

The procedure here is analogous to the steady-state heat dispersion program. The attached program can simulate either wall-cooled or adiabatic reactors. Details are commented in the listing.

```

C PROGRAM NAME 'RINSS2 FORTRAN'
C TREATS 1-ST ORDER INTRINSIC KINETICS
C -----
C THIS BOX FOR DATA OF TEST CASE
C -----
C LAST UPDATE/USE ON 26 JULY 85
C DIMENSION Q(100),R(100),A(100),VEL(100)
C DIMENSION W(100),C(100),T(100)
C DIMENSION BA(100),BB(100)
C DIMENSION EGLOE(100)
C CORREX /RATE/ ZKO,GG
C COMMON /RIN/ DELS,DEFF,BHO,Cp,BETA
C COMMON /RI/ RP,RV,TWALL,DT,DP,VPSP
C THIS PROGRAM CALCULATES FLOWS AND CONCENTRATIONS GIVEN
C ABSOLUT DIMENSIONS.
C VARIABLE **IFLAG**---IF 0 ==> ADIABATIC REACTOR
C OTHERWISE ==> CONSTANT TWALL
C (SEE 'CELLIN' FOR MORE DETAILS)
C DATA IFLAG /1/
C -----
C..... USE CGS UNITS.....
C..... TEMP=DEG KELVIN....
C..... CMC=BMOL/CM**3 ...
C -----
C DATA NLONG,NPRINT /100,5/
C INITIALIZE CONCENTRATION AND TEMPERATURE PROFILES
C DATA C /100*2.0E-8/
C DATA T /100*800.0/
C DATA R /100*0.0/
C REACTION, HEAT TRANSFER, ETC., DATA. . .
CIN = C(1)
CIX = T(1)
ZKO = 4.5 Z8
GG = 1.224
DELS = 2.424
DEFF = 0.001
BHO = 9.5 E-4
CP = 0.25
BV = .00141
BV = .2
CCC BP = 6.32E-4
CCC HW = 3.17E-4
TWALL = 400.0
DT = 3.6
OP = 0.6
VPSP = DP/6.0
CCC QTOT = 81.80
QTCT = 818.0
BETA = OELB / (BHO*CP)
IF (IFLAG -EQ. 0) WRITE(6,3060)
IF (IFLAG .NE. 0) WRITE(6,3070) TWALL
C CALC AREAS BASED ON DTOP AND EA
DTOP = DT / OP
DO 10 I=1,100
  V(I) = 20.0
  Z = DTOP + 0.5
C NOW, TRY ASSIGNING NO. CELLS BASED ON CORRELATIONS...
  Z = DTOP/0.816 + 0.5
  N = Z
  Z = N
  Z = 0.5*Z
  NR = Z
  NA = N-NB
C RESTRICT TO EVEN NO. SEGMENTS
  IF (NA -GT. NB) NB = NA
  N = NA+NB
  WRITE(6,2020) DTOP,N,NA,NB
C SIZE FACII
C SET OP TO DO INCREASING EA'S...
C SIZE EVENLY SPACED BA0II
  ZN = N/2
  DELB = 1.0/ZN
  B(2) = OELB
  DO 80 I=4,N,2
    B(I) = B(I-2) + OELB
80 CONTINUE
C DETERMINE EPS FOR EACH SEGMENT...

```

```

RIN00010
RIN00020
RIN00030
RIN00040
RIN00050
RIN00060
RIN00070
RIN00080
RIN00090
RIN00100
RIN00110
RIN00120
RIN00130
RIN00140
RIN00150
RIN00160
RIN00170
RIN00180
RIN00190
RIN00200
RIN00210
RIN00220
RIN00230
RIN00240
RIN00250
RIN00260
RIN00270
RIN00280
RIN00290
RIN00300
RIN00310
RIN00320
RIN00330
RIN00340
RIN00350
RIN00360
RIN00370
RIN00380
RIN00390
RIN00400
RIN00410
RIN00420
RIN00430
RIN00440
RIN00450
RIN00460
RIN00470
RIN00480
RIN00490
RIN00500
RIN00510
RIN00520
RIN00530
RIN00540
RIN00550
RIN00560
RIN00570
RIN00580
RIN00590
RIN00600
RIN00610
RIN00620
RIN00630
RIN00640
RIN00650
RIN00660
RIN00670
RIN00680
RIN00690
RIN00700
RIN00710
RIN00720
RIN00730
RIN00740
RIN00750
RIN00760
RIN00770
RIN00780
RIN00790
RIN00800

```

```

      ZBAR = 0.3500
C  VOID FRACTION OF FIRST SEGMENT
      CALL VOID(OTOP,0.0,R(2),ZBAR,Z1)
      I=2
      WRITE(6,2010) I,Z1
100  RA(1) = (1.0-Z1)*R(2)*Z(2)
      RA(1) = SQRT( RA(1) )
      RA(2) = R(2)
      RB(1) = Z1*R(2)*R(2)
      RB(1) = SQRT( RB(1) )
      RB(2) = R(2)
      SAX = N-1
      DO 120 I=3,MAX,2
C  VOID FRACTIONS OF RADIAL CELLS BASED ON CORRELATION
      RBG2 = R(I+1)
      RHC1 = R(I-1)
      CALL VOID(OTOP,RHC1,RHC2,ZBAR,ZHAT)
      IW = I+1
      WRITE(6,2010) IW,ZHAT
      IX = R(I+1)*R(I+1) - R(I-1)*R(I-1)
      RA(I) = (1.0-ZHAT)*IX
      RA(I) = R(I-1)*R(I-1) + RA(I)
      RA(I) = SQRT( RA(I) )
      RA(IW) = R(IW)
      RB(I) = ZHAT * IX
      RB(I) = R(I-1)*R(I-1) + RB(I)
      RB(I) = SQRT( RB(I) )
      RB(IW) = R(IW)
120  CONTINUE
      MAX = N-1
      WRITE(6,2150)
      WRITE(6,2160) (RA(I),R(I+1),I=1,MAX,2)
      WRITE(6,2160) (RB(I),R(I+1),I=1,MAX,2)
      CALL ANN(NA,NB,Q,R,A,Z1,Z2,RA,RB)
      N = NA+NB
      DO 200 I=1,N
200  VEL(I) = Q(I)/A(I)
C  WRITE RESULTS
      WRITE(6,2050)
      DO 300 I=2,N,2
      J=I-1
      WRITE(6,2060) I,A(I),Q(I),VEL(I),J,A(J),Q(J),VEL(J)
300  CONTINUE
      WRITE(6,2070) Z1,Z2
      WRITE(6,2150)
      WRITE(6,2160) (R(I),I=1,N)
      CALL MIX1(NA,NB,Q,R)
      WRITE(6,2170)
      WRITE(6,2160) (W(I),I=1,N)
      N = NA + NB
C  NOW, CALC CONCENTRATIONS...
CCC  WRITE(6,2230)
      WRITE(6,3050)
      KOONT = 0
      NP = 0
500  KOONT = KOONT+1
      NP = NP + 1
      WRITE(6,2240) KOONT
      IF(KOONT.GT. NLONG) GOTO 1000
C  A-HALF-CELL
      CALL CELLIS(1,N,OTOP,Q,T,C,IFLAG,RA,RB,RGLGB,OEZLZ)
      IF(NP.LT. NPRINT) GOTO 550
      WRITE(6,3000)
      WRITE(6,3030)
      CABAS = 0.0
      TABAS = 0.0
      RTOT = 0.0
      DO 520 I=2,N,2
      CABAR = CABAS + C(I)*Q(I)
      TABAR = TABAS + T(I)*Q(I)
      I1 = I-1
      WRITE(6,2255) I1,T(I1)
      RWRITE = RGLGB(I1)*OEZLZ
      RTOT = RTOT + RWRITE
      WRITE(6,2250) I,C(I),T(I),RWRITE
520  CONTINUE
      WRITE(6,3040) CABAR,TABAR,RTOT
C
      CONV = 1.0 - CABAR/CIN
      WRITE(6,3045) CONV

```

```

RINO0810
RINO0820
RINO0830
RINO0840
RINO0850
RINO0860
RINO0870
RINO0880
RINO0890
RINO0900
RINO0910
RINO0920
RINO0930
RINO0940
RINO0950
RINO0960
RINO0970
RINO0980
RINO0990
RINO1000
RINO1010
RINO1020
RINO1030
RINO1040
RINO1050
RINO1060
RINO1070
RINO1080
RINO1090
RINO1100
RINO1110
RINO1120
RINO1130
RINO1140
RINO1150
RINO1160
RINO1170
RINO1180
RINO1190
RINO1200
RINO1210
RINO1220
RINO1230
RINO1240
RINO1250
RINO1260
RINO1270
RINO1280
RINO1290
RINO1300
RINO1310
RINO1320
RINO1330
RINO1340
RINO1350
RINO1360
RINO1370
RINO1380
RINO1390
RINO1400
RINO1410
RINO1420
RINO1430
RINO1440
RINO1450
RINO1460
RINO1470
RINO1480
RINO1490
RINO1500
RINO1510
RINO1520
RINO1530
RINO1540
RINO1550
RINO1560
RINO1570
RINO1580
RINO1590
RINO1600

```



```

C B HALF-CELL
  RH(1) = RB(1)
  A(1) = BB(1)*BB(1)
  NAI = N-1
  DO 20 I=3,NAI,2
    RH(I) = RB(I) - R(I-1)
    A(I) = RB(I)*BB(I) - B(I-1)*B(I-1)
  CONTINUE
20 C NOW, DETERMINE FLOWS AND POROSITIES OF A AND B SEGS
C DEPENDS ON NA AND NB
  IF(NA.LE. NB) GOTO 500
C THIS SECTION FOR NA GT NB
C FLOW DISTRIBUTION AND POROSITY
  Z1 = 0.0
  SUM = 0.0
  DO 100 I=1,N,2
    Z1 = Z1 + A(I)
    SUM = SUM + A(I)*SQRT(RH(I))
  100 DO 110 I=1,N,2
    Q(I) = A(I)*SQRT(RH(I))/SUM
  110 CONTINUE
C B SEGMENT
  Z2 = 0.0
  SUM = 0.0
  N1 = N-1
  DO 120 I=2,N1,2
    Z2 = Z2 + A(I)
  120 CONTINUE
  IX = A(N-1)*SQRT(RH(N-1))
  IY = A(N-3)*SQRT(RH(N-3))
  Q(N-1) = Q(N) + Q(N-2)*IX/(IX+IY)
  IX = A(2)*SQRT(RH(2))
  IY = A(4)*SQRT(RH(4))
  Q(2) = Q(1) + Q(3)*IX/(IX+IY)
  NAI = N-3
C DON'T NEED FOLLOWING IF N.LE. 5
  IF(N.LE. 5) GOTO 1000
  DO 130 I=4,NAI,2
    IX = A(I)*SQRT(RH(I))
    IY = A(I-2)*SQRT(RH(I-2))
    ZZ = A(I+2)*SQRT(RH(I+2))
    Q(I) = Q(I-1)*IX/(IX+IY) + Q(I+1)*IX/(IX+ZZ)
  130 DO 500 I=1,N,2
    GOTO 1000
  500 CONTINUE
C THIS SECTION FOR NA=NB
C FLOW DISTRIBUTION AND POROSITY
C A-SEGMENT
  SUM = 0.0
  Z1 = 0.0
  DO 510 I=2,N,2
    Z1 = Z1 + A(I)
    SUM = SUM + A(I)*SQRT(RH(I))
  510 DO 520 I=2,N,2
    Q(I) = A(I)*SQRT(RH(I))/SUM
  520 CONTINUE
C B-SEG
  Z2 = 0.0
  SUM = 0.0
  N1 = N-1
  DO 530 I=1,N1,2
    Z2 = Z2 + A(I)
  530 CONTINUE
C TRI SUBDIVIDING BASED ON SQRT(SH)
  --INSTEAD OF A*SQRT(RH)
  IX = A(N-1)*SQRT(RH(N-1))
  IY = A(N-3)*SQRT(RH(N-3))
  Q(N-1) = Q(N) + Q(N-2)*IX/(IX+IY)
  IX = A(1)*SQRT(RH(1))
  IY = A(3)*SQRT(RH(3))
  Q(1) = Q(2)*IX/(IX+IY)
  NAI = N-3
C DON'T NEED FOLLOWING IF N.LE. 4
  IF(N.LE. 4) GOTO 1000
  DO 540 I=3,NAI,2
    IX = A(I)*SQRT(RH(I))
    IY = A(I-2)*SQRT(RH(I-2))
    ZZ = A(I+2)*SQRT(RH(I+2))
    Q(I) = Q(I-1)*IX/(IX+IY) + Q(I+1)*IX/(IX+ZZ)
  540 CONTINUE

```

```

BXND2410
BXND2420
BXND2430
BXND2440
BXND2450
BXND2460
BXND2470
BXND2480
BXND2490
BXND2500
BXND2510
BXND2520
BXND2530
BXND2540
BXND2550
BXND2560
BXND2570
BXND2580
BXND2590
BXND2600
BXND2610
BXND2620
BXND2630
BXND2640
BXND2650
BXND2660
BXND2670
BXND2680
BXND2690
BXND2700
BXND2710
BXND2720
BXND2730
BXND2740
BXND2750
BXND2760
BXND2770
BXND2780
BXND2790
BXND2800
BXND2810
BXND2820
BXND2830
BXND2840
BXND2850
BXND2860
BXND2870
BXND2880
BXND2890
BXND2900
BXND2910
BXND2920
BXND2930
BXND2940
BXND2950
BXND2960
BXND2970
BXND2980
BXND2990
BXND3000
BXND3010
BXND3020
BXND3030
BXND3040
BXND3050
BXND3060
BXND3070
BXND3080
BXND3090
BXND3100
BXND3110
BXND3120
BXND3130
BXND3140
BXND3150
BXND3160
BXND3170
BXND3180
BXND3190
BXND3200

```

```

1000 RETURN
      END
C
      SUBROUTINE VOID (DTDP, RSO1, RSO2, ZSAB, EPS)
      PI = 2.0*ABSIN(1.0)
      A1 = 0.1863
      A2 = 0.4273
      A3 = 2.4509
      A4 = 2.2011
      ALF = 0.5*DTDP* A2
      B = (A3 - A4)*PI*DTDP/2.0
      C = A3 * PI * DTDP / 2.0
      A = A1 * (1.0-ZSAB) * EXP(-1.0*ALF)
CCC WRITE(6,2000) A, ALF, B, C, DTDP
      R2 = RSO2
      R1 = RSO1
      VADD = 0.0
      V = 0.0
      TEST = 1.0-0.5/DTDP
      IF (RSO2 .LT. TEST) GOTO 100
C THIS SECTION TREATS OUTERMOST ANNULUS. VOID BETWEEN
C WALL AND 0.25DP HAS DIFFERENT FUNCTION....
      VADD = 0.5 - 0.24479*(1.0-ZSAB)
      VADD = VADD*DTDP - 0.125
      VADD = VADD/(DTDP*DTDP)
      B2 = TEST
      IF (RHO1 .GE. TEST) GOTO 200
100 CONTINUE
      V = 0.5*ZSAB*(R2*B2-B1*B1)
      ARG = B-C*B2
      F2 = ALP*COS(ARG) - C*SIN(ARG)
      F2 = F2 * EXP ( ALP*B2 )
      ARG = B-C*B1
      F1 = ALP*COS(ARG) - C*SIN(ARG)
      F1 = F1*EXP ( ALP*B1 )
      V = V + (F2-F1)*A/(ALP*ALP + C*C)
200 VVOID = 2.0*(V + VADD)
      VTOT = RHO2*RHO2 - RHO1*RHO1
      EPS = VVOID/VTOT
C2000 FCENAT(' A, ALP, B, C, DTDP = . .',/,4(21,21.4) )
      RETURN
      END
C
C
      SUBROUTINE WII1(NA, NB, Q, W)
C THIS SUBROUTINE DETERMINES WEIGHT FACTORS FOR
C MIXING AT ANNULUS INLETS
      DIMENSION Q(100), W(100)
      N = NA+NB
      IF (NA .LT. NB) GOTO 200
C THIS SECTION FOR NA GT NB
C NEED WEIGHTS FOR ODD NUMBERED SEGMENTS
      W(N) = 0.0
      W(1) = 1.0
      N2 = N-2
      DO 10 I=3, N2, 2
      I1 = N2 - I + 3
      W(I1) = ( Q(I1+1) - (1.0-W(I1+2))*Q(I1+2) )/Q(I1)
10 CONTINUE
      GOTO 1000
200 CONTINUE
C THIS SECTION FOR NA = NB
C NEED WEIGHTS FOR EVEN NUMBERED SEGMENTS
      W(N) = 0.0
      N2 = N-2
      DO 300 I=2, N2, 2
      I1 = 2-I+2
      W(I1) = ( Q(I1+1) - (1.0-W(I1+2))*Q(I1+2) )/Q(I1)
300 CONTINUE
1000 CONTINUE
      RETURN
      END
      SUBROUTINE WII2(TRANS, NA, NB, Q, W, C)
      DIMENSION W(100), Q(100), C(100)
C THIS SUBROUTINE DETERMINES ANNULUS INLET CONCENTRATIONS
C TRANS=0=>A TO B TRANSITION
C TRANS=1=>B TO A TRANSITION
      N = NA+NB
      IF (NA .LT. NB) GOTO 500
C THIS SECTION FOR NA GT NB

```

```

      IF (ITRANS .NE. 0) GOTO 200
C   A TO B TRANS
C   B'S ARE EVEN NUMBERED SUBSCRIPTS
      N1 = N-1
      DO 100 I=2,N1,2
        C(I) = (1.0-W(I+1))*Q(I+1)*C(I+1)
        C(I) = C(I) + W(I-1)*Q(I-1)*C(I-1)
        C(I) = C(I) / Q(I)
100  CONTINUE
      RETURN
200  CONTINUE
C   B TO A TRANS
C   A'S ARE ODD NUMBERED SUBSCRIPTS
      C(1) = C(2)
      C(N) = C(N-1)
      N2 = N-2
      DO 300 I=3,N2,2
        C(I) = (1.0-W(I))*C(I-1) + W(I)*C(I+1)
300  CONTINUE
      RETURN
500  CONTINUE
C   THIS SECTION FOR NA=NS
      IF (ITRANS .NE. 0) GOTO 700
C   A TO B TRANS
C   B'S ODD NUMBERED SUBSCRIPTS
      C(1) = C(2)
      N1 = N-1
      DO 600 I=3,N1,2
        C(I) = (1.0-W(I+1))*Q(I+1)*C(I+1)
        C(I) = C(I) + W(I-1)*Q(I-1)*C(I-1)
        C(I) = C(I) / Q(I)
600  CONTINUE
      RETURN
700  CONTINUE
C   B TO A TRANSITION
C   A'S EVEN NUMBERED SUBSCRIPTS
      C(N) = C(N-1)
      N2 = N-2
      DO 800 I=2,N2,2
        C(I) = W(I)*C(I+1) + (1.0-W(I))*C(I-1)
800  CONTINUE
      RETURN
      ENC
      FUNCTION TCAT(C,T)
      COMMON /BATE/ ZK0,GG
      COMMON /BIN/ DELH, DEFF, BRO, CP, BETA
      COMMON /HX/ HP, HW, TRALL, DT, DP, VPSP
      IX = GG / (2.0*T*T)
      HJUNK = HP/(DELH*SQRT(DEFF))
      IT = HJUNK / (C + SQRT( IK(T) ) )
      DELT = 1.0/(IT - IX)
      IF (DELT .GT. 0) GOTO 200
C   IN HERE, OUT OF RANGE OF LINEARIZATION...OR ELSE, STABILITY PROBS
      WRITE(6,100)
100  FORMAT(' ---PGN ABORT IN FUNC -TCAT- ---',/,
1 ' ---SECOND LINEARIZ. RANGE ---',/,
2 ' ---OR, STABILITY PROBLEMS ---')
      STOP
200  CONTINUE
      TCAT = T + DELT
      RETURN
      END
C
      FUNCTION IK(T)
      COMMON /BATE/ ZK0, GG
      IX = ZK0 / EXP(GG/T)
      RETURN
      END
C
      SUBROUTINE CELLN(ITRANS,N,QTOT,Q,T,C,IPLAG,BA,BB,BGLCB,DELZ)
C   VARIABLE **IPLAG** -- IF 0 ==> ADIABATIC REACTOR
C   OTHERWISE ==> CONSTANT WALL
      COMMON /BIN/ DELH, DEFF, BRO, CP, BETA
      COMMON /BATE/ ZK0, GG
      COMMON /HX/ HP, HW, TRALL, DT, DP, VPSP
      DIMENSION T(100),C(100),Q(100)
      DIMENSION BA(100),BB(100)
      DIMENSION BGLCB(100)
C
C   SET OF NUMERICAL INTEGRATION PARAMETERS

```



```

      IYZ = BHO*CP*Q(I)*QTOT
      DELT = HP * DELZ * DTDZ/IYZ
      T(I) = T(I) + DELT
1200 CONTINUE
C
C OUTERMOST PLOG EFFECTED BY WALL ALSO
      IX = SQRT(DEFF * IX(T(N-1)))
      IYZ = RA(N-1)*BA(N-1) - RA(N-2)*BA(N-2)
      AREA = 0.5 * PI * 0.25 * DT * DT * IYZ / VPSP
      RGLCB(N) = IX * AREA * C(N)
      DELC = DELZ * (-1.0*RGLCB(N)) / (QTOT*Q(N))
      C(N) = C(N) + DELC
      IF (IFLAG - EQ. 0) GOTO 1300
      IYZ = RHO * CP * Q(N) * QTOT
      ALF = PI * BW * DT / IYZ
      IX = IX(TS1OLD)
      IX = DELH * SQRT(DEFF*IX) * CSOLD / IYZ
      IX = IX*PI*0.25*DT*DT * (RA(N-1)*BA(N-1)-RA(N-2)*BA(N-2)) / VPSP
      IY = IX / 2.0
      DTEZ = IX * ALP * (T(N)-TWALL)
      T(N) = T(N) + DELZ * DTDZ
      IF(T(N) - LT. TWALL) T(N) = TWALL
      GOTO 1310
C THIS SECTION FOR ADIABATIC REACTOR
1300 CONTINUE
      AREA = 0.5*PI*0.25*DT*DT * (RA(N-1)*BA(N-1)-BA(N-2)*BA(N-2)) / VPSP
      IYZ = BHO*CP*Q(N)*QTOT
      DELT = AREA*DELZ*(T(N-1)-T(N))/IYZ
      T(N) = T(N) + DELT
1310 CONTINUE
CCC DO 1400 I=1,N
CCC WRITE(6,2000) I,T(I),C(I)
C1400 CONTINUE
C FOR NHD PELLT TEMPS AT OUTLET
CCC WRITE(6,2000) (I,T(I),C(I),I=1,N)
CALL TPELL(ITRANS,N,QTOT,Q,T,C,IFLAG,RA,RS,TN1OLD,CN1OLD)
CCC WRITE(6,2000) (I,T(I),C(I),I=1,N)
1500 CONTINUE
2000 FCNMT(/, (IS,2X,E13.6,2X,E13.6))
      RETDRN
      END
SUBROUTINE TPELL(ITRANS,N,QTOT,Q,T,C,IFLAG,RA,RS,TN1OLD,CN1OLD)
      DIMENSION Q(100),I(100),C(100),RA(100),RS(100)
      COMMON /H1/ DELH, DEFF, RHO, CP, BETA
      COMMON /RATE/ ZK0, GG
      COMMON /H1/ HP, HW, TWALL, DT, DP, VPSP
C VARIABLE ITRANS-- IF 0 ==> B-HALF-CELL
C OTHERWISE ==> A-HALF-CELL
      IF (ITRANS .NE. 0) GOTO 900
C THIS SECTION FOR B-HALF-CELL
C CALC PELLT TEMPS
      NAX = N-2
      DO 100 I=2,NAX,2
      TSTAR = 0.5*( T(I+1)+T(I-1) )
      CSTAR = 0.5*( C(I+1)+C(I-1) )
      T(I) = TCAT(CSTAR,TSTAR)
100 CONTINUE
C CALC WALL SOLID PLOG TEMP--FCN CF WALL TEMP, TOO.
      IX (IFLAG - EQ. 0) GOTO 140
      IX = IX(T(N-1))
      IX = SQRT(DEFF*IX)
      IX = DELH * IX * C(N-1) / HP
      IY = 0.5 * GG / (T(N-1)*T(N-1))
      BOT = IX * IY - 1.1
      TOP = T(N-1)*( IX*IY - 1.0 )
      TOF = TOP - 0.1*TWALL - IX
      T(N) = TOP / BOT
      GOTO 150
140 CONTINUE
      T(N) = TCAT( C(N-1), T(N-1) )
150 CONTINUE
      RETDRN
C THIS SECTION FOR A-HALF-CELL
900 CONTINUE
      T(I) = TCAT( C(2), T(2) )
      NAX = N-1
      DO 1100 I=3,NAX,2
      CSTAR = 0.5*( C(I-1)+C(I+1) )
      TSTAR = 0.5*( T(I-1)+T(I+1) )
      T(I) = TCAT( CSTAR,TSTAR )

```

RXN05610
 RXN05620
 RXN05630
 RXN05640
 RXN05650
 RXN05660
 RXN05670
 RXN05680
 RXN05690
 RXN05700
 RXN05710
 RXN05720
 RXN05730
 RXN05740
 RXN05750
 RXN05760
 RXN05770
 RXN05780
 RXN05790
 RXN05800
 RXN05810
 RXN05820
 RXN05830
 RXN05840
 RXN05850
 RXN05860
 RXN05870
 RXN05880
 RXN05890
 RXN05900
 RXN05910
 RXN05920
 RXN05930
 RXN05940
 RXN05950
 RXN05960
 RXN05970
 RXN05980
 RXN05990
 RXN06000
 RXN06010
 RXN06020
 RXN06030
 RXN06040
 RXN06050
 RXN06060
 RXN06070
 RXN06080
 RXN06090
 RXN06100
 RXN06110
 RXN06120
 RXN06130
 RXN06140
 RXN06150
 RXN06160
 RXN06170
 RXN06180
 RXN06190
 RXN06200
 RXN06210
 RXN06220
 RXN06230
 RXN06240
 RXN06250
 RXN06260
 RXN06270
 RXN06280
 RXN06290
 RXN06300
 RXN06310
 RXN06320
 RXN06330
 RXN06340
 RXN06350
 RXN06360
 RXN06370
 RXN06380
 RXN06390
 RXN06400

1100 CONTINUE
RETURN
END

SIN06410
SIN06420
SIN06430

Steady-state Reaction (Fickian)

The implicit method (Lee, 1985; Hornbeck, 1975) yields tri-diagonal matrices (of dimension equal to the number of radial increments plus one) which must be inverted at each axial position to yield concentration and temperature vectors. The matrices are simple to invert because of their band characteristic (Hornbeck, 1975). The attached program simulates either adiabatic (hw=0) or wall-cooled (hw=value) reactors. Comments within the listing explain other program steps.

```

C PROGRAM NAME 'PICKED FORTRAN'
C OSZS PICKIAS ANALOGY WITH RADIAL DISPERSION ONLY
C TO GET CONCENTRATION AND TEMPERATURE PROFILES IN PACKED BED REACTOR
C
    IMPLICIT REAL*8 (A-H,O-Z)
    DIMENSION A(21), R(21), C(21), R(21), CCALL(21), ACALL(21)
    DIMENSION COLO(21), CNEW(21), TOLO(21), TNEW(21), TCALL(21)
    COMMON /B1W, ODECAT, VFSP, DELH, HF, ZK0, GG, CIN
    WRITE(6,2000)
C
C TEST CASE
C
C VARIABLE LIMIT...IF 0==>NO DIFF'S LIMITATION
C OTHERWISE==>IS DIFF'S LIMITATION
C
    LIMIT = 1
C
C INPUT DATA
C
C USE C.G.S. UNITS!!!! (CONC==>MCL/CM**3)
C (TEMP==>DEGREES K)
C
C BULK FLOID PROPS
    OINT = 197.0
    USUP = 79.0
    U = OINT
    RHC = 9.5 D-4
    CP = 0.25
C RATE CONSTANT PARAMS
    ZK0 = 4.5 08
    GG = 1.2 04
C HEAT OF REACTION
    ODELH = 2.4 05
C THE 'RATE' FUNCTION DEFINED VIA EFFECTIVENESS FACTOR AND
C INTRINSIC KINETICS. SEE DEF'N IN ROUTINE BELOW.
    ODECAT = 0.001
    DT = 3.6
    OF = 0.6
    VFSP = OF/6.0
C BED PROPERTIES
    IREQ = 0.40
    OSUP = 3.5
    DIAT = OSUP / REQD
    DIFFR = OSUP
    CONOR = 0.00152
C FILM R.L. COEFFS
    RP = .0026
    SET RW=0 FOR ADIABATIC REACTOR
    RW = 0.0
CCC RW = .0025
C INLET CONDITIONS
    CIN = 2.0 D-7
    TIN = 600.0
C WALL TEMPERATURE
    TRALL = TIN
    WRITE(6,2010) RW, TRALL
C NUMERICAL INTEGRATION PARAMETERS
    ROIV = 5.0
    ZH = 0.5*DT/ROIV
    ZL = 0.10
    NVIDE = ROIV + 1
    ZHAI = 100.0
C IWRITE==>DELTA-Z AT WHICH TO WRITE RESULTS...
    ZWRITE = 1.0-ZL
C INITIALIZE PROFILES
    DO 50 I=1,NVIDE
        CCALD(I) = CIN
        TOLO(I) = TIN
50 CONTINUE
    Z = 0.0
C
C CALC UNCHANGING PARTS OF A,B,C MATRICES (FOR CRANK-NICHOLS METHOD)
C ALPHA==>DIFFR FOR CONC ... CONDE FOR TEMP
C B(MAI)==>1 FOR CONC ... (1+GAHSA) FOR TEMP
C
    R(1) = 0.0
    C(1) = -1.0
    R(1) = 0.0
    RAI = NVIDE - 1
    ITZ = 0.5/(ZM*ZH)
    DO 100 I=2,RAI
        FIC00010
        FIC00020
        FIC00030
        FIC00040
        FIC00050
        FIC00060
        FIC00070
        FIC00080
        FIC00090
        FIC00100
        FIC00110
        FIC00120
        FIC00130
        FIC00140
        FIC00150
        FIC00160
        FIC00170
        FIC00180
        FIC00190
        FIC00200
        FIC00210
        FIC00220
        FIC00230
        FIC00240
        FIC00250
        FIC00260
        FIC00270
        FIC00280
        FIC00290
        FIC00300
        FIC00310
        FIC00320
        FIC00330
        FIC00340
        FIC00350
        FIC00360
        FIC00370
        FIC00380
        FIC00390
        FIC00400
        FIC00410
        FIC00420
        FIC00430
        FIC00440
        FIC00450
        FIC00460
        FIC00470
        FIC00480
        FIC00490
        FIC00500
        FIC00510
        FIC00520
        FIC00530
        FIC00540
        FIC00550
        FIC00560
        FIC00570
        FIC00580
        FIC00590
        FIC00600
        FIC00610
        FIC00620
        FIC00630
        FIC00640
        FIC00650
        FIC00660
        FIC00670
        FIC00680
        FIC00690
        FIC00700
        FIC00710
        FIC00720
        FIC00730
        FIC00740
        FIC00750
        FIC00760
        FIC00770
        FIC00780
        FIC00790
        FIC00800
    
```



```

      ZI = I-1
      A(I) = IYZ * (0.5/ZI - 1.0)
      C(I) = -1.0 * IYZ * (0.5/ZI + 1.0)
100  CONTINUE
      A(NWIDE) = -1.0
C
C  START LOOP FOR MARCHING DOWN REACTOR
      ZPRINT = 0.0
250  CONTINUE
      Z = Z + ZL
      ZPRINT = ZPRINT + ZL
      IF (ZPRINT .LT. ZWRITE) GOTO 255
      WRITE(6,2020) Z
      WRITE(6,2030)
255  CONTINUE
C  CONCENTRATION
      A(NWIDE) = -1.0
      B(NWIDE) = 1.0
      R(NWIDE) = 0.0
      R(1) = 0.0
      B(1) = 1.0
      C(1) = -1.0
      IY = 0/ZL - DIFFR/(ZS*ZS)
      IX = 0/ZL + DIFFR/(ZS*ZS)
      RESOLT = (1.0-ZSED)/ZSED
      CCALL(1) = C(1)
      RAX = NWIDE - 1
      DO 300 I=2,RAX
        ACALL(I) = DIFFR*A(I)
        CCALL(I) = DIFFR*C(I)
        B(I) = IX
        R(I) = -1.0*RESOLT * RATE( TOLD(I), COLD(I), LIMIT)
        R(I) = B(I) - ACALL(I)*COLD(I-1) + IY*COLD(I) - CCALL(I)*COLD(I+1)
300  CONTINUE
      ACALL(NWIDE) = A(NWIDE)
C
C  NOW, GET SOLUTION VECTOR
CCC  WRITE(6,3000) (COLD(I), I=1,NWIDE)
      CALL TRIDAG(ACALL, B, CCALL, R, NWIDE, COLD, CNEW)
CCC  WRITE(6,3000) (CNEW(I), I=1,NWIDE)
C
C  TEMPERATURE
      GAMMA = RW/CONDR * ZS
      R(1) = 0.0
      B(1) = 1.0
      C(1) = -1.0
      R(NWIDE) = 1.0 + GAMMA
      BROCP = BROCPF
      R(NWIDE) = GAMMA*TZALL + BROCP
      CCALL(1) = C(1)
      IY = 0/ZL - CONDR/(ZS*ZS)
      IX = 0/ZL + CONDR/(ZS*ZS)
      DO 350 I=1,NWIDE
        TCALL(I) = TOLD(I)*BROCP
350  CONTINUE
      RAX = NWIDE - 1
      DO 400 I=2,RAX
        ACALL(I) = CONDR*A(I)
        B(I) = IX
        CCALL(I) = CONDR*C(I)
        R(I) = DELH*RESOLT * RATE( TOLD(I), COLD(I), LIMIT)
        R(I) = B(I) - ACALL(I)*TCALL(I-1) + IY*TCALL(I)
        R(I) = B(I) - CCALL(I)*TCALL(I+1)
400  CONTINUE
C
C  GET SOLUTION VECTOR
CCC  WRITE(6,3000) (TOLD(I), I=1,NWIDE)
      CALL TRIDAG(ACALL, B, CCALL, R, NWIDE, TCALL, TNEW)
CCC  WRITE(6,3000) (TNEW(I), I=1,NWIDE)
C  CONVERT BACK TO REAL TEMPERATURES
      DO 450 I=1,NWIDE
        TNEW(I) = TNEW(I)/BROCP
450  CONTINUE
CCC  WRITE(6,3000) (TNEW(I), I=1,NWIDE)
C  CALC BULK VALUES, CAT TEMPS, AND RATES.  WRITE RESULTS
C  NO NEED TO DO THIS IF NOT TIME TO PRINT OUT RESULTS
      IF (ZPRINT .LT. ZWRITE) GOTO 550
C  RESET IPRINT AND THEN WRITE RESULTS...
      ZPRINT = 0.0
      CSOR = 0

```

FIC00810
 FIC00820
 FIC00830
 FIC00840
 FIC00850
 FIC00860
 FIC00870
 FIC00880
 FIC00890
 FIC00900
 FIC00910
 FIC00920
 FIC00930
 FIC00940
 FIC00950
 FIC00960
 FIC00970
 FIC00980
 FIC00990
 FIC01000
 FIC01010
 FIC01020
 FIC01030
 FIC01040
 FIC01050
 FIC01060
 FIC01070
 FIC01080
 FIC01090
 FIC01100
 FIC01110
 FIC01120
 FIC01130
 FIC01140
 FIC01150
 FIC01160
 FIC01170
 FIC01180
 FIC01190
 FIC01200
 FIC01210
 FIC01220
 FIC01230
 FIC01240
 FIC01250
 FIC01260
 FIC01270
 FIC01280
 FIC01290
 FIC01300
 FIC01310
 FIC01320
 FIC01330
 FIC01340
 FIC01350
 FIC01360
 FIC01370
 FIC01380
 FIC01390
 FIC01400
 FIC01410
 FIC01420
 FIC01430
 FIC01440
 FIC01450
 FIC01460
 FIC01470
 FIC01480
 FIC01490
 FIC01500
 FIC01510
 FIC01520
 FIC01530
 FIC01540
 FIC01550
 FIC01560
 FIC01570
 FIC01580
 FIC01590
 FIC01600

```

      TSOL = 0
      RSOL = 0
      RLOL = 0
      DELR = ZR
      DO 500 I=2,NWIDE
        RNEW = ROLD + DELR
        AREA = RNEW*RNEW - ROLD*ROLD
        CSOL = CSOL + RNEW*CNEM(I) + ROLD*CNEM(I-1)
        TSOL = TSOL + RNEW*TNEM(I) + ROLD*TNEM(I-1)
        RLOL = RLOL + RATE(I)*CNEM(I),CNEM(I),LIMIT)
        VOL = AREA * ZL * 3.1416
        RLOL = RLOL + VOL
        TSOL = TCAT(TNEW(I),CNEM(I),LIMIT)
        WHITE(6,2040)I,CNEM(I),TNEW(I),TSOL,RLOL
      RSOL = RSOL + RLOL
C   SAVE OLD VALUES
      ROLD = RNEW
500  CONTINUE
      CBOLK = DELR * CSOL / (OT*OT*0.25)
      TBOLK = DELR * TSOL / (DT*DT*0.25)
      RTOL = RSOL
      WHITE(6,2050)CBOLK,TBOLK,RTOL,STOT
      CONV = 1.0 - CBOLK/CIN
      WHITE(6,2060)CONV
C
550  CONTINUE
C   SAVE INTO 'OLD' VECTORS
      DO 600 I=1,NWIDE
        COLD(I) = CNEM(I)
        TOLD(I) = TNEM(I)
600  CONTINUE
      IF(Z.LT.ZNLI)GOTO 250
C
C   FORRATS. . .
2000 FORRAT(5(' '), ' FICK20 FORRAT',5(' '))
2010 FORRAT(' BW=',E13.6,' TWALL(DEG-K)=',E13.6)
2020 FORRAT(' ---Z (CB)',E13.6)
2030 FORRAT(' I',SX,'CONC',11X,'TEMP',11X,'TCAT',11X,'RATE(ROL/S)')
2040 FORRAT(15,' (2X,E13.6)')
2050 FORRAT(' CBOLK=',E13.6,' TBOLK=',E13.6,' TOTAL RATE=',E13.6)
2060 FORRAT(' CONVERSION=',E13.6)
C3000 FORRAT(8(2X,E13.6))
      STOP
      ENO
      SUBROUTINE TWIDAG(A,B,C,R,NWIDE,IOLD,INEW)
      IMPLICIT REAL*8 (A-H,O-Z)
C   NOTE--ONLY DIMENSIONED FOR 20 RADIAL DIVISIONS
C   FOLLOWS FLOW CHART GIVEN BY HORNBECK
C   NWIDE--VECTOR LENGTHS
C   OTHER NOTATION--SEE HORNBECK
      DIMENSION A(21), B(21), C(21), R(21)
      DIMENSION IOLD(21), INEW(21), AA(21), BB(21)
      A(1) = 0.0
      C(NWIDE) = 0.0
      DO 50 I=1,NWIDE
        AA(I) = A(I)
        BB(I) = B(I)
        INEW(I) = IOLD(I)
50  CONTINUE
      AA(NWIDE) = AA(NWIDE)/B(NWIDE)
      BB(NWIDE) = BB(NWIDE)/B(NWIDE)
C   CALC INTERMEDIATE VARIABLES
      DO 100 I=2,NWIDE
        J = NWIDE - I + 2
        TEMP = 1.0/(R(J-1) - AA(J)*C(J-1))
        AA(J-1) = AA(J-1) * TEMP
        BB(J-1) = (BB(J-1) - C(J-1)*BB(J)) * TEMP
100  CONTINUE
C
C   NOW, SOLUTION VECTOR
      INEW(1) = BB(1)
      DO 200 I=2,NWIDE
        INEW(I) = BB(I) - AA(I)*INEW(I-1)
200  CONTINUE
      RETURN
      END
      FUNCTION RATE(T,C,LIMIT)
      IMPLICIT REAL*8 (A-H,O-Z)
      CONSEC/RIN/DECAT,VPSR,DELR,RP,ZK0,GG,CIN
C   CALC SOLID TEMP FROM LINEARIZED FORM

```

FIC01610
 FIC01620
 FIC01630
 FIC01640
 FIC01650
 FIC01660
 FIC01670
 FIC01680
 FIC01690
 FIC01700
 FIC01710
 FIC01720
 FIC01730
 FIC01740
 FIC01750
 FIC01760
 FIC01770
 FIC01780
 FIC01790
 FIC01800
 FIC01810
 FIC01820
 FIC01830
 FIC01840
 FIC01850
 FIC01860
 FIC01870
 FIC01880
 FIC01890
 FIC01900
 FIC01910
 FIC01920
 FIC01930
 FIC01940
 FIC01950
 FIC01960
 FIC01970
 FIC01980
 FIC01990
 FIC02000
 FIC02010
 FIC02020
 FIC02030
 FIC02040
 FIC02050
 FIC02060
 FIC02070
 FIC02080
 FIC02090
 FIC02100
 FIC02110
 FIC02120
 FIC02130
 FIC02140
 FIC02150
 FIC02160
 FIC02170
 FIC02180
 FIC02190
 FIC02200
 FIC02210
 FIC02220
 FIC02230
 FIC02240
 FIC02250
 FIC02260
 FIC02270
 FIC02280
 FIC02290
 FIC02300
 FIC02310
 FIC02320
 FIC02330
 FIC02340
 FIC02350
 FIC02360
 FIC02370
 FIC02380
 FIC02390
 FIC02400

```

      TSC1 = TCAT(T,C,LIMIT)
      IF( C .GT. (0.001*CIN)) GOTO 50
      RATE = 0
      GOTO 1000
50    CONTINUE
      IF(LIMIT .NE. 0) GOTO 100
C    THIS SECTION FOR NO DIFFUSION LIMITATIONS...
      RATE = C * IK(TSOL)
      GOTO 1000
100   CONTINUE
      RATE = (C/VPSP) * DSQRT( DECAT*IK(TSOL) )
1000  RETURN
      END
      FUNCTION TCAT(T,C,LIMIT)
      IMPLICIT REAL*8 (A-H,O-Z)
      COMMON /RIS/ DECAT, VPSP, DELH, HP, ZKO, GG, CIN
      IF(C .GT. (0.01*CIN)) GOTO 30
      DELT = 0.0
      GOTO 200
30    CONTINUE
      IF(LIMIT .NE. 0) GOTO 40
C    THIS SECTION FOR NO DIFF'N LIMITATIONS
      II = DELH * IK(T) * C * VPSP
      II = HP / II
      YY = GG/(T*T)
      DELI = 1.0/(II-YY)
C    TEST SMALL DELTA-T FOR TEST CASE
CCC   DELT = 2.0
CCC   GOTO 50
90    CONTINUE
      II = DELH * C * DSQRT( DECAT*IK(T) )
      II = HP/II
      YY = GG*0.5/(T*T)
      DELI = 1.0/(II-II)
50    CONTINUE
      IF(DELH .GT. 0.0) GOTO 200
C    HAVE STABILITY (OR LINEARIZ) PROBLEMS IN HERE...
      WRITE(6,100)
100   FORMAT('-----PGH ABOIT IN FUNC -TCAT- ----',/,
1     ' * --- STABILITY OR LINEARIZ PROBLEMS!!!!!!')
      STOP
200   CONTINUE
      TCAT = T + DELT
      RETURN
      END
      FUNCTION IK(T)
      IMPLICIT REAL*8 (A-H,O-Z)
      COMMON /RIS/ DECAT, VPSP, DELH, HP, ZKO, GG, CIN
      IK = ZKO / EXP( GG/T )
      RETURN
      END

```

FIC02410
 FIC02420
 FIC02430
 FIC02440
 FIC02450
 FIC02460
 FIC02470
 FIC02480
 FIC02490
 FIC02500
 FIC02510
 FIC02520
 FIC02530
 FIC02540
 FIC02550
 FIC02560
 FIC02570
 FIC02580
 FIC02590
 FIC02600
 FIC02610
 FIC02620
 FIC02630
 FIC02640
 FIC02650
 FIC02660
 FIC02670
 FIC02680
 FIC02690
 FIC02700
 FIC02710
 FIC02720
 FIC02730
 FIC02740
 FIC02750
 FIC02760
 FIC02770
 FIC02780
 FIC02790
 FIC02800
 FIC02810
 FIC02820
 FIC02830
 FIC02840
 FIC02850
 FIC02860
 FIC02870
 FIC02880
 FIC02890
 FIC02900
 FIC02910

BIBLIOGRAPHY

- Akella, L.M., Reactor Design and Analysis for Exothermic Reactions and Characterization of Ethylene Oxide Reactions, University of Florida, Ph.D. Dissertation (1983).
- Aris, R., "On the Dispersion of a Solute in a Fluid Flowing through a Tube," Proc. Royal Soc. London, A235, p. 67 (1956).
- Aris, R., "On the Dispersion of Linear Kinematic Waves," Proc. Royal Soc. London, A245, p. 268 (1958).
- Aris, R., "On the Dispersion of a Solute by Diffusion, Convection" Proc. Royal Soc. London, A252, p. 538 (1959).
- Aris, R., and N.R. Amundson, "Some Remarks on Longitudinal Mixing or Diffusion in Fixed Beds," AIChE Journal, vol. 3, p. 280 (1957).
- Awasthi, R.C., and K. Vasudeva, "On Mean Residence Times in Flow Systems," Chemical Engineering Science, vol. 38, p. 313 (1983).
- Baron, T., "Generalized Graphical Method for the Design of Fixed Bed Catalytic Reactors," Chemical Engineering Progress, vol. 4, p. 118 (1952).
- Baumeister, E.B., and C.O. Bennett, "Fluid-particle Heat Transfer in Packed Beds," AIChE Journal, vol. 4, p. 69 (1958).
- Beek, J., "Design of Packed Catalytic Reactors," Advances in Chemical Engineering, vol. 3, p. 203 (1962).
- Benati, R.R., and C.G. Brosilow, "Void Fraction Distribution in Beds of Spheres," AIChE Journal, vol. 8, p. 359 (1962).
- Bennett, Charles H., "Serially Deposited Amorphous Aggregates of Hard Spheres," J. Appl. Phys., vol. 43, p. 2727 (1972).
- Bennett, C.O., and J.E. Myers. Momentum, Heat and Mass Transfer (Third Edition). New York: McGraw-Hill Book Company. 1982.

- Bernard, R.A., and R.H. Wilhelm, "Turbulent Diffusion in Fixed Beds of Packed Solids," Chemical Engineering Progress, vol. 46, p. 233 (1950).
- Beveridge, G., and R.S. Schechter, Optimization: Theory and Practice. New York: McGraw-Hill Book Company. 1970.
- Bird, R.B., W.E. Stewart and E.N. Lightfoot. Transport Phenomena. New York: John Wiley and Sons. 1960.
- Bischoff, K.B., and O. Levenspiel, "Fluid Dispersion--Generalization and Comparison of Mathematical Models" Chemical Engineering Science, vol. 17, p. 245 (1962).
- Bischoff, K.B., and E.A. McCracken, "Tracer Tests in Flow Systems," Industrial and Engineering Chemistry, vol. 58, No. 7, p. 18 (1966).
- Botterill, J.S.M., and A.O.O. Denloye, "A Theoretical Model of Heat Transfer to a Packed or Quiescent" Chemical Engineering Science, vol. 33, p. 509 (1978).
- Bowers, K.L., and J.W. Thomas, "Effective Modeling of Time-Dependent, Maldistributed Flow in Packed Beds," AIChE Journal, vol. 31, p. 871 (1985).
- Buffham, B.A., "The Effects of Intrasolid Resistance and Axial Mixing on Transient" Chemical Engineering, vol. 2, p. 71 (1971).
- Bunnell, D.G., H.B. Irvin, R.W. Olson and J.M. Smith, "Effective Thermal Conductivities in Gas-Solid Systems," Industrial and Engineering Chemistry, vol. 41, p. 1977 (1949).
- Burghardt, A., and T. Zaleski, "Longitudinal Dispersion at Small and Large Peclet Numbers in Chemical" Chemical Engineering Science, vol. 23, p. 575 (1968).
- Cairns, E.J., and J.M. Prausnitz, "Longitudinal Mixing in Packed Beds," Chemical Engineering Science, vol. 12, p. 20 (1960).
- Calderbank, P.H., and L.A. Pogorski, "Heat Transfer in Packed Beds," Trans. Instn. Chem. Engrs., Vol. 35, p. 195 (1957).
- Carberry, J.J., "First Order Rate Processes and Axial Dispersion in Packed Bed Reactors," The Canadian Journal of Chemical Engineering, vol. 35, p. 207 (1958).
- Carberry, J.J. Chemical and Catalytic Reaction Engineering. New York: McGraw-Hill Book Company. 1976.

- Carberry, J.J., and R.H. Bretton, "Axial Dispersin of Mass in Flow Through Mixed Beds," AICHE Journal, vol. 4, p. 367 (1958).
- Carbonell, R.G., "Flow Non-uniformities in Packed Beds: Effect on Dispersion," Chemical Engineering Science, vol. 35, p. 1347 (1980).
- Chang, H., "A Non-Fickian Model of Packed-Bed Reactors," AICHE Journal, vol. 28, p. 208 (1982).
- Chang, H., "Effective Diffusion and Conduction in Two-phase Media: a Unified Approach," AICHE Journal, vol. 29, p. 846 (1983).
- Chen, B.H., A.F. McMillan, and S.T. Wang, "An Analytical Solution for Dispersion in Packed Beds" Chemical Engineering Science, vol. 38, p. 257 (1983).
- Choi, C.Y., and D.D. Perlmutter, "A Unified Treatment of the Inlet Boundary Conditions for Dispersive Flow" Chemical Engineering Science, vol. 31, p. 250 (1976).
- Chung, S.F., and C.Y. Wen, "Longitudinal Dispersion of Liquid Flowing" AICHE Journal, vol. 14, p. 857 (1968).
- Clement, K., and S.B. Jorgensen, "Experimental Investigation of Axial and Radial Thermal Dispersion" Chemical Engineering Science, vol. 38, p. 835 (1981).
- Coberly, C.A., and W.A. Marshall, "Tempeature Gradients in Gas Streams Flowing through Fixed Granular Beds," Chemical Engineering Progress, vol. 47, p. 141 (1951).
- Cohen, Yoram and A.B. Metzner, "Wall Effects in Laminar Flow of Fluids through Packed Beds," AICHE Journal, vol. 27, p. 705 (1981).
- Colburn, A.P., "Heat Transfer and Pressure Drop in Empty, Baffled, and Packed Tubes" Industrial and Engineering Chemistry, vol. 23, p. 910 (1931).
- Coulson, J.M., "The Flow of Fluids through Granular Beds: Effect of Particle Shape" Transactions of the Institution of Chemical Engineers (London), vol. 27, p. 237 (1949).
- Crider, J.E., and A.S. Foss, "Effective Wall Heat Transfer Coefficients and Thermal Resistances" AICHE Journal, vol. 11, p. 1012 (1965).

- Danckwerts, P.V., "Continuous Flow Systems Distribution of Residence Times," Chemical Engineering Science, vol. 2, p. 1 (1953).
- Daugherty, R.L., and J.B. Franzini, Fluid Mechanics with Engineering Applications. New York: McGraw-Hill, Inc. 1977.
- Deans, H.A., and L. Lapidus, "A Computational Model for Predicting and Correlating the Behavior" AIChE Journal, vol 6., p. 656 (1960).
- Deckwer, W., and E.A. Mahlmann, "Boundary Conditions of Liquid Phase Reactors with Axial Dispersion," The Chemical Engineering Journal, vol. 11, p. 19 (1976).
- deWasch, A.P., and G.F. Froment, "Heat Transfer in Packed Beds," Chemical Engineering Science, vol. 27, p. 567 (1972).
- Dodds, J.A., "The Porosity and Contact Points in Multicomponents" Journal of Colloid and Interface Science, vol. 77, p. 317 (1980).
- Dorweiler, V.P., and R.W. Fahien, "Mass Transfer at Low Flow Rates in a Packed Column" AIChE Journal, vol. 5, p. 139 (June, 1959).
- Duarte, S., I. Pereira, O.M. Martinez, O.A. Ferretti and N.O. Lemcoff, "Theoretical Prediction of Heterogeneous One-Dimensional Heat Transfer Coefficients for Fixed-Bed Reactors," AIChE Journal, vol. 31, p. 868 (1985).
- Ebach, E.A., and R.R. White, "Mixing of Fluids Flowing through Beds of Packed Solids," AIChE Journal, vol. 4, p. 161 (1958).
- Edwards, M.F., and J.F. Richardson, "Gas Dispersion in Packed Beds," Chemical Engineering Science, vol. 23, p. 109 (1968).
- Eidsath, A., R.G. Carbonell, S. Whitaker, and L.R. Hermann, "Dispersion in Pulsed Systems---III Comparison between Theory" Chemical Engineering Science, vol. 38, p. 1803 (1983).
- Epstein, N., "Gas-particle Heat and Mass Transfer in Packed Beds of Spheres" Industrial and Engineering Chemistry Fundamentals, vol. 4, p. 238 (1965).
- Ergun, S., "Fluid Flow through Packed Columns," Chemical Engineering Progress, vol. 48, p. 89 (1952).
- Ergun, S., and A.A. Orning, "Fluid Flow through Randomly Packed Columns and Fluidized Beds," Industrial and Engineering Chemistry, vol. 41, p. 1179 (1949).
- Evans, E.V., and C.N. Kenney, "Gaseous Dispersion in Packed Beds at Low Reynolds Numbers," Trans. Instn. Chem. Engrs., vol. 44, p. T189 (1966).

- Fahien, R.W., and J.M. Smith, "Mass Transfer in Packed Beds," AIChE Journal, vol. 1, p. 28 (1955).
- Fedors, R.F., "A Relationship between Maximum Packing of Particles and Particle Size," Powder Technology, vol. 22, p. 71 (1979).
- Froment, G.F., "Fixed Bed Catalytic Reactors--Current Design Status," Industrial and Engineering Chemistry, vol. 59, p. 18 (1967).
- Froment, G.F., "Fixed Bed Reactors Steady State Conditions," Proc. 5 Europ/2nd Int. Symp. on Chem. Reaction Engng., Paper A5-1, Elsevier, Amsterdam (1972).
- Froment, G.F., and K.B. Bischoff. Chemical Reactor Analysis and Design. New York: John Wiley and Sons. 1979.
- Galloway, L.R., W. Komarnicky, and N. Epstein, "Effect of Packing Configuration on Mass and Heat Transfer" The Canadian Journal of Chemical Engineering, p. 139 (1957).
- Grabmuller, H., and H. Schadlich, "Residence Time Distribution of Plug Flow in a Finite Packed-Bed" Chemical Engineering Science, vol. 38, p. 1543 (1983).
- Greenkorn, R.A., and D.P. Kessler, Transfer Operations. New York: McGraw-Hill Book Company, 1972.
- Gunn, D.J., "Mixing in Packed and Fluidized Beds," The Chemical Engineer, p. CE153 (1968).
- Gunn, D.J., "Theory of Axial and Radial Dispersion in Packed Beds," Trans. Instn. Chem. Engrs., vol. 47, p. T351, (1969).
- Gunn, D.J., and R. England, "Dispersion and Diffusion in Beds of Porous Particles," Chemical Engineering Science, vol. 26, p. 1413 (1971).
- Gunn, D.J., and M. Khalid, "Thermal Dispersion and Wall Heat Transfer in Packed Beds," Chemical Engineering Science, vol. 30, p. 261 (1976).
- Gunn, D.J., and C. Pryce, "Dispersion in Packed Beds," Trans. Instn. Chem. Engrs., vol. 47, p. T341 (1969).
- Hall, R.E., and J.M. Smith, "Design of Gas-Solid Catalytic Reactors," Chemical Engineering Progress, vol. 45, p. 459 (1949).

- Hanratty, T.J., "Nature of Wall Heat Transfer Coefficient in Packed Beds," Chemical Engineering Science, vol. 8, p. 209 (1954).
- Haughey, D.P., and G.S.G. Beveridge, "Local Voidage Variation in a Randomly Packed Bed of Equal-Sized Spheres," Chemical Engineering Science, vol. 21, p. 905 (1966).
- Hibilaro, L.G., "Residence Time Distributions in Regions of Continuous Flow Systems," Chemical Engineering Science, vol. 34, p. 697 (1979).
- Hiby, J.W., "Longitudinal and Transverse Mixing During Single-phase Flow" Interaction Between Fluids and Particles, p. 312 (1963).
- Hinduja, M.J., A Non-Fickian Model for Dispersion in Packed Beds, Rice University, Ph.D. Dissertation (1977).
- Hinduja, M.J., S. Sundaresan, and R. Jackson, "A Crossflow Model of Dispersion in Packed Bed Reactors," AIChE Journal, vol. 26, p. 274 (1980).
- Hirai, Eiji, "The Void of a Packed Tower", Chemical Engineering (Japan), vol. 18, p. 22 (1954).
- Hoffmann, H., "Der derzeitige Stand bei der Vorausberechnung der Verweilzeitverteilung" Chemical Engineering Science, vol. 14, p. 193 (1961).
- Hong, J.C., Design and Control of Fixed-Beds Affected by Catalyst Deactivation, University of Florida, Ph.D. Dissertation (1984).
- Hornbeck, R.W. Numerical Methods. Englewood Cliffs, N.J.: Prentice-Hall, Inc. 1975.
- Hsiang, T.C., and H.W. Haynes, "Axial Dispersion in Small Diameter Beds of Large Spherical Particles" Chemical Engineering Science, vol. 32, p. 678 (1977).
- Hughmark, G.A., "Momentum, Heat and Mass Transfer for Fixed and Homogeneous Fluidized Beds," Industrial and Engineering Chemistry Fundamentals, vol. 18, p. 1020 (1972).
- Hughmark, G.A., "Heat and Mass Transfer for Spherical Particles in a Fluid Field," Industrial and Engineering Chemistry Fundamentals, vol. 19, p. 198 (1980).

- Jacques, G.L., and T. Vermeulen, Longitudinal Dispersion in Solvent-Extraction Columns: Peclet Numbers for Ordered and Random Packings, Report UCRL-8029, U.S. Atomic Energy Commission (1957). (Performed at University of California, Berkeley, contract number W-7405-eng-8).
- Karabelas, A.J., T.H. Wegner, and T.J. Hanratty, "Flow Pattern in a Close Packed Cubic Array of Spheres" Chemical Engineering Science, vol. 28, p. 673 (1973).
- Kayser, H.G., "A Methodical Investigation of Interactions between Flow and Structure" Dechema Monographs, vol. 32, p. 116 (1959).
- Klinkenberg, A., H.J. Krajenbrink, and H.A. Lauwerier, "Diffusion in a Fluid Moving at Uniform Velocity in a Tube", Industrial and Engineering Chemistry, vol. 45, p. 1202 (1953).
- Klinkenberg, A., and F. Sjenitzer, Holding-time Distributions of the Gaussian Type, Chemical Engineering Science, vol. 5, p. 258 (1956).
- Kramers, H., and G. Alberda, "Frequency Response of Continuous Flow Systems," Chemical Engineering Science, vol. 2, p. 173 (1953).
- Kubo, K., T. Aratani, A. Mishima, and T. Yano, "Mutual Relation Between the Streamlines and the Residence Time Curve" The Chemical Engineering Journal, vol. 18, p. 209 (1979).
- Kunii, D., and J.M. Smith, "Heat Transfer Characteristics of Porous Rocks," AIChE Journal, vol. 6, p. 71 (1960).
- Kunii, D., M. Suzuki and N. Ono, "Heat Transfer from Wall Surface to Packed Beds at High Reynolds Number," Journal of Chemical Engineering of Japan, vol. 1. p. 21 (1968).
- Kwong, S.S., and J.M. Smith, "Radial Heat Transfer in Packed Beds," Industrial and Engineering Chemistry, vol. 49, p. 894 (1957).
- Lapidus, L., "Flow Distribution and Diffusion in Fixed-bed Two-phase Reactors," Industrial and Engineering Chemistry, vol. 49, p. 1000 (1957).
- Lapidus, L., and N.R. Amundson (Editors). Chemical Reactor Theory: A Review. Prentice Hall, Inc. 1977
- Lapin, A., "Pressure Drop for Gases Flowing across Packed Beds," Chemical Engineering Progress, vol. 58, p. 47 (1962).

- Latinen, G.A., Mechanisms of Fluid-phase Mixing in Fixed and Fluidized Beds of Uniformly Sized Spherical Particles, Princeton University, Ph.D. Dissertation, (1951).
- Lee, H.H., "An Approximate Approach to Design and Analysis of Fixed Bed Catalytic Reactors," AIChE Journal, vol. 27, p. 558 (1981).
- Lee, H.H., Heterogeneous Reactor Design. Boston: Butterworth Publishers, 1985.
- LeGoff, P., D. LeClerc, and J. Dodds, "The Structure of Packed Beds: Continuity of Research in Nancy and Some New Results," Powder Technology, vol. 42, p. 47 (1985).
- Lerou, J.J., and G.F. Froment, "Velocity, Temperature and Conversion Profiles in Fixed Bed Catalytic Reactors," Chemical Engineering Science, vol. 32, p. 853 (1977).
- Leva, M., "Heat Transfer to Gases through Packed Tubes, General Correlation", Industrial and Engineering Chemistry, vol. 39, p. 357 (1947a).
- Leva, M., "Pressure Drop through Packed Tubes, Part I: A General Correlation," Chemical Engineering Progress, vol. 43, p. 549 (1947b).
- Leva, M., and M. Grummer, "Pressure Drop through Packed Tubes, Part II: Effect of Surface Roughness," Chemical Engineering Progress, vol. 43, p. 633 (1947a).
- Leva, M., and M. Grummer, "Pressure Drop through Packed Tubes, Part III: Prediction of Voids" Chemical Engineering Progress, vol. 43, p. 713 (1947b).
- Leva, M., and M. Grummer, "Heat Transfer to Gases through Packed Tubes, Effect of Particle", Industrial and Engineering Chemistry, vol. 40, p. 415 (1948).
- Levenspiel, O. Chemical Reaction Engineering. New York: John Wiley and Sons. 1962.
- Levenspiel, O., "Patterns of Flow in Chemical Process Vessels," Advances in Chemical Engineering, Academic Press, vol. 4, p. 95 (1963).
- Levenspiel, O. and T.J. Fitzgerald, "A Warning on the Misuse of the Dispersion Model," Chemical Engineering Science, vol. 38, p. 489 (1983).

- Li, C., and B. A. Finlayson, "Heat Transfer in Packed Beds--A Reevaluation," Chemical Engineering Science, vol. 32, p. 1055 (1977).
- Liles, A. W., Axial Mixing of Liquids Flowing through Packed Beds, Ohio State University, Ph.D. Thesis (1959).
- Liles, A. W., and C. J. Geankoplis, "Axial Diffusion of Liquids in Packed Beds and End Effects," vol. 6, p. 591 (1960).
- Lippert, E. and P. Schneider, "Combined Isothermal Diffusion and Forced Flow of a Binary Gaseous," Chemical Engineering Communications, vol. 3, p. 65 (1979).
- Luus, R., and T. H. I. Jaakola, "Optimization by Direct Search and Systematic Reduction of the Size of Search Region," AIChE Journal, vol. 19, p. 760 (1973).
- Marivoet, J., P. Teodoroiu, and S. J. Wajc, "Porosity, Velocity and Temperature Profiles in Cylindrical Packed Beds," Chemical Engineering Science, vol. 29, p. 1836 (1974).
- Martin, J. J., W. L. McCabe, and C. C. Monrad, "Pressure Drop through Stacked Spheres, Effect of Orientation," Chemical Engineering Progress, vol. 47, p. 91 (1951).
- McCabe, W. L., and J. C. Smith. Unit Operations of Chemical Engineering (Third Edition). New York: McGraw-Hill Book Company. 1976.
- McHenry, K. W., and R. H. Wilhelm, "Axial Mixing of Binary Gas Mixture Flowing in a Random Bed of Spheres," AIChE Journal, vol. 3, p. 83 (1957).
- Mears, D. F., "The Role of Axial Dispersion in Trickle-flow Laboratory Reactors," Chemical Engineering Science, vol. 26, p. 1361 (1971).
- Mickley, H. S., K. A. Smith, and E. I. Korchak, "Fluid Flow in Packed Beds," Chemical Engineering Science, vol. 20, p. 237 (1965).
- Miller, S. F., and C. J. King, "Axial Dispersion in Liquid Flow through Packed Beds," AIChE Journal, vol. 12, p. 767 (1966).
- Olbrich, W.E., J. G. Agnew, and O. E. Potte, "Dispersion in Packed Beds and the Cell Model," Trans. Instn. Chem. Engrs., vol. 44, p. T207 (1966).
- Oliveros, G., and J. M. Smith, "Dynamic Studies of Dispersion and Channeling in Fixed Beds," AIChE Journal, vol. 28, p. 751 (1982).

- Ouchiyaama, N., and T. Tanaka, "Porosity of a Mass of Solid Particles Having a Range of Sizes," Industrial and Engineering Chemistry Fundamentals, vol. 20, p. 66 (1981).
- Ouchiyaama, N., and T. Tanaka, "Porosity Estimation for Random Packings of Spherical Particles," Industrial and Engineering Chemistry Fundamentals, vol. 23, p. 490 (1984).
- Patterson, W.R., and J.J. Carberry, "Fixed Bed Catalytic Reactor Modeling, the Heat Transfer Problem", Chemical Engineering Science, vol. 38, p. 175 (1983).
- Pillai, K.K., "Voidage Variation at the Wall of a Packed Bed of Spheres," Chemical Engineering Science, vol. 32, p. 59 (1977).
- Plautz, D.A., and H.A. Johnstone, "Heat and Mass Transfer in Packed Beds," AIChE Journal, vol. 1, p. 193 (1955).
- Ranz, W.E., and W.R. Marshall, Jr. CEP, vol. 48, p. 141 (1952), (Cited in Bird et al., 1960, p. 409).
- Rasmuson, A., "Exact Solution of a Model for Diffusion and Transient Adsorption," AIChE Journal, vol. 27, p. 1032 (1981).
- Rasmuson, A., and I. Neretnieks, "Exact Solution of a Model for Diffusion in Particles," AIChE Journal, vol. 26, p. 686 (1980).
- Ray, W.H., M. Marek, and S. Elnashaie, "The Effect of Heat and Mass Dispersion on Tubular Reactor Performance," Chemical Engineering Science, vol. 27, p. 1527 (1972).
- Reilly, P.M., "Unsteady State Heat Transfer in Stationary Packed Beds," AIChE Journal, vol. 3, p. 513 (1957).
- Ridgway, K., and K.J. Tarbuck, "Voidage Fluctuations in Randomly-packed Beds of Spheres," Chemical Engineering Science, vol. 23, p. 1147 (1968).
- Roble, L.H., R.M. Baird, and J.W. Tierney, "Radial Profile Variations in Packed Beds," AIChE Journal, vol. 4, p. 460 (1958).
- Roemer, G., J.S. Dranoff, and J.M. Smith, "Diffusion in Packed Beds at Low Flow Rates," Industrial and Engineering Chemistry Fundamentals, vol. 1, p. 284 (1962).

- Schertz, W.W., and K.B. Bischoff, "Thermal and Material Transport in Nonisothermal Packed Beds," AIChE Journal, vol. 15, p. 597 (1969).
- Schlunder, E.U., "Transport Phenomena in Packed Bed Reactors," ACS Symposium Series, vol. 72 (5th International Symposium on Chemical Reaction Engineering in Houston, Texas), p. 11 (1978).
- Schmalzer, D.K., and H.E. Hoelscher, "Detector Effects in Packed Bed Measurements," AIChE Journal, vol. 17, p. 241 (1971a).
- Schmalzer, D.K., and H.E. Hoelscher, "A Stochastic Model of Packed-bed Mixing and Mass Transfer," AIChE Journal, vol. 17, p. 104 (1971b).
- Schotte, W., "Thermal Conductivity of Packed Beds," AIChE Journal, vol. 6, p. 63 (1960).
- Schwartz, C.E., and J.M. Smith, "Flow Distribution in Packed Beds," Industrial and Engineering Chemistry, vol. 45, p. 1209 (1953).
- Scott, D.S., W. Lee, and J. Papa, "The Measurement of Transport Coefficients in Gas-Solid" Chemical Engineering Science, vol. 29, p. 2155 (1974).
- Sherwood, T.K., and R.L. Pigford. Absorption and Extraction. New York: McGraw-Hill Book Company. 1952. (Cited in Bird, et al., 1960, p. 408).
- Sloane, N.J.A., "The Packing of Spheres," Scientific American, vol. 250, p. 116 (1984).
- Smith, J.M. Chemical Engineering Kinetics. New York: McGraw-Hill Book Company. 1981.
- Standard, G., "The Thermodynamic Significance of the Danckwerts' Boundary Conditions," Chemical Engineering Science, vol. 23, p. 645 (1968).
- Standish, N., "Comment on the Velocity Profiles in Packed Beds," Chemical Engineering Science, vol. 39, p. 1530 (1984).
- Standish, N., and G. McGregor, "The Average Shape of a Mixture of Particles in a Packed Bed," Chemical Engineering Science, vol. 33, p. 618 (1978).
- Stanek, V., and V. Eckert, "A Study of the Area Porosity Profiles in a Bed of Equal-diameter" Chemical Engineering Science, vol. 34, p. 933 (1979).

- Strang, D.A., and C.J. Geankoplis, "Longitudinal Diffusivity of Liquids in Packed Beds," Industrial and Engineering Chemistry, vol. 50 p. 1305 (1958).
- Sundaresan, S., N.R. Amundson, and R. Aris, "Observation on Fixed-bed Dispersion Models: The Role," AIChE Journal, vol. 26, p. 529 (1980).
- Suzuki, M., and J.M. Smith, "Effect of Transport Processes on Conversion in a Fixed Bed Reactor," AIChE Journal, vol. 16, p. 882 (1970).
- Tan, C.S., and J.M. Smith, "Catalyst Particle Effectiveness with Unsymmetrical Boundary Conditions," Chemical Engineering Science, vol. 33, p. 1601 (1980).
- Taylor, G.I., "Dispersion of Soluble Matter in Solvent Flowing Slowly through a Tube," Proc. Roy. Soc. London, A219, p. 186 (1953).
- Taylor, G.I., "Conditions under which Dispersion of a Solute in a Stream of Solvent Can," Proc. Roy. Soc. London, A225, p. 473, (1954a).
- Taylor, G.I., "The Dispersion of Matter in Turbulent Flow through a Pipe," Proc. Roy. Soc. London, A223, p. 446 (1954b).
- Turner, J.C.R., "The Interpretation of Residence-time Measurements in Systems," Chemical Engineering Science, vol. 26, p. 549 (1971).
- Turner, J.C.R., and D. Vortmeyer, "Answer to the Letter of Prof. Standish," Chemical Engineering Science, vol. 39, p. 1531 (1984).
- Vortmeyer, D., and J. Schuster, "Evaluation of Steady Flow Profiles," Chemical Engineering Science, vol. 38, p. 1691 (1983).
- Vortmeyer, D., and R.P. Winter, "Impact of Porosity and Velocity Distribution on the Theoretical Prediction of Fixed-bed Chemical Reactor Performance," ACS Symposium Series, vol. 196 (7th International Symposium on Chemical Reaction Engineering in Boston, Massachusetts), p. 49 (1982).
- Vortmeyer, D., and R.P. Winter, "On the Validity Limits of Packed Bed Reactor Continuum Models," Chemical Engineering Science, vol. 39, p. 1430 (1984).
- Wakao, N., "Particle-to-fluid Transfer Coefficients and Fluid Diffusivities," Chemical Engineering Science, vol. 31, p. 1115 (1976).

- Wakao, N., S. Kaguei, and T. Funazkri, "Effect of Fluid Dispersion Coefficients on Particle-to-fluid Heat," Chemical Engineering Science, vol. 34, p. 325 (1979).
- Wakao, N., and K. Kato, "Effective Thermal Conductivity of Packed Beds," Journal of Chemical Engineering of Japan, vol. 2, p. 24 (1969).
- Wehner, J.F., and R.H. Wilhelm, "Boundary Conditions of Flow Reactor," Chemical Engineering Science, vol. 6, p. 89 (1956).
- Wen, C.Y. and L.T. Fan. Models for Flow Systems and Chemical Reactors. New York: Marcel Dekker, Inc. 1975.
- Whitaker, S., "Forced Convection Heat Transfer Correlations for Flow in Pipes", AIChE Journal, vol. 18, p. 361 (March 1972).
- Wolff, H., K. Radeke, and D. Gelbin, "Heat and Mass Transfer in Packed-Beds--The Use of Weight," Chemical Engineering Science, vol. 34, p. 101 (1979).
- Yagi, S., and D. Kunii, "Studies on Heat Transfer Near Wall Surface in Packed Beds," AIChE Journal, vol. 6, p. 97 (1960).
- Yagi, S., D. Kunii, and N. Wakao, "Studies on Axial Effective Thermal Conductivities in Packed Beds," AIChE Journal, vol. 6, p. 543 (1960).
- Yagi, S., and N. Wakao, "Heat and Mass Transfer from Wall to Fluid in Packed Beds," AIChE Journal, vol. 5, p. 79 (1959).
- Yoshida, F., D. Ramaswami, and O.A. Hougen, "Temperatures and Partial Pressures at the Surfaces of Catalyst Particles," AIChE Journal, vol. 8, p. 5 (1962).

BIOGRAPHICAL SKETCH

The author was born on July 18, 1958, in Washington, D.C. She received her B.S.E. and M.S.E. in chemical engineering from the University of South Florida in 1980. After working for three years as a process control engineer in the chemical intermediates industry, she enrolled at the University of Florida for further graduate studies. Her career interests are in process research and design.

I certify that I have read this study and that in my opinion it conforms to acceptable standards of scholarly presentation and is fully adequate, in scope and quality, as a dissertation for the degree of Doctor of Philosophy.



Hong H. Lee, Chairman
Professor of Chemical Engineering

I certify that I have read this study and that in my opinion it conforms to acceptable standards of scholarly presentation and is fully adequate, in scope and quality, as a dissertation for the degree of Doctor of Philosophy.



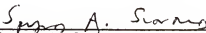
Gerasimos K. Lyberatos
Assistant Professor of Chemical
Engineering

I certify that I have read this study and that in my opinion it conforms to acceptable standards of scholarly presentation and is fully adequate, in scope and quality, as a dissertation for the degree of Doctor of Philosophy.



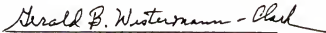
Patrick J. McKenna
Associate Professor of Mathematics

I certify that I have read this study and that in my opinion it conforms to acceptable standards of scholarly presentation and is fully adequate, in scope and quality, as a dissertation for the degree of Doctor of Philosophy.



Spyros A. Svoronos
Assistant Professor of Chemical
Engineering

I certify that I have read this study and that in my opinion it conforms to acceptable standards of scholarly presentation and is fully adequate, in scope and quality, as a dissertation for the degree of Doctor of Philosophy.



Gerald B. Westermann-Clark
Associate Professor of Chemical
Engineering

This dissertation was submitted to the Graduate Faculty of the College of Engineering and to the Graduate School and was accepted as partial fulfillment of the requirements for the degree of Doctor of Philosophy.

Hubert A. Bavis

Dean, College of Engineering

December
1985

Dean, Graduate School